8-7-2020

Can Mixed Ligand and Catalytic Solvent Effects Transform Single Electron Transfer Living Radical Polymerization (SET-LRP) into a Commercializable Process?

Devendra Surendrakumar Maurya
University of Pennsylvania, maurya@sas.upenn.edu

Can Mixed Ligand and Catalytic Solvent Effects Transform Single Electron Transfer Living Radical Polymerization (SET-LRP) into a Commercializable Process?

Abstract

Currently most of the SET-LRP and ATRP techniques uses tris(2-dimethylaminoethyl)amine (Me$_6$-TREN) as ligand which is 80 time more expensive than its precursor tris(2-aminoethyl)amine (TREN). TREN is much less expensive than Me$_6$-TREN but at the same time is much less efficient, thus limiting the commercial applications of SET-LRP and ATRP mediated by TREN.[1-6] In this work the efficiency of TREN was increased via two mechanisms: (i) the mixed ligand effect, (ii) the catalytic effect of solvent. Me$_6$-TREN and TREN mixed ligand effect was studied in programed "biphasic" mixtures of the dipolar aprotic solvents N-methylpyrrolidone (NMP), dimethylformamide (DMF) and N,N-dimethylacetamide (DMAc) with H$_2$O and in the homogenous dimethyl sulfoxide (DMSO) system with methyl acrylate(MA) as monomer, initiated by bis(2-bromopropionyl)-ethane (BPE). From the kinetic studies, molecular weight evolution and chain end analysis it was concluded that Me$_6$-TREN complemented TREN to enhance its apparent rate constant of propagation, monomer conversion, and molecular weight control in the absence of externally added Cu(II)Br$_2$. The catalytic effect of DMSO was studied with Me$_6$-TREN, mixed-ligand and TREN and a liner external order of reaction was observed. The catalytic activity of DMSO in SET-LRP with near 100% chain end revitalized TREN as an excellent ligand in SET-LRP. Since the highest rate of reaction in mixed-ligand system is observed at a 1/1 ratio of ligands, this suggested three possible mechanisms: (i) either a fast exchange of ligands in the catalytic system, (ii) a new single dynamic ligand generated by hydrogen-bonding of the two ligands, (iii) or a combination of both (i) and (ii).

Keywords

Single Electron Transfer Living Radical Polymerization, SET-LRP, Mixed Ligand Effect, Catalytic Solvent Effect, Living Polymerization, Living Radical Polymerization

Disciplines

Chemistry

Creative Commons License

AN ABSTRACT OF THE CAPSTONE REPORT OF

Devendra Surendrakumar Maurya for the degree of Master of Chemical Sciences

Title: Can Mixed Ligand and Catalytic Solvent Effects Transform Single Electron Transfer Living Radical Polymerization (SET-LRP) into a Commercializable Process?

Project conducted at: *University of Pennsylvania, 231 South 34th Street Philadelphia, PA 19104*

Supervisor: Professor *Virgil Percec*
Dates of Project: January 2019-August 2020

Abstract approved: Virgil Percec, Academic Advisor

Currently most of the SET-LRP and ATRP techniques uses tris(2-dimethylaminoethyl)amine (Me_6-TREN) as ligand which is 80 time more expensive than its precursor tris(2-aminoethyl)amine (TREN). TREN is much less expensive than Me_6-TREN but at the same time is much less efficient, thus limiting the commercial applications of SET-LRP and ATRP mediated by TREN.[1-6] In this work the efficiency of TREN was increased via two mechanisms: (i) the mixed ligand effect, (ii) the catalytic effect of solvent. Me_6-TREN and TREN mixed ligand effect was studied in programed "biphasic" mixtures of the dipolar aprotic solvents N-methylpyrrolidone (NMP), dimethylformamide (DMF) and N,N-dimethylacetamide (DMAc) with H_2O and in the homogenous dimethyl sulfoxide (DMSO) system with methyl acrylate(MA) as monomer, initiated by bis(2-bromopropionyl)-ethane (BPE). From the kinetic studies, molecular weight evolution and chain end analysis it was concluded that Me_6-TREN complemented TREN to enhance its apparent rate constant of propagation, monomer conversion, and molecular weight control in the absence of externally added $Cu(II)Br_2$. The catalytic effect of DMSO was studied with Me_6-TREN, mixed-ligand and TREN and a liner external order of reaction was observed. The catalytic activity of DMSO in SET-LRP with near 100% chain end revitalized TREN as an excellent ligand in SET-LRP. Since the highest rate of reaction in mixed-ligand system is observed at a 1/1 ratio of ligands, this suggested three possible mechanisms: (i) either a fast exchange of ligands in the catalytic system, (ii) a new single dynamic ligand generated by hydrogen-bonding of the two ligands, (iii) or a combination of both (i) and (ii).

Can Mixed Ligand and Catalytic Solvent Effects Transform Single Electron Transfer Living Radical Polymerization (SET-LRP) into a Commercializable Process?

By
Devendra Surendrakumar Maurya

A CAPSTONE REPORT

submitted to the

University of Pennsylvania
in partial fulfillment of
the requirements for
the degree of

Masters of Chemical Sciences

Presented July 28th, 2020
Commencement August 7th, 2020

Master of Chemical Sciences Capstone Report of <u>*Devendra Surendrakumar Maurya*</u> presented on July 28th, 2020.

APPROVED:

Virgil Percec, representing *Organic Chemistry*

I understand that my Capstone Report will become part of the permanent collection of the University of Pennsylvania Master of Chemical Sciences Program. My signature below authorizes release of my final report to any reader upon request.

Devendra Surendrakumar Maurya, Author

Acknowledgment

Table of Content

List of Figures

List of Tables

List of Schemes

List of Appendices

Chapter 1
Replacing Cu(II)Br$_2$ with Me$_6$-TREN in Biphasic Cu(0)/TREN Catalyzed SET-LRP Reveals the Mixed-Ligand Effect
(Reproduced with permission from Refence No 1. Copyright (2020) American Chemical Society.)

Introduction

Living Polymerization

Polymers are heavily used chemical products ranging from medical implants to coatings on the sea vessels. The polymers are interesting because of their physical properties, unlike the small molecular weight molecules, which are interesting because of their chemical properties.[2] Chiefly of which is the low density to strength ratio making them popular in commercial applications. Polymer chains consist of repeating units of one or more monomers.[2] Not all the chain of a polymer has the same molecular weight. Their molecular weight and the distribution define many of the properties of the polymers. The main drive in polymer chemistry is to control the polymer architecture, polymer chain end functionality, molecular weight and lower the polydispersity (chain length distribution). Living polymerization technique gives us the above benefits by living end groups which can be of three types a) non-terminated end group b) reversibly activated and deactivated end group and c) reversibly activated and deactivated end group by chain transfer to give the desired polymer.[3a] Biological macromolecules such as proteins and nucleic acids are monodisperse, contrast to polymers. Currently, monodisperse macromolecules or polymers such us dendrimers and even synthetic peptides and nucleic acids can be prepared only by iterative (protection deprotection) methods.

Conventional chain growth polymerization has four steps initiation, propagation, termination and chain transfer. Living polymerization on other hand have no or minimum termination and chain transfer. In 1936 Ziegler, reported that anionic polymerization of styrene and butadiene initiated with an alkyl lithium initiator does not have termination and chain transfer.[4] The work on living polymerization was done before the term living polymerization was introduced, for example polymerization of ethylene oxide initiated by alkoxides by Flory.[2,3] In 1956 Szwarc coined the term "living polymerization" for the anionic polymerization of styrene initiated by sodium naphthalene.[4] Szwarc observed that when additional monomer was added to polymer, the polymer chain would continue to grow suggesting living chain end in polymer. The definition proposed by Szwarc was "living polymer are polymers that retain their ability to propagated and grown to a desired size while their degree of termination or chain transfer is still negligible".[5] Experimentality, living polymerization is characterized by a linear kinetic plot, a linear molecular weight distribution versus conversion, low polydispersity, and perfect or near perfect chain end-functionality chain end-functionality.

The termination in polymerization is monitored by consumption of monomer as a function of time. The semi-logarithmic kinetic plot of ln([M]$_0$/[M]) versus time should be linear for living polymerization (**Figure 1.1a**).[6] [M]$_0$ is the initial concentration of monomer and [M]

is the concentration of monomer at a given time. A linear plot suggests a constant number of active polymer chain with no termination.[6] The rate of polymerization only depend on the concentration of monomer, when there no termination.[6] Any deceleration in liner plot indicate termination and any acceleration indicate slow initiation.
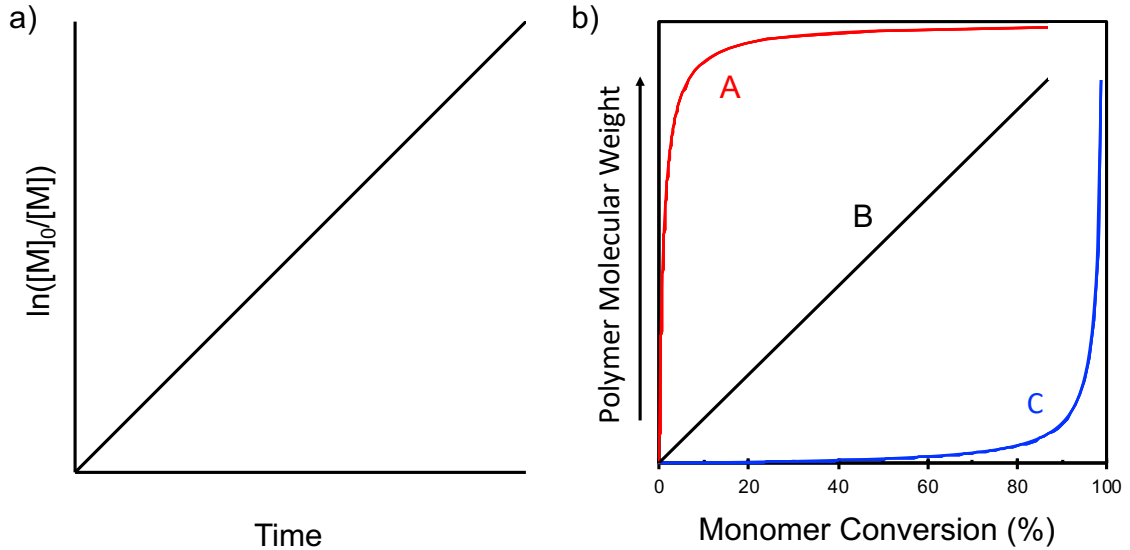
Figure 1.1. a) Evolution of monomer conversion plot versus time b) Molecular weight conversion curves for various kinds of polymerization methods: (A) freeradical polymerization; (B) living polymerization and (C) condensation polymerization.[1]

Degree of polymerization (DP) is determined by the ratio of the concentration of monomer versus initiator (**Equation 1**). Without any termination all the active polymer chain grow at same rate and molecular weight is equal to DP. In ideal living polymerization the molecular weight is directly proportional to conversion (**Figure 1.1b**, line B). While in radical polymerization, high molecular weight polymer is formed in initial stage (**Figure 1.1b**, curve A) and in condensation polymerization high molecular weight polymer is formed only as the conversion approaches 100 % (**Figure 1.1b**, curve C).[2] When chain transfer reaction take place in polymerization, molecular weight of polymer is less than predicted DP. When inefficient initiation or chain coupling take place in polymerization, molecular weight of polymer is more than predicted DP.

$$\text{Degree of Polymerization (DP)} = \frac{[\text{monomer}]}{[\text{initiater}]} \qquad (1)$$

Another property of living polymerization is the very narrow molecular weight distribution (M_w/M_n) polymer is obtained. M_n is number average molecular weight and M_w is weight average molecular weight. The M_w/M_n is defined by Poisson distribution (**Equation 2**).[2] The M_w/M_n decreases with conversion and comes to an ideal value of 1.0 where all polymer chains have the same length. Any increase in M_w/M_n versus conversion suggest chain breaking reactions. [6]

$$\frac{M_w}{M_n} = 1 + \frac{1}{DP} = 1 + \frac{1}{\left(\frac{[M]_o}{[I]_o} \times conv\right)} \tag{2}$$

Lastly, the chain end-functionalization is demonstrated by modifying chain end to a particular group or using polymer as macroinitiator for another polymerization. The perfect or near perfect chain end-functionality is used for two application: polymer architectural controller and functionalized end group.[2]

Single Electron Transfer Living Radical Polymerization (SET-LRP)

SET-LRP mechanism is shown in **Figure 1.2**. An example of living polymerizations in which Cu(0) acts as a catalyst to activate an alkyl halide by an outer sphere electron donation (reductive dehalogenation) to radicals while Cu(II)X$_2$ acts as radical deactivator to provide a LRP. The step propagation of polymer take place by addition of monomer to grouing radical chain. Cu(I)X produced during the activation step of this reaction disproportionates into highly active Cu(0) and Cu(II)X$_2$ in the presence of a disproportioning solvent such as a polar, a protic solvent or water and a ligand that stabilizes Cu(II)X$_2$ better than Cu(I)X such as tris[2-(dimethylamino)ethyl] amine (Me$_6$-TREN) and tris(2-aminoethyl)amine (TREN). (**Figure 1.2**, **Scheme 1.2**). In atom transfer radical polymerization (ATRP), Cu(I) acts as a catalyst to activate by an inner sphere electron donation and an excess of Cu(II), which is required for deactivation, is generated by irreversible bimolecular termination to provide the persistent radical effect,[5] while in SET-LRP disproportionation rather than termination is responsible for the creation of CuX$_2$. A wide range of important polymers such as acrylates, methacrylates, acrylamides, acrylonitrile, and vinyl chloride with excellent control of molecular weight, molecular weight distribution, chain end functionality, and quantitative conversion can be synthesis by SET-LRP.[8,10,11,12]
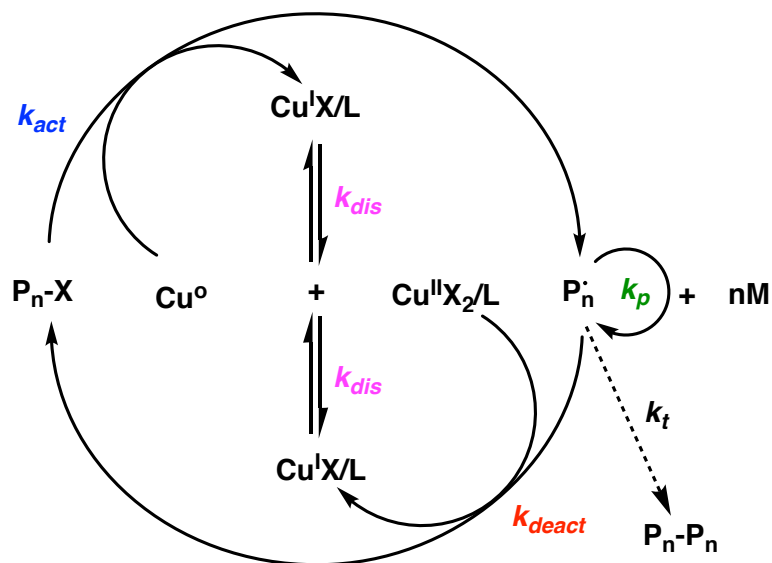
Figure 1.2. Mechanism of SET-LRP[9]

The mechanistically fundamental step in Cu(0)-mediated SET-LTP is disproportionation reaction of Cu(I)X into Cu(0) atomic species and Cu(II)X$_2$. The disproportionation either be promote or disfavor by appropriate solvent and N-ligand combination.[9-18] The frequently used ligand in SET-LRP is Tris(2-dimethylaminoethyl)amine (Me$_6$-TREN) [9,10,13], which is more expensive than its precursor tris(2-aminoethyl)amine(TREN)[9,28], because it favors the disproportionation process by preferentially binding Cu(II)X$_2$ rather than Cu(I)X.[19] However, the use of its precursor, tris(2-aminoethyl)amine (TREN),[10,20-22] which is about 80 times less expensive than Me$_6$-TREN[28], and poly(ethylene imine) (PEI)[9] also proved successful for the polymerization of vinyl chloride (VC) during the first days of SET-LRP. Likewise, TREN[23-25] and N,N,N',N'',N''-pentamethyldiethylenetriamine (PMDETA)[9,26,27] are also alternative ligands to Me$_6$-TREN for the Cu(0) wire-catalyzed SET-LRP of acrylates and methacrylates in homogeneous SET-LRP.

Solvent play an important role in disproportionation Cu(I)X and chain end functionality of polymer. Disproportionating solvents, such as dimethyl sulfoxide (DMSO), provided high chain end functionality for a SET-LRP catalyzed by Cu(0) wire, powder, coins, and other.[25,28] In nondisproportionating solvents including polar solvents like acetonitrile [29] and nonpolar solvents like toluene[26], the chain end functionality of the resulting polymers is much lower. The incompatibility of SET-LRP with polar nondisproportionating solvents and nonpolar nondisproportionating solvents was resolved designing "programmed" biphasic organic solvent-H$_2$O programmed biphasic systems to mediate the disproportionation of Cu(I)X/N-ligand, thus expanding the library of accessible solvents.[30-34]. In "programmed" biphasic, SET-LRP is an interfacial process in which disproportionation and activation events take place independently in the aqueous and organic compartments, respectively, whereas the "self-controlled" reversible deactivation occurs at the interface. [35] In previous report, the replacement of Me$_6$-TREN with TREN was not so successful in aqueous–organic "programmed" biphasic systems using Cu(0) wire catalyst, although it is very efficient in single phase SET-LRP experiments.[36-40] In biphasic organic solvent–water systems, the external addition of Cu(II)Br$_2$ was necessary to complement the performance of TREN and retain living character.[36] Large amount of Cu(II)X$_2$ decreases the chain end functionality of the polymer.[25,28,41].

The concept of mixed-ligand systems emerged as an efficient and simple methodology to obtain superior catalytic activity in transition-metal-catalyzed enantioselective reactions.[42] Nearly at the same time, Feringa's laboratory reported that heterocombinations of chiral monodentate ligands were more effective than homocombinations for Rh-catalyzed C–C cross-coupling reactions.[43] This concept was also employed for Pd-catalyzed C–N[44,45] and C–S[46] cross-coupling reactions as well as for Ni-catalyzed Suzuki-type cross-coupling and borylation reactions.[47] However, the benefits of using mixed-ligand catalysts have only been noted so far in few metal-catalyzed polymerization experiments.[48-50]

The goal of this chapter is to increase the efficiency of TREN using concept of mixed-ligand systems without addition of external Cu(II)X$_2$. The objective of this chapter is to investigated mixed-ligand concept in different solvent by changing different ligand system in reaction system. In the first series of experiments, the performance of the "programmed" biphasic SET-LRP of MA in various Me$_6$-TREN/TREN ligand ratios will be compared to

determine the efficiency mixed-ligand systems. The reaction kinetics will be measured by periodically taking a sample from the reaction mixture and analyzing it for conversion and molecular weight distribution using ^{1}H NMR and gel permeation chromatography (GPC), respectively. The solvent affects the disproportionation of Cu(I)X, hence studying the different solvents with mixed-ligands will help us determine the efficiency mixed-ligand systems. Visualization experiment will be carried out to understand the mechanism of programmed" biphasic SET-LRP. Finally, the living livingness of the polymers obtained from mixed-ligand systems will be compared to individual ligand using NMR and MALDI-TOF analysis by using thio-bromo "click" chemistry to determine the chain-end functionality of the resulting polymers.

Materials and Methods

Reagents

Methyl acrylate (MA) (99%, Acros) was passed over a short column of basic Al_2O_3 before use in order to remove the radical inhibitor. Tris(2-aminoethyl)amine (TREN) (99%, Acros), Cu(0) wire (20 gauge wire, 0.812 mm diameter from Fisher), and dimethylformamide (DMF) (99.8%, Sigma-Aldrich) were used as received. N,N-Dimethylacetamide anhydrous (DMAc) (99.8%, Sigma-Aldrich) and N-methylpyrrolidone (NMP) (99%, Sigma-Aldrich) were distilled before use. Deionized water was used in all SET-LRP experiments. Triethylamine (NEt$_3$) (>99.5% Chemimpex) was distilled under N2 over CaH2. Bis(2-bromopropionyl)ethane (BPE) was synthesized by esterification of ethylene glycol with 2-bromopropionyl bromide in the presence pyridine according to our previously reported method.[51] Hexamethylated tris(2-aminoethyl)amine (Me$_6$-TREN) was synthesized according to a literature procedure.[52]

Techniques

400 MHz ^{1}H NMR spectra were recorded on a Bruker AVANCE NEO 400 NMR instrument at 27 °C in CDCl$_3$ containing tetramethylsilane (TMS) as internal standard. Gel permeation chromatography (GPC) analysis of the polymer samples was performed using a Shimadzu LC-20AD high-performance liquid chromatograph pump, a PE Nelson Analytical 900 Series integration data station, a Shimadzu RID-10A refractive index (RI) detector, and three AM gel columns (a guard column, 500 Å, 10 μm and 104 Å, 10 μm). THF (Fisher, HPLC grade) was used as eluent at a flow rate of 1 mL/min^{-1}. The number-average (M_n) and weight-average (M_w) molecular weights of PMA samples were determined with poly(methyl methacrylate) (PMMA) standards purchased from American Polymer Standards. MALDI-TOF spectra were obtained on a Voyager DE (Applied Biosystems) instrument with a 337 nm nitrogen laser (3 ns pulse width). For all polymers, the accelerating potential was 25 kV, the grid was 92.5, the laser power was 2200–2500 a.u., and a positive ionization mode was used. The sample analysis was performed with 2-(4-hydroxyphenylazo) benzoic acid as the matrix. Solutions of the matrix (25 mg/mL in THF), NaCl (2 mg/mL in deionized H$_2$O), and polymer (10 mg/mL) were prepared separately. The solution for MALDI-TOF analysis was obtained by mixing the matrix, polymer, and salt solutions in a 5/1/1 volumetric ratio. Then 0.5 μL portions of the mixture were deposited onto three wells of sample plate and dried in air at room temperature before subjected to MALDI- TOF analysis.

Typical Procedure for SET-LRP of MA in "Programmed" Biphasic Mixtures using Mixed-Ligand Systems

Stock solutions with different ligand ratios (Me$_6$-TREN/TREN as 0.05 M/0 M, 0.0375 M/0.0125 M, 0.025 M/0.025 M, 0.0125 M/0.0375 M, 0 M/0.05 M) in water were prepared. The monomer (MA, 11.1 mmol, 1.00 mL), organic solvent (DMF, DMAc, or NMP, 0.4 mL), water stock solution (0.005 mmol Ligand, 0.1 mL), and initiator (BPE, 0.05 mmol, 16.6 mg) were added to a 25 mL Schlenk tube. The reaction mixture was then

deoxygenated by six freeze–pump–thaw cycles. After these cycles, the Schlenk tube was opened under a positive flow of nitrogen to add the Cu(0) wire wrapped around a Teflon-coated stir bar. Two more freeze–pump–thaw cycles were carried out while holding the stir bar above the reaction mixture using an external magnet. After that, the Schlenk tube was filled with N_2, and the reaction mixture was placed in a water bath at 25 °C. Then, the stir bar wrapped with the Cu(0) wire was dropped gently into the reaction mixture. The introduction of the Cu(0) wire defines t = 0. Samples were taken at different reaction times by purging the side arm of the Schlenk tube with nitrogen for 2 minutes using a deoxygenated syringe and stainless steel needles. The collected samples were dissolved in $CDCl_3$ and quenched by air bubbling. After that, the monomer conversion was measured by 1H NMR spectroscopy. In order to determine the molecular weight and polydispersity of the samples, the solvent and the residual monomer were removed under vacuum. Finally, samples were dissolved in THF and passed through a short and small basic Al_2O_3 chromatographic column to remove any residual copper and subsequently were analyzed by GPC. The resulting PMA was precipitated in cold methanol and dried under vacuum until constant weight to perform chain end analysis by ^{1}H NMR spectroscopy, before and after the thioetherification reaction.

General Procedure for the Chain End Modification of PMA via Thio-Bromo "Click" Reaction

In a 10 mL test tube sealed with a rubber septum, thiophenol (0.05 equivalents) and distilled triethylamine (NEt_3, 0.05 equivalents) were added into a solution of the corresponding polymer (0.01 equivalents) in acetonitrile (1 mL) under a nitrogen flow. The reaction mixture was stirred at room temperature for 3 hours. Then, the resulting modified PMA was precipitated in cold methanol and washed with methanol several times. The resulting modified polymers were dried under vacuum until constant weight.

Result and Discussion

The Mixed-Ligand Effect During the Biphasic SET-LRP of MA in NMP–Water Mixture using Me$_6$-TREN and TREN as Ligands

From the reported literature, the use of mixed-ligand of Me$_6$-TREN and TREN was not employed before in SET-LRP or any other metal-catalyzed LRP technique. The performance of Me$_6$-TREN and TREN was first investigate by mediating the "programmed" biphasic SET-LRP of MA in NMP- water mixture (8/2 v/v). N-methylpyrrolidone (NMP) dipolar aprotic solvent is not one of the most efficient SET-LRP solvent in homogenous solution,[53] but becomes excellent in biphasic systems with water.[34,36] The chemical structure of both ligands and a schematic illustration for the Cu(0) wire-catalyzed SET-LRP of MA initiated from the bifunctional initiator bis(2-bromopropnionyl)ethane (BPE) are depicted in **Scheme 1.1**. Triplicate kinetic experiments were performed under the following reaction conditions: [MA]$_0$/[BPE]$_0$/[L]$_0$ = 222/1/ 0.1 using 9.0 cm of nonactivated Cu(0) wire. The molar ratio between Me$_6$-TREN and TREN was varied from 1:0 to 0:1 while maintaining the total amount of ligand, relative to initiator, constant at 10 mol %.

Scheme 1.1. Biphasic SET-LRP of MA Initiated from BPE and Catalyzed with Nonactivated Cu(0) Wire Using Various Molar Combinations of Me$_6$-TREN and TREN[a]
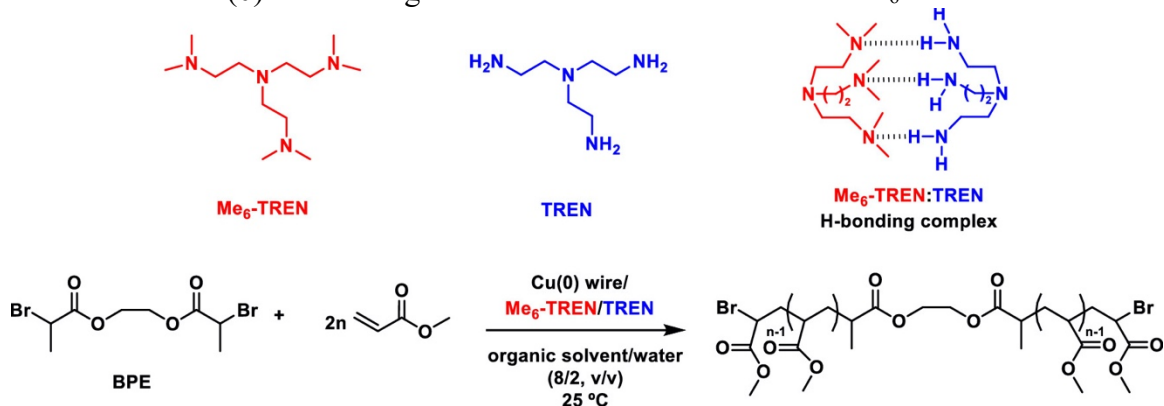
[a] Organic solvents investigated herein are NMP, DMF, and DMAc.

From **Table 1.1**, **Figure 1.3**, and **Figure 1.4a**, it was observer that any of the tested mixed ligand compositions provided higher apparent rate of polymerization ($k_p{}^{app}$) than those obtained in the control experiments performed in the presence of either Me$_6$-TREN or TREN. For example, the replacement of 2.5 mol % of Me$_6$-TREN with TREN increased the $k_p{}^{ap}$ from 0.068 min^{-1} (**Figure 1.3a**) to 0.078 min^{-1} (**Figure 1.3b**), while retaining first-order kinetics. Similar trends were observed using the inverse ligand composition (**Figure 1.3d**). Moreover, in both cases a slight increase in monomer conversion was also noted (**Appendix 1a**). Nevertheless, the superior catalytic activity was observed wherein 1:1 molar combinations of both ligands. Under these conditions, the SET-LRP of MA proceeded approximately 1.2 and 1.3-fold faster than control experiments with Me$_6$-TREN and TREN, respectively. This particular mixed-ligand system also enabled the highest monomer conversion (**Appendix 1a**). In addition, the synergistic effect between both ligands also improved the control over molecular weight distribution attained by SET-LRP.

Representative GPC data shown in **Figure 1.5** illustrate the evolution of molecular weight as a function of conversion during these experiments. GPC chromatograms revealed monomodal polymer peak distributions shifting to higher molecular weight while increasing conversion. However, significantly higher than expected M_n^{GPC} values were obtained at low conversion for the control experiment using TREN without Me$_6$-TREN (**Figure 1.5e**). When using only TREN ligands a nonlinear evolution of molecular weight was detected during the early stages of the polymerization (right panel of **Figure 1.3e**). Likewise, the broadest PMA at ultimate monomer conversion was obtained when only TREN ligands was used ($M_w/M_n = 1.39$ at 81% conversion). In previous publications, the addition of Cu(II)Br$_2$ additive was used to significantly improve molecular weight control under these conditions.[36-40] In this case, GPC analysis revealed that Me$_6$-TREN was complementary and made TREN a very efficient ligand without using the externally added Cu(II)Br$_2$. As can be seen in **Appendix 1a**, replacing only 2.5 mol % of TREN with Me$_6$-TREN improved significantly the molecular weight distribution evolution throughout polymerization (compare panels e and d of **Figure 1.3**). As expected, increasing further the amount of hexamethylated ligand resulted in a better-defined polymer (**Appendix 1a**). Note that the average M_w/M_n was below 1.2 using the equimolar combination of ligands (**Figure 1.3,1.4** and **Table 1.1**). Meanwhile, whereas initiator efficiency (I_{eff}) was around 75% for both control experiments, the use of mixed-ligand systems significantly enhanced this value (**Figure 1.3** and **Table 1.1**). Again, the most important effect was observed at 1:1 molar ratio between ligands. In this case, the I_{eff} was determined to be above 90%. Overall, these results demonstrate that the mixed-ligand catalytic system consisting of nonactivated Cu(0) wire and Me$_6$-TREN/TREN is an effective catalyst for the SET-LRP of MA under biphasic reaction conditions.

Table 1.1. Dependence of k_p^{app} on the Dimension of the Cu(0) Wire in the SET-LRP of MA Initiated with BPE in NMP/water(8/2,v/v) at 25 °C[a]

entry	Wire length (cm) 20G	Reaction conditions	k_p^{app} (min^{-1})	k_p^{app}/k_p^{app}(TREN)	M_w/M_n	I_{eff}(%)
1	9.0	[MA]/[BPE]/[Me$_6$-TREN] 222/1/0.1	0.068	1.1	1.08	75
2	9.0	[MA]/[BPE]/[Me$_6$-TREN]/[TREN] 222/1/0.075/0.025	0.078	1.3	1.15	87
3	9.0	[MA]/[BPE]/[Me$_6$-TREN]/[TREN] 222/1/0.05/0.05	0.080	1.3	1.18	85
4	9.0	[MA]/[BPE]/[Me$_6$-TREN]/[TREN] 222/1/0.025/0.075	0.076	1.3	1.21	96
5	9.0	[[MA]/[BPE]/[TREN] 222/1/0.1	0.060	1.0	1.42	77

[a]Reaction conditions: monomer = 1 mL; solvent + water = 0.5 mL. The v/v ratio must be multiplied by 10 to obtain % solvent/% water. The value of v + v must be divided by 20 to obtain the total volume of solvents, 0.5 mL.
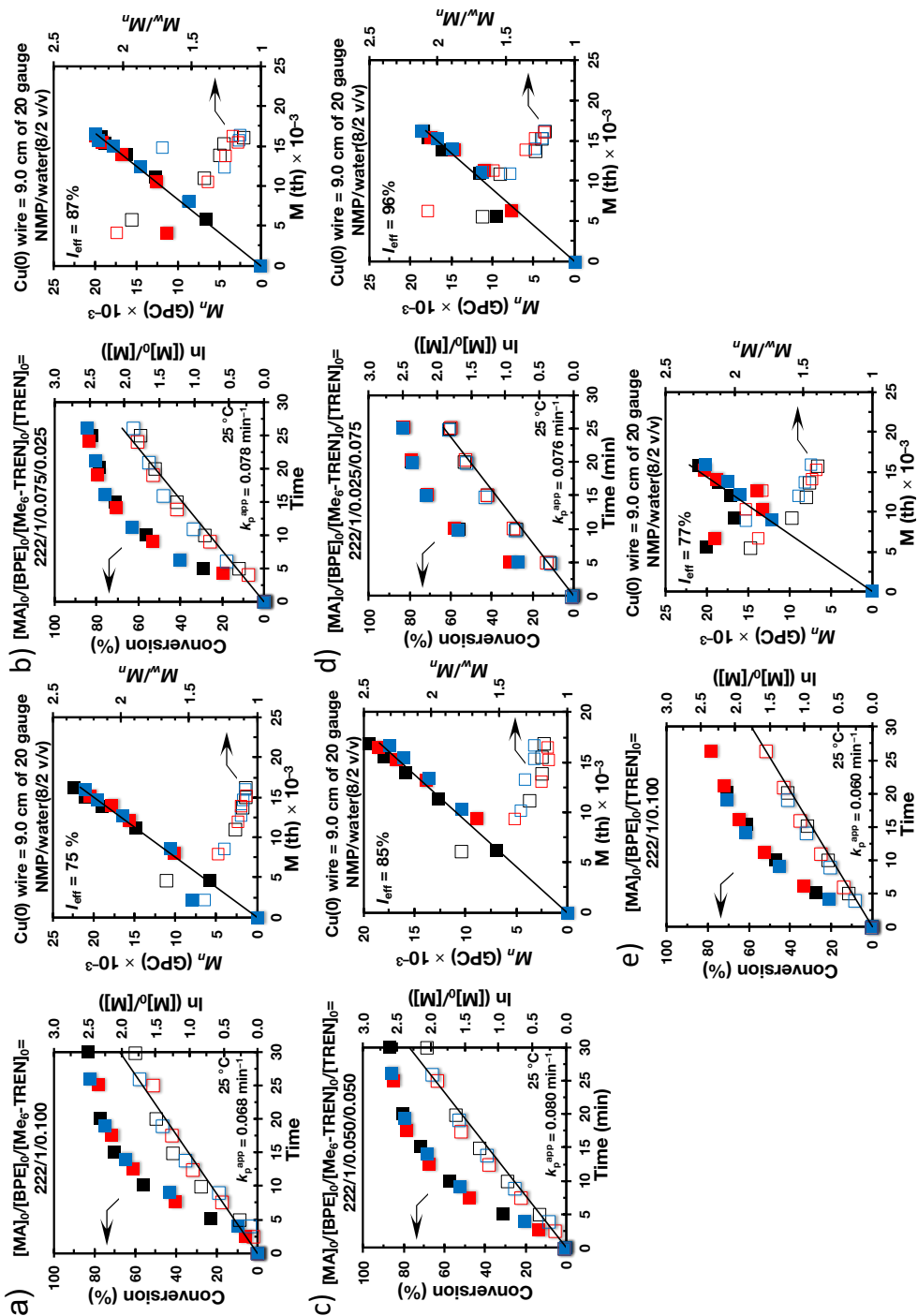
Figure 1.3. Kinetic plots, molecular weight, and polydispersity evolution for the SET-LRP of MA in NMP/water mixture (8/2, v/v) initiated with BPE and catalyzed by the 9.0 cm nonactivated Cu(0) wire at 25 °C. Experimental data in different colors were obtained from different kinetics experiments sometimes performed by different researches. k_p^{app} and I_{eff} are the average values of three experiments. Reaction conditions: MA = 1 mL, NMP = 0.4 mL, water = 0.1 mL, $[MA]_0/[BPE]_0/[L]_0 = 222/1/0.1$.

10
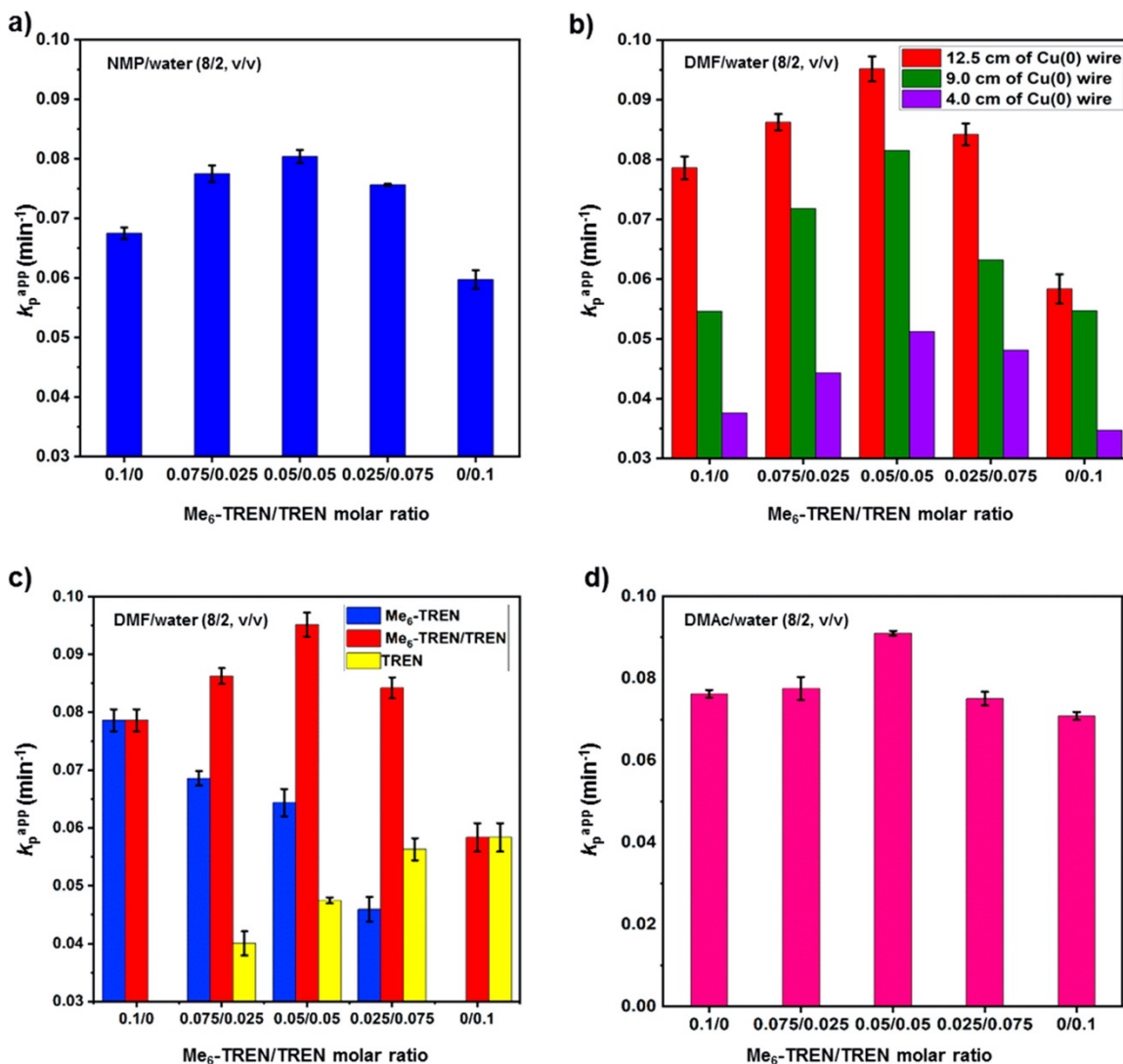
Figure 1.4. Evolution of k_p^{app} for the SET-LRP of MA initiated with BPE in various "programmed" biphasic reaction mixtures at 25 °C. (a) NMP/water mixture (8/2, v/v) using 9.0 cm nonactivated Cu(0) wire as catalyst. (b) DMF/water mixture (8/2, v/v) using 12.5, 9.0, and 4.0 cm of nonactivated Cu(0) wire as catalyst. (c) DMF/water mixture (8/2, v/v) using 12.5 cm of nonactivated Cu(0) wire as catalyst and (d) DMAc/water mixture (8/2, v/v) using 9.0 cm of nonactivated Cu(0) wire as catalyst. Reaction conditions: MA = 1 mL, organic solvent = 0.4 mL, water = 0.1 mL, and $[MA]_0/[BPE]_0/[L]_0$ = 222/1/0.1 (a,b, and d) $[MA]_0/[BPE]_0/[L]_0$ = 222/1/0.1–0.0 (c).

a) [Me$_6$-TREN]$_0$/[TREN]$_0$ = 0.1/0

M_n (th) = 4,720
M_n (GPC) = 5,770
M_w/M_n = 1.66

M_n (th) = 11,120
M_n (GPC) = 14,830
M_w/M_n = 1.16

M_n (th) = 16,260
M_n (GPC) = 22,470
M_w/M_n = 1.08

— 23%
— 56%
— 83%

b) [Me$_6$-TREN]$_0$/[TREN]$_0$ = 0.075/0.025

M_n (th) = 5,860
M_n (GPC) = 6,640
M_w/M_n = 1.92

M_n (th) = 11,130
M_n (GPC) = 12,750
M_w/M_n = 1.40

M_n (th) = 16,120
M_n (GPC) = 19,190
M_w/M_n = 1.12

— 44%
— 58%
— 74%

c) [Me$_6$-TREN]$_0$/[TREN]$_0$ = 0.05/0.05

M_n (th) = 6,250
M_n (GPC) = 7,020
M_w/M_n = 1.77

M_n (th) = 14,030
M_n (GPC) = 15,910
M_w/M_n = 1.17

M_n (th) = 16,950
M_n (GPC) = 19,490
M_w/M_n = 1.16

— 31%
— 72%
— 87%

d) [Me$_6$-TREN]$_0$/[TREN]$_0$ = 0.025/0.075

M_n (th) = 6,280
M_n (GPC) = 7,750
M_w/M_n = 2.07

M_n (th) = 13,940
M_n (GPC) = 14,750
M_w/M_n = 1.35

M_n (th) = 16,180
M_n (GPC) = 18,660
M_w/M_n = 1.22

— 31%
— 71%
— 83%

e) [Me$_6$-TREN]$_0$/[TREN]$_0$ = 0/0.1

M_n (th) = 5,560
M_n (GPC) = 19,960
M_w/M_n = 1.87

M_n (th) = 11,910
M_n (GPC) = 17,180
M_w/M_n = 1.47

M_n (th) = 15,790
M_n (GPC) = 20,890
M_w/M_n = 1.39

— 27%
— 60%
— 81%

Figure 1.5. Representative GPC traces of the evolution of molecular weight as a function of conversion for the SET-LRP of MA in a mixture of NMP/water (8/2, v/v) and catalyzed by the 9.0 cm nonactivated Cu(0) wire at 25 °C in the presence of various ligand compositions. Reaction conditions: MA = 1 mL, NMP = 0.4 mL, water = 0.1 mL, [MA]$_0$/[BPE]$_0$/[L]$_0$ = 222/1/0.1.

The Mixed-Ligand Effect During the Biphasic SET-LRP of MA in DMF–Water Mixture using Me$_6$-TREN and TREN as Ligands

The accuracy of the trend disclosed above was tested with an additional set of control experiments using different Cu(0) wire lengths in a DMF-water mixture (8/2, v/v). Thus, the SET-LRP of MA was investigated using wire lengths of 12.5, 9.0, and 4.0 cm while maintaining the rest of the polymerization conditions unchanged (**Figure 1.4**). **Appendix 2–4** show the corresponding kinetic plots and evolution of experimental M_n and M_w/M_n versus theoretical M_{th}. Kinetic experiments using 9.0 cm of nonactivated Cu(0) wire showed the same trend (**Figure 1.4b**, green columns) as in the case of **Figure 1.4a**. The biphasic SET-LRP of MA in a DMF/water (8/2, v/v) mixture was faster using mixed-ligand systems. However, again, the highest k_p^{app} and I$_{eff}$ values were observed at 1:1 molar ratio of Me$_6$-TREN and TREN (**Table 1.2**). Under these conditions, SET-LRP was approximately 1.5-fold faster than the control experiment with either Me$_6$-TREN or TREN. Indeed, monomer conversion was also slightly improved when the mixed-ligand systems 0.075/0.025 (82%) and 0.05/0.05 (87%) were used (**Table 1.2** entry 7 and 8). Mixed-ligand effects were also noted for the polymerization using 12.5 and 4.0 cm of Cu(0) wire. Previous reports demonstrated that SET-LRP catalysts utilize a surface-mediated activation.[29,54] Accordingly, the use of 12.5 cm of Cu(0) wire provided the faster series of polymerizations, whereas with the shortest wire length reactions were slower (**Figure 1.4b**, red and purple columns, respectively). For example, at the 1:1 molar ratio between ligands, the k_p^{app} values decrease as follows, 0.095 min^{-1} (12.5 cm), 0.082 min^{-1} (9.0 cm), and 0.051 min^{-1} (4.0 cm) (**Table 1.2** entry 3, 8 and 13). Nevertheless, the evolution of k_p^{app} values as a function of ligand ratio reiterates again the benefit of employing a combination of both ligands. These results suggest the existence of an optimum molar ratio between ligands. Accordingly, both monomer conversion and I_{eff} also showed higher values in the mixed-ligand systems for the polymerization using 4.0 cm of Cu(0) wire. However, the highest amount of catalyst did not provide a clear trend (compare **Appendix 1b,c** with **Appendix 1d**).

An additional set of control experiments were performed to highlight the occurrence of fast exchange between the two ligands at all compositions (**Figure 1.4c**). The SET-LRP of MA was investigated using decreasing ligand loading using either Me$_6$-TREN or TREN and no coligand. The corresponding kinetic plots are shown in **Appendix 5**, panels a-c (Me$_6$-TREN) and **Appendix 5**, panels d-f (TREN). The control experiments from **Figure 1.4c** demonstrate both for the case of TREN (yellow colored experiments) and of Me$_6$-TREN (blue colored experiments) a continuous decrease of the rate of polymerization as the concentration of the ligand decreases. These experiments contrast the experiments in which mixed-ligand with identical compositions as the single ligands are used (see red colored experiments). In these series of experiments an increase in rate is obtained as the ratio between the two ligands tends to approach the 1/1 ratio. This trend demonstrates the mixed-ligand effect. The fact that the most important effects have been systematically observed at a 1/1 molar ratio suggests that in addition to a fast exchange between the two ligands, a new single dynamic ligand generated by H-bonding should be considered in future mechanistic investigations (**Scheme 1.1**).

The interaction between both ligands was confirmed by ^{1}H NMR analysis of their equimolar mixture prepared in CDCl$_3$. **Figure 1.6** shows that signal corresponding to amine protons of TREN shifts downfield (0.15 ppm) and becomes broader in the presence of Me$_6$-TREN, suggesting the formation of a more rigid complex than TREN or Me$_6$-TREN.

Table 1.2. Dependence of k_p^{app} on the Dimension of the Cu(0) Wire in the SET-LRP of MA Initiated with BPE in DMF/water(8/2,v/v) at 25 °C^a

entry	Wire length (cm)	Reaction conditions	k_p^{app} (min^{-1})	k_p^{app}/k_p^{app}(TREN)	M_w/M_n	I_{eff}(%)
1	12.5	[MA]/[BPE]/[Me$_6$-TREN] 222/1/0.1	0.079	1.4	1.12	79
2	12.5	[MA]/[BPE]/[Me$_6$-TREN]/[TREN] 222/1/0.075/0.025	0.086	1.5	1.14	78
3	12.5	[MA]/[BPE]/[Me$_6$-TREN]/[TREN] 222/1/0.05/0.05	0.095	1.6	1.21	78
4	12.5	[MA]/[BPE]/[Me$_6$-TREN]/[TREN] 222/1/0.025/0.075	0.084	1.4	1.23	80
5	12.5	[[MA]/[BPE]/[TREN] 222/1/0.1	0.058	1.0	1.36	79
6	9.0	[MA]/[BPE]/[Me$_6$-TREN] 222/1/0.1	0.055	1.0	1.09	76
7	9.0	[MA]/[BPE]/[Me$_6$-TREN]/[TREN] 222/1/0.075/0.025	0.057	1.0	1.08	82
8	9.0	[MA]/[BPE]/[Me$_6$-TREN]/[TREN] 222/1/0.05/0.05	0.082	1.5	1.09	87
9	9.0	[MA]/[BPE]/[Me$_6$-TREN]/[TREN] 222/1/0.025/0.075	0.063	1.1	1.13	78
10	9.0	[[MA]/[BPE]/[TREN] 222/1/0.1	0.055	1.0	1.25	66
11	4.0	[MA]/[BPE]/[Me$_6$-TREN] 222/1/0.1	0.038	1.1	1.14	81
12	4.0	[MA]/[BPE]/[Me$_6$-TREN]/[TREN] 222/1/0.075/0.025	0.044	1.3	1.14	82
13	4.0	[MA]/[BPE]/[Me$_6$-TREN]/[TREN] 222/1/0.05/0.05	0.051	1.4	1.16	86
14	4.0	[MA]/[BPE]/[Me$_6$-TREN]/[TREN] 222/1/0.025/0.075	0.048	1.4	1.28	66
15	4.0	[[MA]/[BPE]/[TREN] 222/1/0.1	0.035	1.0	1.40	51

^{a}Reaction conditions: monomer = 1 mL; solvent + water = 0.5 mL. The v/v ratio must be multiplied by 10 to obtain % solvent/% water. The value of v + v must be divided by 20 to obtain the total volume of solvents, 0.5 mL.
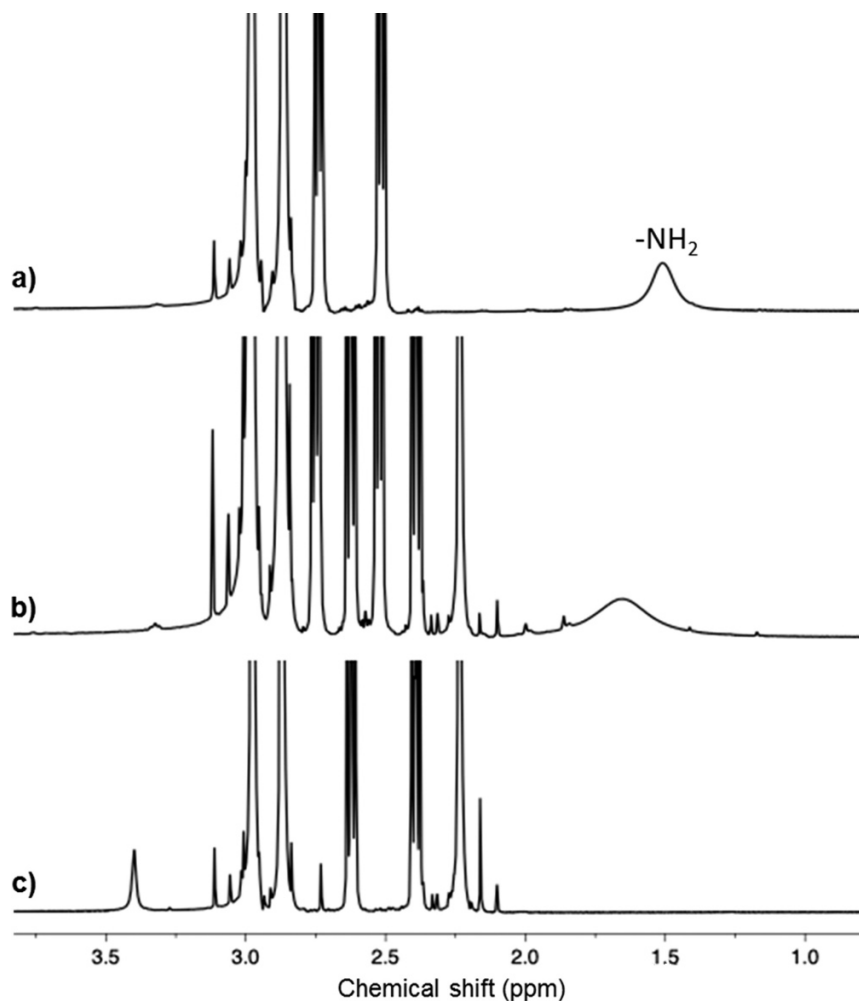
Figure 1.6. ^{1}H NMR spectra at 400 MHz of (a) TREN, (b) 1:1 molar ratio mixture of TREN and Me$_6$-TREN, and (c) Me$_6$-TREN in CDCl$_3$ at 25 °C.

The Mixed-Ligand Effect During the Biphasic SET-LRP of MA in DMAc–Water Mixture using Me$_6$-TREN and TREN as Ligands

In the last series of kinetics, it was examined the solvent screening with a DMAc-water mixture also at 8/2 (v/v). The SET-LRP of MA was investigated using only 9.0 cm of nonactivated Cu(0) wire. In this case, all the tested compositions showed two first-order kinetic regimes with a slower second domain (**Appendix 6**). The same behavior was previously observed during the homogeneous SET-LRP of MA in DMAc with lower loadings of water.[53] On the basis of previous reports, this result may be attributed to rapid activation combined with insufficient disproportionation, which favors bimolecular termination events between growing chains. Nevertheless, even under these conditions, the 1:1 molar ratio of Me$_6$-TREN and TREN provided the fastest polymerization (**Figure 1.4d** and **Table 1.3**). Moreover, I_{eff} values also were higher for mixed-ligand systems, but no clear trend was observed on monomer conversion (**Appendix 1e**). As in all previously tested systems, with the transition from TREN to Me$_6$-TREN, the resulting PMA showed narrower molecular weight distribution (**Appendix 6** and **Table 1.3**).

15

Table 1.3. Dependence of k_p^{app} on the Dimension of the Cu(0) Wire in the SET-LRP of MA Initiated with BPE in DMAc/water(8/2,v/v) at 25 °C[a]

entry	Wire length (cm)	Reaction conditions	k_p^{app} (min^{-1})	k_p^{app}/k_p^{app}(TREN)	M_w/M_n	I_{eff}(%)
1	9.0	[MA]/[BPE]/[Me$_6$-TREN] 222/1/0.1	0.076	1.1	1.11	78
2	9.0	[MA]/[BPE]/[Me$_6$-TREN]/[TREN] 222/1/0.075/0.025	0.077	1.1	1.16	83
3	9.0	[MA]/[BPE]/[Me$_6$-TREN]/[TREN] 222/1/0.05/0.05	0.091	1.3	1.29	87
4	9.0	[MA]/[BPE]/[Me$_6$-TREN]/[TREN] 222/1/0.025/0.075	0.075	1.0	1.36	87
5	9.0	[[MA]/[BPE]/[TREN] 222/1/0.1	0.071	1.0	2.14	60

[a]Reaction conditions: monomer = 1 mL; solvent + water = 0.5 mL. The v/v ratio must be multiplied by 10 to obtain % solvent/% water. The value of v + v must be divided by 20 to obtain the total volume of solvents, 0.5 mL.
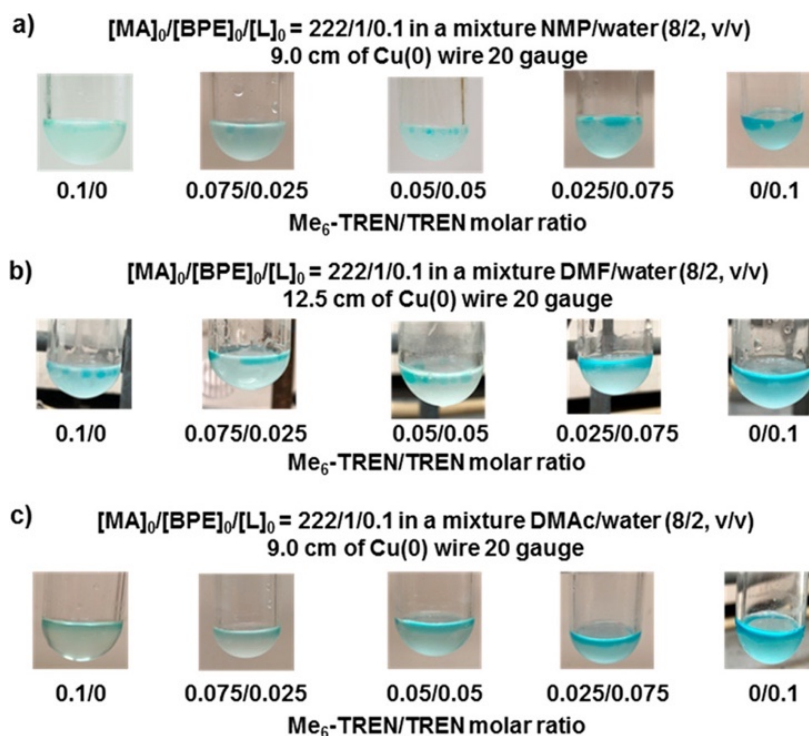
Figure 1.7. Visualization of the reaction mixture after the biphasic SET-LRP of MA initiated with BPE using various ligand compositions. (a) NMP/water (8/2, v/v), (b) DMF/water (8/2, v/v), and (c) DMAc/water (8/2, v/v). Reaction conditions: MA = 1 mL, organic solvent = 0.4 mL, water = 0.1 mL, [MA]$_0$/[BPE]$_0$/[L]$_0$ = 222/1/0.1.

Visualization of the Reaction Mixtures at the End of the Polymerization: How Biphasic SET-LRP Takes Place?

NMP, DMF, and DMAc are dipolar aprotic solvents miscible with water. However, irrespective of the ligand or mixture of ligands used, the SET-LRP of MA in aqueous mixtures of these solvents containing 20% water proceeds under biphasic reaction

16

conditions as can be seen in the series of digital images recorded at the end of the polymerizations (**Figure 1.7**).

Note that these biphasic reaction mixtures are "programmed" by the partition of the Cu(I)Br/mixed-ligand generated during the activation step in the organic phase, to the water phase, where it disproportionates into atomic Cu(0) and Cu(II)Br$_2$. Under these conditions, dissociation of I-X and P$_n$-X is achieved in the organic phase through a heterolytic outer-sphere SET-process wherein the outer sphere electron donor Cu(0) transfers an electron to I-X/P$_n$-X resulting, depending of the structure of the initiator, in a radical anion [P$_n$/P-X]$^{•-}$, which degrades in a stepwise or concerted pathway to P$_n^{•\delta+}$ and X$^-$ (**Scheme 1.2**).[11-13] Detailed mechanism and definitions by both IUPAC Organic and Electrochemistry Divisions were discussed in previous reviews. [11-13]

Scheme 1.2. Schematic Representation of Cu(0)-Catalyzed SET-LRP in Organic-Water "Programmed" Biphasic Reaction Mixtures[a]

Organic phase containing solvent, monomer, polymer and "free" Cu(0) nanoparticles.

Aqueous phase containing Cu(I)X/L$_1$/L$_2$ which instantaneously disporportionates into atomic Cu(0) and Cu(II)X$_2$/L$_1$/L$_2$, traces of monomer and organic solvent. Excess "nascent" atomic Cu(0) that did not activate nucleates and grow on the existing Cu(0) surface (e.g. powder, wire, plates,...).

Interphase between organic and aqueous phases where deactivation process takes place.

[a]Color code: organic phase, green; aqueous phase, blue; interphase, red.

Subsequently, Cu(I)X species generated during or after the SET event, are partitioned from the organic phase into the aqueous phase associated with an N-ligand. This process is determined by the much higher solubility of Cu(I)X/L in the aqueous phase rather than in

organic phase. In the water phase, the Cu(I)X/L species quantitatively disproportionate (equilibrium constant for disproportionation, $K_{disp} = 0.89 \times 10^6$–$5.8 \times 10^7$)[55,56] to generate the atomic Cu(0) activator and Cu(II)X$_2$/L deactivator. While water is miscible with dipolar aprotic solvents, the solution of Cu(II)Br$_2$/L in water is not miscible with the solution of the dipolar aprotic solvent containing MA. This immiscibility is responsible for the transition from a single-phase reaction mixture to a biphasic reaction mixture. Cu(0) atomic species activate the dormant species, and the excess of Cu(0) nucleates and grows on the existing Cu(0) surface (e.g., powder, wire, plates, etc.),[57] increasing its area and therefore the reactivity of the original Cu(0) surface. Propagation takes place in the organic phase via the addition of the monomer to the growing radicals. However, the Cu(II)X$_2$-mediated deactivation of the propagating macroradicals is thought to occur at the interphase between organic and aqueous phase via reverse outer-sphere oxidation of P$_n$• to P$_n$-X (**Scheme 1.2**). Accordingly, after SET-LRP, the organic phase consisting mainly of PMA and residual monomer dissolved in the organic solvent was almost colorless, whereas the water droplets were bluish because they contain Cu(II)Br$_2$/L complexes with only some traces of organic solvent and monomer (**Figure 1.7**). The images in **Figure 1.7** also revealed a slight increase in the blue color of the water phase as the concentration of TREN increases. This trend may indicate a negligible increase in the extent of bimolecular termination that is too low to be detected by NMR and MALDI-TOF analysis experiments. A similar color change going from Me$_6$-TREN to TREN was observed during the control experiments using ethyl acetate instead of MA (**Appendix 7**). [EA]$_0$ in **Appendix 7** refers to ethyl acetate that has been used as a nonreactive model for methyl acrylate.

Structural Analysis of PMA before and after Thio-Bromo "Click" Functionalization

A combination of 400 MHz ^{1}H NMR and MALDI-TOF measurements before and after reacting -Br end-groups of PMA with thiophenol via thio-bromo "click" reaction[58,59] were used to assess the livingness of polymers prepared using various molar ratios between Me$_6$-TREN and TREN. Low molar mass polymers were prepared using the three above investigated "programmed" biphasic mixtures targeting SET-LRP of MA at a [MA]$_0$/[BPE]$_0$ = 60. **Figure 1.8** shows representative ^{1}H NMR spectra of PMA samples isolated at high conversion after biphasic SET-LRP in DMF/water mixture (8/2, v/v) using 1:0, 1:1, and 0:1 molar ratios of Me$_6$-TREN and TREN.

Within the experimental error, the integral of signal c, corresponding to the CH$_3$- groups of the middle-chain initiator residue, and signal a,k, corresponding to the middle-chain CH$_2$ groups and CH-Br end-groups, did not provide any evidence of termination events. Irrespective of the ligand composition, the bromine chain-end functionality was in all cases >98% at monomer conversion >90%.
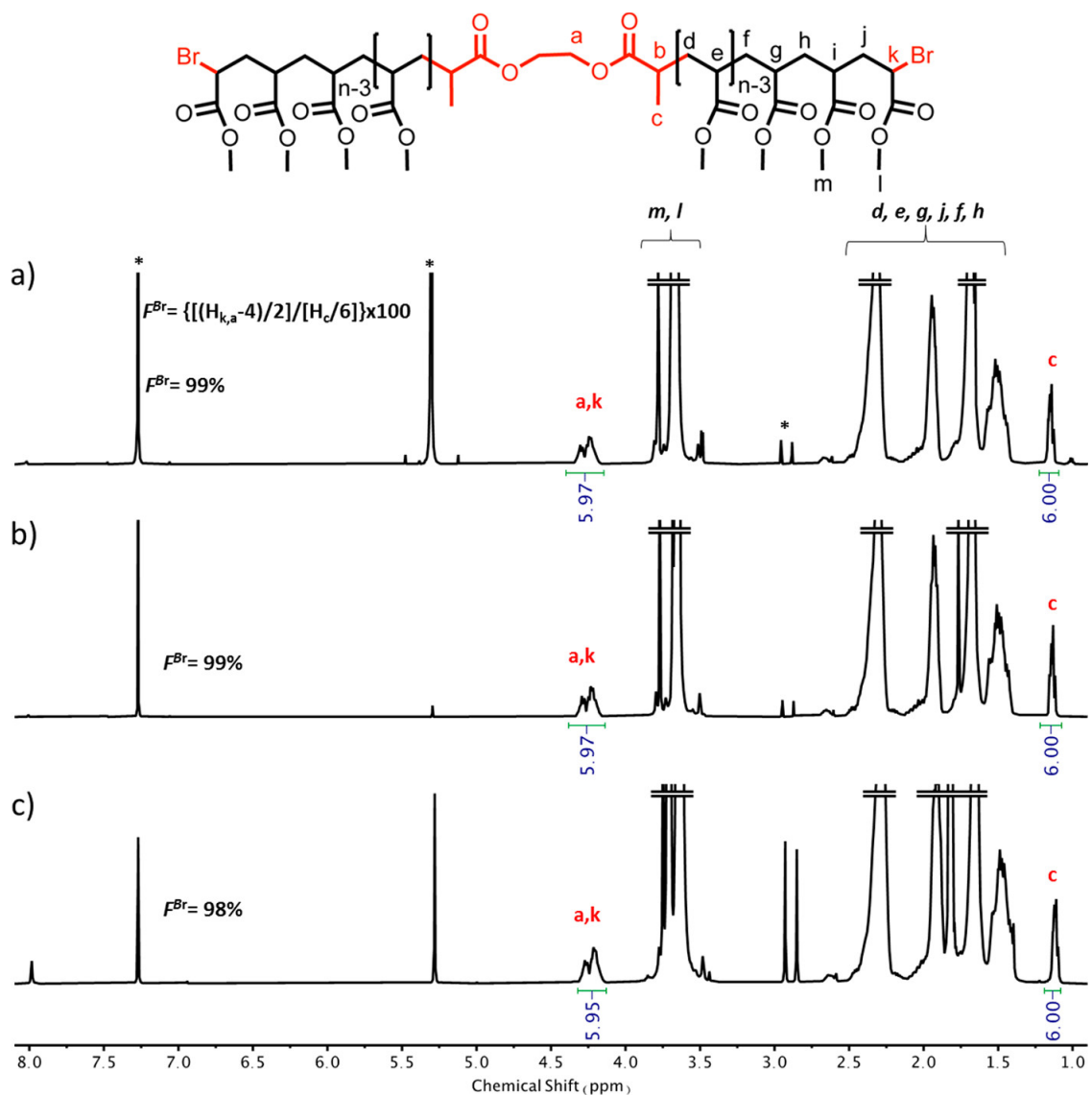
Figure 1.8. ^1H NMR spectra at 400 MHz of α,ω-di(bromo)PMA at (a) 93% monomer conversion ($M_n = 6480$ and $M_w/M_n = 1.14$) ([MA]$_0$/[BPE]$_0$/[Me$_6$-TREN]$_0$ = 60/1/0.1); (b) 91% monomer conversion ($M_n = 6100$ and $M_w/M_n = 1.25$) ([MA]$_0$/[BPE]$_0$/[Me$_6$-TREN]$_0$/[TREN]$_0$ = 60/1/0.05/0.05); (c) 94% monomer conversion ($M_n = 5990$ and $M_w/M_n = 1.25$) ([MA]$_0$/[BPE]$_0$/[TREN]$_0$ = 60/1/0.1). Polymerization conditions: MA = 1 mL, DMF = 0.4 mL, water = 0.1 mL using 12.5 cm of nonactivated Cu(0) wire 20-gauge wire. ^1H NMR resonances from residual solvents are indicated with *.

a) PMA before thioetherification

Conversion = 91%
M_{th} = 5028
$M_{n,GPC}$ = 6096; M_w/M_n = 1.25
$M_{n,MALDI}$ = 3982; M_w/M_n = 1.17

b) PMA after thioetherification

Conversion = 91%
M_{th} = 5028
$M_{n,GPC}$ = 8259; M_w/M_n = 1.17
$M_{n,MALDI}$ = 4932; M_w/M_n = 1.08
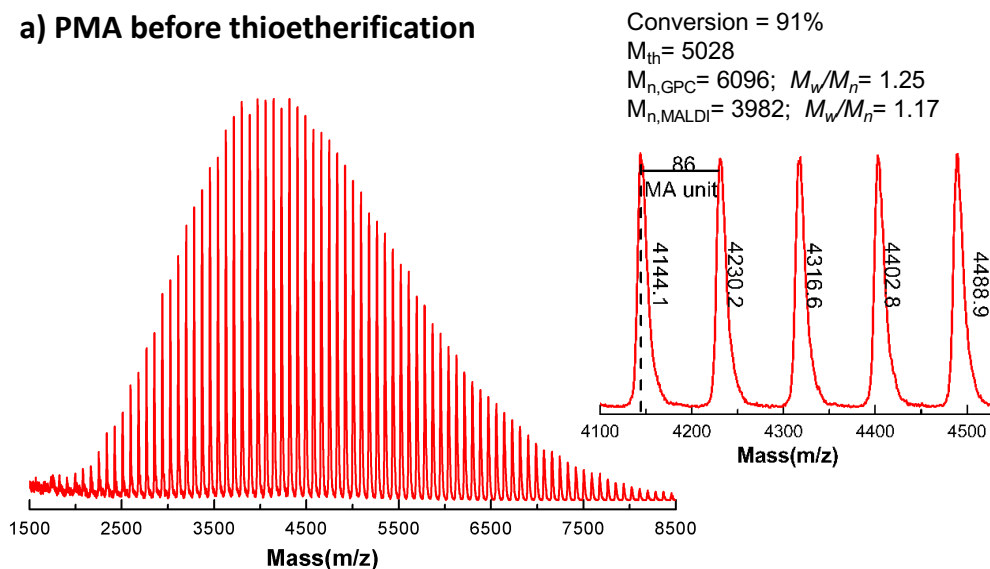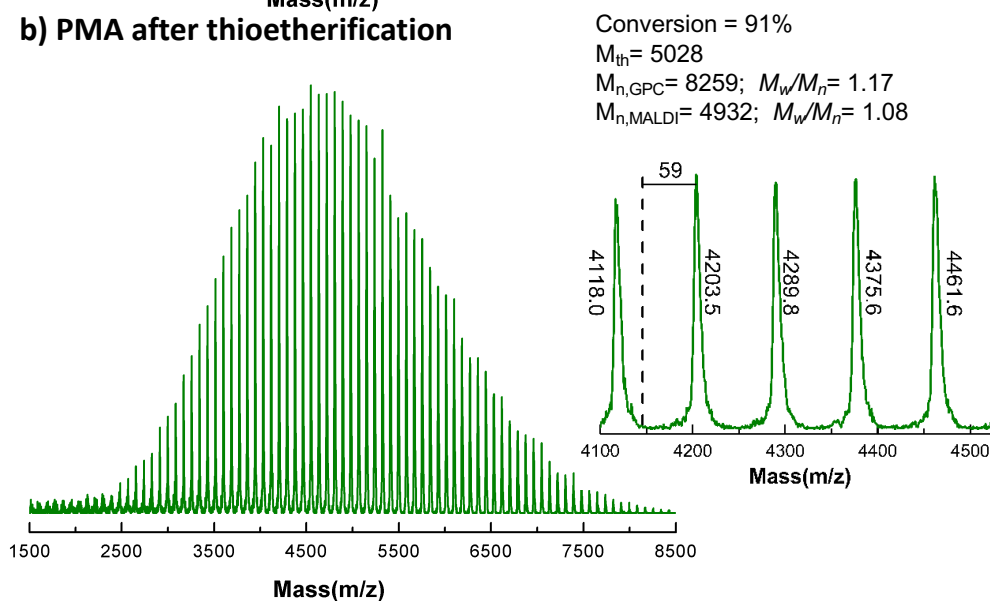
Figure 1.9. MALDI-TOF of α,ω-di(bromo)PMA isolated at 91% monomer conversion from SET-LRP of MA in DMF/water (8/2, v/v) mixture initiated with BPE and catalyzed by nonactivated Cu(0) wire at 25 °C: (a) before and (b) after "thio-bromo "click". Polymerization conditions: MA = 1 mL, DMF = 0.4 mL, water = 0.1 mL using 12.5 cm of nonactivated Cu(0) wire 20-gauge wire ([MA]$_0$/[BPE]$_0$/[TREN]$_0$ = 60/1/0.05/0.05). The dotted line in expansion after thioetherification shows the original peak from before thioetherification, while 58 represents the increase in molar mass after thioetherification i.e., 2x[SPh (109. 2) – Br (79.9)] = 58.57 for each chain end.

The chain-end functionality of PMA calculated after thio-bromo "click" reaction with thiophenol also supports the near perfect functionality of the synthesized PMA (**Appendix 8**). The MALDI-TOF analysis of the prepared samples was also consistent with these results. **Figure 1.9** depicts representative MALDI-TOF spectra of PMA synthesized using equimolar amounts of Me_6-TREN and TREN analyzed before and after the thioetherification reaction. The polymer isolated after SET-LRP showed one distribution which can be assigned to the corresponding bromine-terminated polyacrylate chains ionized with Na^+. After thioetherification with thiophenol, the original series of peaks vanished and appeared 59 mass units above. This is the expected mass difference value considering the replacement of -Br atoms (2×79.9) by -SPh moieties (2×109.2) at both polymer chain-ends. MALDI-TOF analysis of PMA prepared using Me_6-TREN and TREN showed also high levels of chain end functionality (**Appendix 9** and **Appendix 10**, respectively). Likewise, equivalent samples prepared in NMP/water and DMAc/water (8/2, v/v) mixtures provided also evidence of chain-end functionality close to 100% in all cases (see **Appendix 11– Appendix 20**).

Conclusion

The use of TREN and Me$_6$-TREN mixed-ligand system to mediate the Cu(0) wire-catalyzed SET-LRP MA in various "programmed" biphasic mixtures based on dipolar aprotic solvents and water is reported. Kinetic data and chain end analysis demonstrate that Me$_6$-TREN can complement and make TREN a very efficient ligand in the absence of externally added Cu(II)Br$_2$. During the SET-LRP of MA in 8/2 (v/v) aqueous mixtures of NMP, DMF, and DMAc with H$_2$O the use of the mixed-ligand system demonstrated an enhanced rate of polymerization, monomer conversion, and molecular weight control. The fact that the most important effect is observed at 1/1 molar ratio between ligands suggests that in addition to a fast exchange between the two ligands, a new single dynamic ligand generated by hydrogen-bonding should be considered in future mechanistic investigations. The rate of polymerization at 1/1 molar ratio between the two ligands is higher than that obtained with each of the individual ligand at the same molar concentration. At the same time, SET-LRP experiments performed in biphasic systems with H$_2$O do not require the use of the activated Cu(0) wire. The high chain end functionality generated in the absence of externally added Cu(II)Br$_2$ makes the SET-LRP in the presence of the mixed-ligand the method of choice for the synthesis of biomacromolecules.

References

(1)   Feng, X.; Maurya, D. S.; Bensabeh, N.; Moreno, A.; Oh, T.; Luo, Y.; Lejnieks, J.; Galià, M.; Miura, Y.; Monteiro, M. J.; Lligadas, G.; Percec, V. Replacing Cu(II)Br$_2$ with Me$_6$-TREN in Biphasic Cu(0)/TREN Catalyzed SET-LRP Reveals the Mixed-Ligand Effect. *Biomacromolecules* **2020**, *21*, 250– 261.

(2)   Webster, O. W. Living Polymerization Methods. Science **1991**, *251*, 887–894.

(3)   a) Grubbs, R. B.; Grubbs, R. H. 50th Anniversary Perspective: Living Polymerization—Emphasizing the Molecule in Macromolecules. *Macromolecules* **2017**, *50*, 6979–6997. b) Flory, P. J. Molecular Size Distribution in Ethylene Oxide Polymers. J. Am. Chem. Soc. **1940**, *62*, 1561−1565.

(4)   Ziegler, K. Die Bedeutung der alkalimetallorganischen Verbindungen für die Synthese. Angew. Chem. **1936**, *49*, 499−502.

(5)   Szwarc, M. "Living" Polymers. Nature **1956**, *178*, 1168−1169.

(6)   Matyjaszewski, K. General Concepts and History of Living Radical Polymerization.vIn Handbook of Radical Polymerization; John Wiley & Sons, Inc.: Hoboken, NJ, USA, 2002; pp 361–406.

(7)   Fischer, H. The Persistent Radical Effect: A Principle for Selective Radical Reactions and Living Radical Polymerizations. *Chem. Rev.* **2001**, *101* (12), 3581–3610.

(8)   Lligadas, G.; Grama, S.; Percec, V. Recent Developments in the Synthesis of Biomacromolecules and Their Conjugates by Single Electron Transfer–Living Radical Polymerization. *Biomacromolecules* **2017**, *18* (4), 1039–1063.

(9)   Percec, V.; Guliashvili, T.; Ladislaw, J. S.; Wistrand, A.; Stjerndahl, A.; Sienkowska, M. J.; Monteiro, M. J.; Sahoo, S. Ultrafast Synthesis of Ultrahigh Molar Mass Polymers by Metal-Catalyzed Living Radical Polymerization of Acrylates, Methacrylates, and Vinyl Chloride Mediated by SET at 25 °C. *J. Am. Chem. Soc.* **2006**, *128*, 14156– 14165.

(10)   Percec, V.; Popov, A. V.; Ramirez-Castillo, E.; Monteiro, M.; Barboiu, B.; Weichold, O.; Asandei, A. D.; Mitchell, C. M. Aqueous Room Temperature Metal-Catalyzed Radical Polymerization of Vinyl Chloride. *J. Am. Chem. Soc.* **2002**, *124*, 4940– 4941.

(11)   Rosen, B. M.; Percec, V. Single-Electron Transfer and Single-Electron Transfer Degenerative Chain Transfer Living Radical Polymerization. *Chem. Rev.* **2009**, *109*, 5069– 5119.

(12)   Zhang, N.; Samanta, S. R.; Rosen, B. M.; Percec, V. Single Electron Transfer in Radical Ion and Radical-Mediated Organic, Materials and Polymer Synthesis. *Chem. Rev.* **2014**, *114*, 5848– 5958.

(13)   Lligadas, G.; Grama, S.; Percec, V. Single-Electron Transfer Living Radical Polymerization Platform to Practice, Develop and Invent. *Biomacromolecules* **2017**, *18*, 2981– 3008.

(14)   Boyer, C.; Corrigan, N. A.; Jung, K.; Nguyen, D.; Nguyen, T. K.; Adnan, N. N.; Oliver, S.; Shanmugam, S.; Yeow, J. Copper-Mediated Living Radical Polymerization (Atom Transfer Polymerization and Copper(0) Mediated Polymerization): From Fundamentals to Bioapplications. *Chem. Rev.* **2016**, *116*, 1803– 1949.

(15) Anastasaki, A.; Nikolaou, V.; Nurumbetov, G.; Wilson, O.; Kempe, K.; Quinn, J. F.; Davis, T. P.; Whittaker, M. R.; Haddleton, D. M. Cu(0)-Mediated Living Radical Polymerization: a Versatile Tool for Materials Synthesis. *Chem. Rev.* **2016**, *116*, 835– 877.

(16) Anastasaki, A.; Nikolaou, V.; Haddleton, D. M. Cu(0)-Mediated Living Radical Polymerization: Recent Highlights and Applications: a Perspective. *Polym. Chem.* **2016**, *7*, 1002– 1026.

(17) Rosen, B. M.; Jiang, X.; Wilson, C. J.; Nguyen, N. H.; Monteiro, M. J.; Percec, V. The Disproportionation of Cu(I)X Mediated by Ligand and Solvent Into Cu(0) and Cu(II)X2 and Its Implications for SET-LRP. *J. Polym. Sci., Part A: Polym. Chem.* **2009**, *47*, 5606– 5628.

(18) Levere, M. E.; Nguyen, N. H.; Leng, X.; Percec, V. Visualization of the Crucial Step in SET-LRP. *Polym. Chem.* **2013**, *4*, 1635– 1647.

(19) Rosen, B. M.; Percec, V. A Density Functional Theory Computational Study of the Role of Ligand on the Stability of Cu(I) and Cu(II) Species Associated with ATRP and SET-LRP. *J. Polym. Sci., Part A: Polym. Chem.* **2007**, *45*, 4950– 4964.

(20) Sienkowska, M. J.; Rosen, B. M.; Percec, V. SET-LRP of Vinyl Chloride Initiated with CHBr$_3$ in DMSO at 25 °C. *J. Polym. Sci., Part A: Polym. Chem.* **2009**, *47*, 4130– 4140.

(21) Hatano, T.; Rosen, B. M.; Percec, V. SET-LRP of Vinyl Chloride Initiated with CHBr$_3$ and Catalyzed by Cu(0)-Wire/TREN in DMSO at 25 °C. *J. Polym. Sci., Part A: Polym. Chem.* **2010**, *48*, 164– 172.

(22) Percec, V.; Popov, A. V.; Ramirez-Castillo, E.; Weichold, O. Living Radical Polymerization of Vinyl Chloride Initiated with Iodoform and Catalyzed by Nascent Cu(0)/Tris(2-aminoethyl)amine or Polyethyleneimine in Water at 25 °C Proceeds by a New Competing Pathways Mechanism. *J. Polym. Sci., Part A: Polym. Chem.* **2003**, *41*, 3283– 3299.

(23) Nguyen, N. H.; Levere, M. E.; Percec, V. TREN versus Me$_6$-TREN as Ligands in SET-LRP of Methyl Acrylate. *J. Polym. Sci., Part A: Polym. Chem.* **2012**, *50*, 35– 46.

(24) Nicol, E.; Derouineau, T.; Puaud, F.; Zaitsev, A. Synthesis of Double Hydrophilic Poly(ethylene oxide)-b-poly(2-hydroxyethyl acrylate) by Single-Electron Transfer-Living Radical Polymerization. *J. Polym. Sci., Part A: Polym. Chem.* **2012**, *50*, 3885– 3894.

(25) Nguyen, N. H.; Levere, M. E.; Percec, V. SET-LRP of Methyl Acrylate to Complete Conversion with Zero Termination. *J. Polym. Sci., Part A: Polym. Chem.* **2012**, *50*, 860– 873.

(26) Voorhaar, L.; Wallyn, S.; Du Prez, F. E.; Hoogenboom, R. Cu(0)-Mediated Polymerization of Hydrophobic Acrylates Using High-Throughput Experimentation. *Polym. Chem.* **2014**, *5*, 4268– 4276.

(27) Simula, A.; Nikolaou, V.; Alsubaie, F.; Anastasaki, A.; Haddleton, D. M. The Effect of Ligand, Solvent and Cu(0) Source on the Efficient Polymerization of Polyether Acrylates and Methacrylates in Aqueous and Organic Media. *Polym. Chem.* **2015**, *6*, 5940– 5950.

(28) Nguyen, N. H.; Levere, M. E.; Kulis, J.; Monteiro, M. J.; Percec, V. Analysis of the Cu(0)-Catalyzed Polymerization of Methyl Acrylate in Disproportionating and Nondisproportionating Solvents. *Macromolecules* **2012**, *45*, 4606–4622.

(29) Lligadas, G.; Rosen, B. M.; Bell, C. A.; Monteiro, M. J.; Percec, V. Effect of Cu(0) Particle Size on The Kinetics of SET-LRP in DMSO and Cu-Mediated Radical Polymerization in MeCN at 25°C. *Macromolecules* **2008**, *41*, 8365– 8371.

(30) Smail, R. B.; Jezorek, R. L.; Lejnieks, J.; Enayati, M.; Grama, S.; Monteiro, M. J.; Percec, V. Acetone-Water Biphasic Mixtures as Solvents for Ultrafast SET-LRP of Hydrophobic Acrylates. *Polym. Chem.* **2017**, *8*, 3102– 3123.

(31) Enayati, M.; Jezorek, R. L.; Smail, R. B.; Monteiro, M. J.; Percec, V. Ultrafast SET-LRP in Biphasic Mixtures of the Non-Disproportionating Solvent Acetonitrile with Water. *Polym. Chem.* **2016**, *7*, 5930– 5942.

(32) Enayati, M.; Smail, R. B.; Grama, S.; Jezorek, R. L.; Monteiro, M. J.; Percec, V. The Synergistic Effect During Biphasic SET-LRP in Ethanol-Nonpolar Solvent-Water Mixtures. *Polym. Chem.* **2016**, *7*, 7230– 7241.

(33) Enayati, M.; Jezorek, R. L.; Monteiro, M. J.; Percec, V. Ultrafast SET-LRP of Hydrophobic Acrylates in Multiphase Alcohol-Water Mixtures. *Polym. Chem.* **2016**, *7*, 3608– 3621.

(34) Grama, S.; Lejnieks, J.; Enayati, M.; Smail, R. B.; Ding, L.; Lligadas, G.; Monteiro, M. J.; Percec, V. Searching for Efficient SET-LRP Systems *via* Biphasic Mixtures of Water with Carbonates, Ethers and Dipolar Aprotic Solvents. *Polym. Chem.* **2017**, *8*, 5865– 5874.

(35) Jezorek, R. L.; Enayati, M.; Smail, R. B.; Lejnieks, J.; Grama, S.; Monteiro, M. J.; Percec, V. The Stirring Rate Provides a Dramatic Acceleration of the Ultrafast Interfacial SET-LRP in Biphasic Acetonitrile-Water Mixtures. *Polym. Chem.* **2017**, *8*, 3405– 3424.

(36) Moreno, A.; Grama, S.; Liu, T.; Galià, M.; Lligadas, G.; Percec, V. SET-LRP Mediated by TREN in Biphasic Water-Organic Solvent Mixtures Provides the Most Economical and Efficient Process. *Polym. Chem.* **2017**, *8*, 7559– 7574.

(37) Moreno, A.; Galià, M.; Lligadas, G.; Percec, V. SET-LRP in Biphasic Mixtures of the Nondisproportionating Solvent Hexafluoroisopropanol with Water. *Biomacromolecules* **2018**, *19*, 4480– 4491.

(38) Moreno, A.; Liu, T.; Galià, M.; Lligadas, G.; Percec, V. Acrylate-Macromonomers and Telechelics of PBA by Merging Biphasic SET-LRP of BA, Chain Extension with MA and Biphasic Esterification. *Polym. Chem.* **2018**, *9*, 1961– 1971.

(39) Moreno, A.; Jezorek, R. L.; Liu, T.; Galià, M.; Lligadas, G.; Percec, V. Macromonomers, Telechelics and More Complex Architectures of PMA by a Combination of Biphasic SET-LRP and Biphasic Esterification. *Polym. Chem.* **2018**, *9*, 1885– 1899.

(40) Moreno, A.; Liu, T.; Ding, L.; Buzzacchera, I.; Galià, M.; Möller, M.; Wilson, C. J.; Lligadas, G.; Percec, V. SET-LRP in Biphasic Mixtures of Fluorinated Alcohols with Water. *Polym. Chem.* **2018**, *9*, 2313– 2327.

(41) (a) Nyström, F.; Soeriyadi, A. H.; Boyer, C.; Zetterlund, P. B.; Whittaker, M. R. End-Group Fidelity of Copper(0)-Meditated Radical Polymerization at High Monomer Conversion: an ESI-MS Investigation. *J. Polym. Sci., Part A: Polym. Chem.* **2011**, *49*, 5313– 5321. (b) Boyer, C.; Atme, A.; Waldron, C.; Anastasaki, A.; Wilson, P.;

Zetterlund, P. B.; Haddleton, D.; Whittaker, M. R. Copper(0)-Mediated Radical Polymerisation in a Self-Generating Biphasic System. *Polym. Chem.* **2013**, *4*, 106– 112. (c) Boyer, C.; Soeriyadi, A. H.; Zetterlund, P. B.; Whittaker, M. R. Synthesis of Complex Multiblock Copolymers via a Simple Iterative Cu(0)-Mediated Radical Polymerization Approach. *Macromolecules* **2011**, *44*, 8028– 8033.d) Basuki, J. S.; Esser, L.; Duong, H. T. T.; Zhang, Q.; Wilson, P.; Whittaker, M. R.; Haddleton, D. M.; Boyer, C.; Davis, T. P. Magnetic Nanoparticles with Diblock Glycopolymer Shells Give Lectin Concentration-Dependent MRI Signals and Selective Cell Uptake. *Chem. Sci.* **2014**, *5*, 715– 726. (e) Soeriyadi, A. H.; Boyer, C.; Nyström, F.; Zetterlund, P. B.; Whittaker, M. R. High-Order Multiblock Copolymers via Iterative Cu(0)-Mediated Radical Polymerizations (SET-LRP): Toward Biological Precision. *J. Am. Chem. Soc.* **2011**, *133*, 11128– 11131. (f) Alsubaie, F.; Anastasaki, A.; Nikolaou, V.; Simula, A.; Nurumbetov, G.; Wilson, P.; Kempe, K.; Haddleton, D. M. Investigating the Mechanism of Copper(0)-Mediated Living Radical Polymerization in Aqueous Media. *Macromolecules* **2015**, *48*, 6421– 6432.(g) Whitfield, R.; Parkatzidis, K.; Rolland, M.; Truong, N. P.; Anastasaki, A. Tuning Dispersity by Photoinduced Atom Transfer Radical Polymerisation: Monomodal Distributions with Ppm Copper Concentration. *Angew. Chem., Int. Ed.* **2019**, *58*, 13323– 13328. (h) Jones, G. R.; Li, Z.; Anastasaki, A.; Lloyd, D. J.; Wilson, P.; Zhang, Q.; Haddleton, D. M. Rapid Synthesis of Well-Defined Polyacrylamide by Aqueous Cu(0)-Mediated Reversible-Deactivation Radical Polymerization. *Macromolecules* **2016**, *49*, 483– 489. (i) Whitfield, R.; Anastasaki, A.; Truong, N. P.; Wilson, P.; Kempe, K.; Burns, J. A.; Davis, T. P.; Haddleton, D. M. Well-Defined PDMAEA Stars via Cu(0)-Mediated Reversible Deactivation Radical Polymerization. *Macromolecules* **2016**, *49*, 8914– 8924.

(42) Reetz, M. T.; Sell, T.; Meiswinkel, A.; Mehler, G. A New Principle in Combinatorial Asymmetric Transition-Metal Catalysis: Mixtures of Chiral Monodentate P Ligands. *Angew. Chem., Int. Ed.* **2003**, *42*, 790– 793.

(43) Duursma, A.; Hoen, R.; Schuppan, J.; Hulst, R.; Minnaard, A. J.; Feringa, B. L. First Examples of Improved Catalytic Asymmetric C-C Bond Formation Using the Monodentate Ligand Combination Approach. *Org. Lett.* **2003**, *5*, 3111– 3113.

(44) Fors, B. P.; Buchwald, S. L. A Multiligand Based Pd Catalyst for C-N Cross-Coupling Reactions. *J. Am. Chem. Soc.* **2010**, *132*, 15914– 15917.

(45) Fan, Y.; Xia, Y.; Tang, J.; Ziarelli, F.; Qu, F.; Rocchi, P.; Iovanna, J. L.; Peng, L. An Efficient Mixed-Ligand Pd Catalytic System to Promote C-N Coupling for the Synthesis of N-Arylaminotriazole Nucleosides. *Chem. - Eur. J.* **2012**, *18*, 2221– 2225.

(46) Cong, M.; Fan, Y.; Raimundo, J. M.; Xia, Y.; Liu, Y.; Quéléver, G.; Qu, F.; Peng, L. C-S Coupling Using a Mixed-Ligand Pd Catalyst: A Highly Effective Strategy for Synthesizing Arylthio-Substituted Heterocycles. *Chem. - Eur. J.* **2013**, *19*, 17267– 17272.

(47) (a) Percec, V.; Golding, G. M.; Smidrkal, J.; Weichold, O. NiCl$_2$(dppe)-Catalyzed Cross-Coupling of Aryl Mesylates, Arenesulfonates, and Halides with Arylboronic Acids. *J. Org. Chem.* **2004**, *69*, 3447– 3452. (b) Wilson, D. A.; Wilson, C. J.; Rosen, B. M.; Percec, V. Two-Step, One-Pot Ni-Catalyzed Neopentylglycolborylation and Complementary Pd/Ni-Catalyzed Cross-Coupling with Aryl Halides, Mesylates, and

Tosylates. *Org. Lett.* **2008**, *10.* (c) Moldoveanu, C.; Wilson, D. A.; Wilson, C. J.; Corcoran, P.; Rosen, B. M.; Percec, V. Neopentylglycolborylation of Aryl Chlorides Catalyzed by the Mixed Ligand System NiCl₂(dppp)/dppf. *Org. Lett.* **2009**, *11*, 4974– 4977. (d) Wilson, D. A.; Wilson, C. J.; Moldoveanu, C.; Resmerita, A. M.; Corcoran, P.; Hoang, L. M.; Rosen, B. M.; Percec, V. Neopentylglycolborylation of Aryl Mesylates and Tosylates Catalyzed by Ni-Based Mixed-Ligand Systems Activated with Zn. *J. Am. Chem. Soc.* **2010**, *132*, 1800– 1801. (e) Leowanawat, P.; Resmerita, A. M.; Moldoveanu, C.; Liu, C.; Zhang, N.; Wilson, D. A.; Hoang, L. M.; Rosen, B. M.; Percec, V. Zero-Valent Metals Accelerate the Neopentylglycolborylation of Aryl Halides Catalyzed by NiCl₂-Based Mixed-Ligand Systems. *J. Org. Chem.* **2010**, *75*, 7822– 7828.(f) Moldoveanu, C.; Wilson, D. A.; Wilson, C. J.; Leowanawat, P.; Resmerita, A. M.; Liu, C.; Rosen, B. M.; Percec, V. *J. Org. Chem.* **2010**, *75*, 5438– 5452, .(g) Leowanawat, P.; Zhang, N.; Resmerita, A.-M.; Rosen, B. M.; Percec, V. Ni(COD)₂/PCy₃ Catalyzed Cross-Coupling of Aryl and Heteroaryl Neopentylglycolboronates with Aryl and Heteroaryl Mesylates and Sulfamates in THF at Room Temperature. *J. Org. Chem.* **2011**, *76*, 9946– 9955. (h) Leowanawat, P.; Zhang, N.; Safi, M.; Hoffman, D. J.; Fryberger, M. C.; George, A.; Percec, V. trans-Chloro(1-Naphthyl)bis(triphenylphosphine)nickel(II)/PCy₃ Catalyzed Cross-Coupling of Aryl and Heteroaryl Neopentylglycolboronates with Aryl and Heteroaryl Mesylates and Sulfamates at Room Temperature. *J. Org. Chem.* **2012**, *77*, 2885– 2892. (i) Leowanawat, P.; Zhang, N.; Percec, V. Nickel Catalyzed Cross-Coupling of Aryl C-O Based Electrophiles with Aryl Neopentylglycolboronates. *J. Org. Chem.* **2012**, *77*, 1018– 1025.(j) Zhang, N.; Hoffman, D. J.; Gutsche, N.; Gupta, J.; Percec, V. Comparison of Arylboron-Based Nucleophiles in Ni-Catalyzed Suzuki-Miyaura Cross-Coupling with Aryl Mesylates and Sulfamates. *J. Org. Chem.* **2012**, *77*, 5956– 5964, DOI: 10.1021/jo300547v. (k) Leowanawat, P.; Zhang, N.; Safi, M.; Hoffman, D. J.; Fryberger, M. C.; George, A.; Percec, V. trans-Chloro(1-Naphthyl)bis(triphenylphosphine)nickel(II)/PCy₃ Catalyzed Cross-Coupling of Aryl and Heteroaryl Neopentylglycolboronates with Aryl and Heteroaryl Mesylates and Sulfamates at Room Temperature. *J. Org. Chem.* **2012**, *77*, 2885– 2892.(l) Malineni, J.; Jezorek, R. L.; Zhang, N.; Percec, V. An Indefinitely Air-Stable σ-Ni^{II} Precatalyst for Quantitative Cross-Coupling of Unreactive Aryl Halides and Mesylates with Aryl Neopentylglycolboronates. *Synthesis* **2016**, *48*, 2795– 2807.(m) Malineni, J.; Jezorek, R. L.; Zhang, N.; Percec, V. Ni^{II}Cl(1-Naphthyl)(PCy₃)₂, An Air-Stable σ-Ni^{II} Precatalyst for Quantitative Cross-Coupling of Aryl C-O Electrophiles with Aryl Neopentylglycolboronates. *Synthesis* **2016**, *48*, 2808– 2815.

(48) Li, K.-T.; Shieh, D. C. Polymerization of 2,6-Dimethylphenol with Mixed-Ligand Copper Complexes. *Ind. Eng. Chem. Res.* **1994**, *33*, 1107– 1112.

(49) Matyjaszewski, K.; Wei, M.; Xia, J.; McDermott, N. E. Controlled/"Living" Radical Polymerization of Styrene and Methyl Methacrylate Catalyzed by Iron Complexes. *Macromolecules* **1997**, *30*, 8161– 8164.

(50) Iizuka, E.; Wakioka, M.; Ozawa, F. Mixed-Ligand Approach to Palladium-Catalyzed Direct Arylation Polymerization: Synthesis of Donor-Acceptor Polymers with Dithienosilole (DTS) and Thienopyrroledione (TPD) Units. *Macromolecules* **2015**, *48* (9), 2989– 2993.

(51) Lligadas, G.; Percec, V. Synthesis of Perfectly Bifunctional Polyacrylates by Single-Electron-Transfer Living Radical Polymerization. *J. Polym. Sci., Part A: Polym. Chem.* **2007**, *45*, 4684– 4695.

(52) Ciampolini, M.; Nardi, N. Five-Coordinated High-Spin Complexes of Bivalent Cobalt, Nickel, and Copper with Tris(2-dimethylaminoethyl)amine. *Inorg. Chem.* **1966**, *5*, 41– 44.

(53) Nguyen, N. H.; Rosen, B. M.; Jiang, X.; Fleischmann, S.; Percec, V. New Efficient Reaction Media for SET-LRP Produced from Binary Mixtures of Organic Solvents and H_2O. *J. Polym. Sci., Part A: Polym. Chem.* **2009**, *47*, 5577– 5590.

(54) Nguyen, N. H.; Rosen, B. M.; Lligadas, G.; Percec, V. Surface-Dependent Kinetics of Cu(0)-Wire-Catalyzed Single-Electron Transfer Living Radical Polymerization of Methyl Acrylate in DMSO at 25°C. *Macromolecules* **2009**, *42*, 2379– 2386.

(55) Ahrland, S.; Rawsthorne, J.; Haaland, A.; Jerslev, B.; Schaffer, C. E.; Sunde, E.; Sørensen, N. A. The Stability of Metal Halide Complexes in Aqueous Solution. VII. The Chloride Complexes of Copper(I). *Acta Chem. Scand.* **1970**, *24*, 157– 172.

(56) Ciavatta, L.; Ferri, D.; Palombari, R. On the equilibrium Cu^{2+} + Cu(s) $\rightleftarrows 2Cu^{+}$. *J. Inorg. Nucl. Chem.* **1980**, *42*, 593– 598.

(57) Nguyen, N. H.; Sun, H.-J.; Levere, M. E.; Fleischmann, S.; Percec, V. Where is Cu(0) Generated by Disproportionation During SET-LRP?. *Polym. Chem.* **2013**, *4*, 1328– 1332.

(58) Rosen, B. M.; Lligadas, G.; Hahn, C.; Percec, V. Synthesis of Dendrimers Through Divergent Iterative Thio-Bromo "Click" Chemistry. *J. Polym. Sci., Part A: Polym. Chem.* **2009**, *47*, 3931– 3939.

(59) Rosen, B. M.; Lligadas, G.; Hahn, C.; Percec, V. Synthesis of Dendritic Macromolecules Through Divergent Iterative Thio-Bromo "Click" Chemistry and SET-LRP. *J. Polym. Sci., Part A: Polym. Chem.* **2009**, *47*, 3940– 3948.

Chapter 2
The Me$_6$-TREN/TREN Mixed-Ligand Effect During SET-LRP in the Catalytically Active DMSO Revitalizes TREN into an Excellent Ligand

(Reproduced with permission from Refence No 1. Copyright (2020) American Chemical Society.)

Introduction

In last chapter, the efficiency of tris(2-aminoethyl)amine (TREN) ligand in SET-LRP was improved using mixed-ligand concept and thus expanding the solvents which can be used in "programmed" biphasic SET-LRP. The mixed-ligand concept represents an inexpensive but extremely efficient methodology to design new catalytic systems without synthetic efforts.[2] Almost simultaneously with its development, Feringa reported heterocombinations of chiral monodentate ligands as more efficient than homocombinations in Rh-catalyzed C–C cross-coupling.[3] At the same time the mixed-ligand strategy was expanded to Pd-catalyzed C–N[4,5] and C–S[6] cross-coupling and to Ni-mediated Suzuki cross-coupling and borylation.[7] The advantages of the mixed-ligand catalytic systems have been observed only in several polymerization reactions.[8-10]

A suitable solvent/N-ligand mixture is demanded for Cu(0)-catalyzed single electron transfer-living radical polymerization (SET-LRP)[11-18] in order to facilitate the disproportionation of Cu(I)X into Cu(0) and Cu(II)X$_2$.[19,20] Tris(2-dimethylaminoethyl)amine (Me$_6$-TREN) is a common ligand used in SET-LRP,[11,12,15] since it favors the disproportionation by preferentially binding Cu(II)X$_2$ rather than Cu(I)X.[21] Nevertheless, the precursor of Me$_6$-TREN, tris(2-aminoethyl)amine (TREN)[12,22-24] that is about 80 times less expensive than Me$_6$-TREN, and poly(ethylene imine) (PEI)[11] was also used for SET-LRP of vinyl chloride (VC), acrylates, and methacrylates during the first days of SET-LRP. Likewise, TREN[25-27] and *N,N,N′,N″,N′*-pentamethyldiethylenetriamine (PMDETA)[11,28,29] were also employed in SET-LRP.

In previous report, the replacement of Me$_6$-TREN with TREN was not so successful in aqueous–organic "programmed" biphasic systems using Cu(0) wire catalyst,"[30-34] although TREN is known for its efficiency in single-phase SET-LRP. Biphasic organic solvent–water SET-LRP complex systems demand the addition of Cu(II)Br$_2$ in order to retain the living character when TREN is used as a ligand. In this particular case, SET-LRP is an interfacial process that was discussed in more details in previous publications.[35] The Cu(0)-mediated SET-LRP in bi(multi)phasic mixtures of organic solvents with water is very important and opens new methodologies since the organic solvent does not have to facilitate the disproportionation of Cu(I)X/N-ligand, as in the classic SET-LRP.[36-40] The first mixed-ligand effect in a SET-LRP system was observed in the water–organic solvent "programmed" biphasic systems when Me$_6$-TREN was successfully employed to replace the externally added Cu(II)X$_2$ with Me$_6$-TREN.[11]

In most organic reactions the rate of reaction is dependent upon the reactant concentration. When the amount of solvent is increased, the reactant concentration decreases and the rate

of reaction decreases. In the catalytic effect of solvent during SET-LRP the opposite effect was observed.[12a] By increasing the amount of DMSO during the polymerization of MA with Methyl-2-bromopropionate (MBP) catalyzed by Cu(0) powder, the apparent rate of polymerization increases with the increased amount of DMSO.

The goal of this chapter is to increase the efficiency of TREN using catalytic activity of DMSO and mixed-ligand concept. There are two objectives of this chapter, first by measuring apparent rate of polymerization at different volume of DMSO to establish catalytic activity of DMSO and secondly investigated mixed-ligand concept in two different concentrations of the DMSO solvent by changing different ligand system in reaction system. In first series of experiment, the catalytic activity of DMSO solvent was studied in both Me_6-TREN and TREN and in the mixed-ligand Me_6-TREN/TREN-mediated SET-LRP of MA initiated with BPE at 25 °C and catalyzed with nonactivated Cu(0) wire. In second series of experiment, the mixed-ligand effect of Me_6-TREN/TREN was investigated at two different concentrations of the DMSO solvent by measuring reaction kinetics and molecular weight distribution using ^{1}H NMR and gel permeation chromatography (GPC), respectively. Finally, by determination of the chain-end functionality of the resulting polymers by a combination of NMR and MALDI-TOF before and after thio-bromo "click" reaction which will demonstrated that the catalytic activity of DMSO.

Materials and Methods

Reagents

Methyl acrylate (MA; 99%, Acros) was passed over a short column of basic Al_2O_3 to remove its radical inhibitor. Tris(2-aminoethyl)amine (TREN; 99%, Acros), Cu(0) wire (20 gauge wire, 0.812 mm diameter from Fisher), and dimethyl sulfoxide (DMSO; 99.8%, Sigma-Aldrich) were used as received. Triethylamine (NEt₃; >99.5% Chemimpex) was distilled under N_2 from CaH_2. Bis(2-bromopropionyl)ethane (BPE) was synthesized by esterification of ethylene glycol with 2-bromopropionyl bromide in the presence pyridine.[41] Hexamethylated tris(2-aminoethyl)amine (Me_6-TREN) was synthesized by a literature procedure.[42]

Techniques

^{1}H NMR (400 MHz) spectra were recorded on a Bruker AVANCE NEO 400 NMR instrument at 27 °C in $CDCl_3$ containing tetramethylsilane (TMS) as internal standard. Gel permeation chromatography (GPC) analysis of the polymer samples was performed using a Shimadzu LC-20AD high-performance liquid chromatograph pump, a PE Nelson Analytical 900 Series integration data station, a Shimadzu RID-10A refractive index (RI) detector, and three AM gel columns (a guard column, 500 Å, 10 μm and 10^4 Å, 10 μm). THF (Fisher, HPLC grade) was used as eluent at a flow rate of 1 mL min^{-1}. The number-average (M_n) and weight-average (M_w) molecular weights of PMA were determined with poly(methyl methacrylate) (PMMA) standards from American Polymer Standards. MALDI-TOF spectra were obtained on a Voyager DE (Applied Biosystems) instrument with a 337 nm nitrogen laser (3 ns pulse width). The accelerating potential was 25 kV, the grid was 92.5, the laser power was 2200–2500, and a positive ionization mode was used. The sample analysis was performed with 2-(4-hydroxyphenylazo) benzoic acid as the matrix. Solutions of the matrix (25 mg/mL in THF), NaCl (2 mg/mL in deionized H_2O), and polymer (10 mg/mL) were prepared independently. The solution for MALDI-TOF analysis was obtained by mixing the matrix, polymer, and salt solutions in a 5/1/1 volumetric ratio. Subsequently, 0.5 μL portions of the mixture were deposited onto three wells of sample plate and dried in air at room temperature before being subjected to MALDI-TOF analysis.

Standard Procedure for SET-LRP of MA in DMSO Using Me₆-TREN, TREN, and the Mixed-Ligand Me₆-TREN/TREN Methodology

Stock solutions prepared with different ratios of Me_6-TREN to TREN such as 0.02/0 M, 0.015/0.005 M, 0.01/0.01 M, 0.005/0.015 M, and 0/0.02 M in DMSO were first made. The monomer (MA, 22.2 mmol, 2.00 mL), organic solvent (DMSO if necessary), DMSO stock solution (0.02 mmol ligand, 1 mL), and initiator (BPE, 0.1 mmol, 33.2 mg) were added in this order to a 25 mL Schlenk tube. The mixture was deoxygenated by six freeze–pump–thaw cycles. Subsequently, the Schlenk tube was opened under a positive flow of nitrogen to add the Cu(0) wire wrapped around a Teflon-coated stir bar. Two more freeze–pump–thaw cycles were carried out while holding the stir bar above the reaction mixture with the

31

help of an external magnet. The Schlenk tube was filled with N_2, and the reaction was placed in a water bath at 25 °C. Then, the stir bar wrapped with the Cu(0) wire was dropped gently into the reaction. The introduction of the Cu(0) wire defines $t = 0$. Samples were taken at different times by purging the side arm of the Schlenk tube with nitrogen for 2 minutes using a deoxygenated syringe and stainless steel needles. Samples were dissolved in $CDCl_3$ and quenched by air bubbling. After that, the monomer conversion was measured by ^1H NMR spectroscopy. In order to determine the molecular weight and polydispersity of the samples, the solvent and the residual monomer were removed under vacuum. Finally, samples were dissolved in THF and passed through a short small basic Al_2O_3 chromatographic column to remove any residual copper and analyzed by GPC. The resulting PMA was precipitated in cold methanol and dried under vacuum until constant weight to perform chain-end analysis by ^1H NMR spectroscopy, before and after the thioetherification of the chain ends.

General Method for the Chain-End Thioetherification of PMA via Thio-Bromo "Click" Reaction

In a 10 mL test tube sealed with a rubber septum, thiophenol (0.05 equivalents) and distilled triethylamine (NEt_3, 0.05 equivalents) were added into a solution of the corresponding polymer (0.01 equivalents) in acetonitrile (1 mL) under a nitrogen flow. The mixture was stirred at room temperature for 3 hours. Then, the resulting modified PMA was precipitated in cold methanol and washed with methanol several times. The resulting polymer was dried under vacuum to a constant weight.

Results and Discussion

Determination of the External Order of Reaction in DMSO During SET-LRP Catalyzed with Nonactivated Cu(0) Wire in DMSO

A close to first order external order of reaction in the DMSO used as solvent was observed when Cu(0) powder was employed as catalyst in SET-LRP.[12a,43-48] This external first order of reaction in DMSO demonstrated the catalytic activity of DMSO when SET-LRP was performed in DMSO as solvent.[12a] Three series of experiments were carried out with nonactivated Cu(0) wire as catalyst, MA as monomer, and Me_6-TREN, TREN, and mixtures of Me_6-TREN/TREN in different concentrations of DMSO at 25 °C. BPE was used as initiator in all cases.

The structures of the two ligands and an equation of the Cu(0) wire-catalyzed SET-LRP of MA initiated with bis(2-bromopropnionyl)ethane (BPE) are outlined in **Scheme 2.1**. Duplicate and triplicate kinetics were carried out under the following conditions: $[MA]_0/[BPE]_0/[L]_0 = 222/1/0.2$ using 9.0 cm of nonactivated Cu(0) wire.

Scheme 2.1. SET-LRP of MA Initiated with BPE and Catalyzed with Nonactivated Cu(0) Wire by Employing Various Ratios of Me_6-TREN and TREN in the Catalytically Active DMSO at 25 °C

Me₆-TREN   TREN   Me₆-TREN:TREN (1:1) H-bonded complex

BPE   MA   PMA
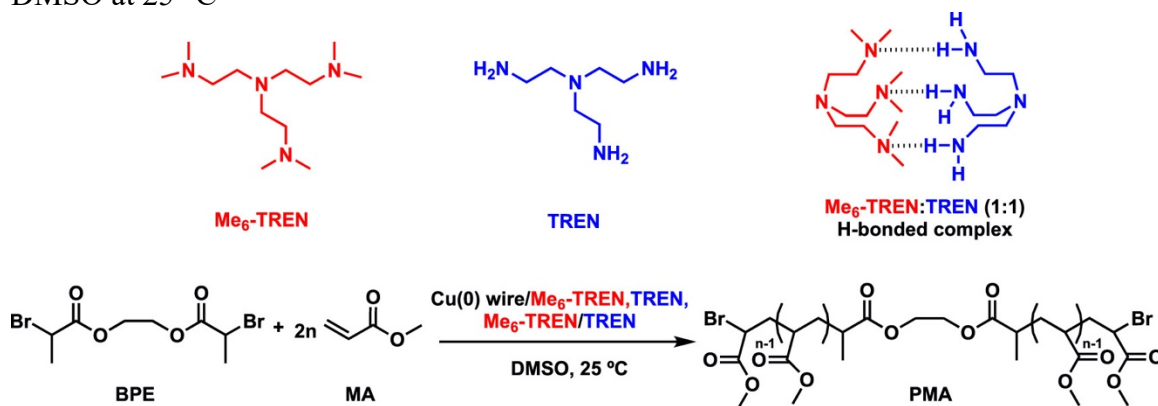
Figure 2.1a reports the kinetic data for the experiments performed with Me_6-TREN as ligand, **Figure 2.1b** shows the data obtained with TREN, while **Figure 2.1c** shows the data obtained with the mixed-ligand system Me_6-TREN/TREN. Selected kinetic experiments from which these external orders of reaction in DMSO were obtained for Me_6-TREN (**Figure 2.2a,c,e**) and TREN (**Figure 2.2b,d,f**) as ligands are reported in **Figures 2.2** when the DMSO concentration was varied from 1.0 to 1.5 and to 1.8 mL of DMSO with 2 mL of MA. Kinetic experiments with all other DMSO concentrations employed in **Figure 2.1a–c** are shown in **Appendix 21–25**. First order reaction kinetics in monomer were observed for all DMSO concentrations from **Figures 2.2** and **Appendix 21–25**. A continuous increase in the rate of polymerization and of the corresponding apparent rate constant, k_p^{app}, as the concentration of the DMSO increased or the overall concentration of the MA decreased was observed in all cases (**Figures 2.2** and **Appendix 21–25**).
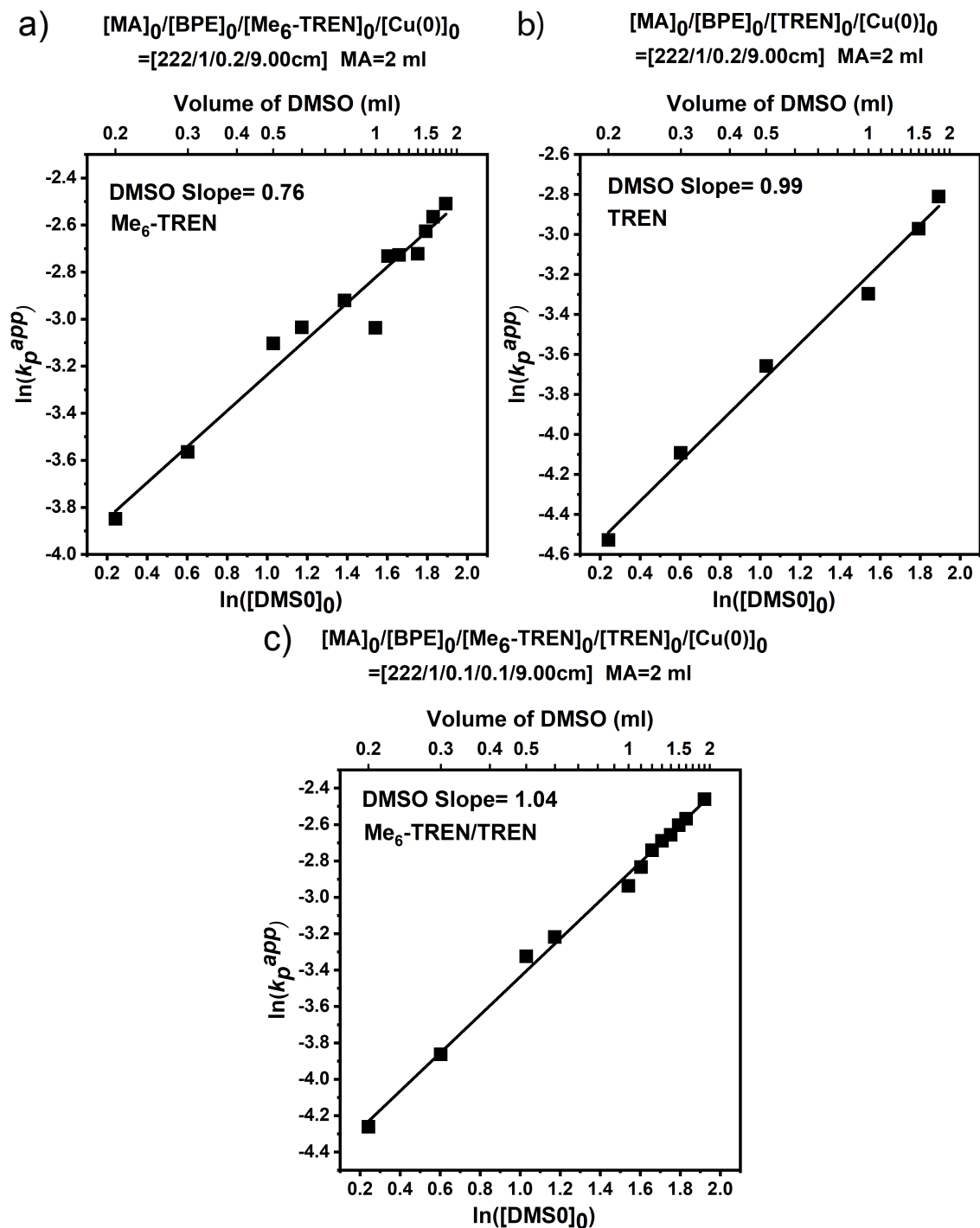
Figure 2.1. Determination of the external order of reaction in $[DMSO]_0$ for the Cu(0) wire/ligand-catalyzed polymerization of methyl acrylate (MA) in DMSO at 25 °C, initiated with BPE. $\ln(k_p^{app})$ vs $\ln([DMSO]_0)$ with DMSO varied from 0.2 to 1.9 mL, with 2 mL of MA for (a) $[MA]_0/[BPE]_0/[Me_6\text{-}TREN]_0/[Cu(0)]_0$ = 222/1/0.2/9 cm; (b) $[MA]_0/[BPE]_0/[TREN]_0/[Cu(0)]_0$ = 222/1/0.2/9 cm; (c) $[MA]_0/[BPE]_0/[Me_6\text{-}TREN]_0/[TREN]_0/[Cu(0)]_0$ = 222/1/0.1/0.1/9 cm.
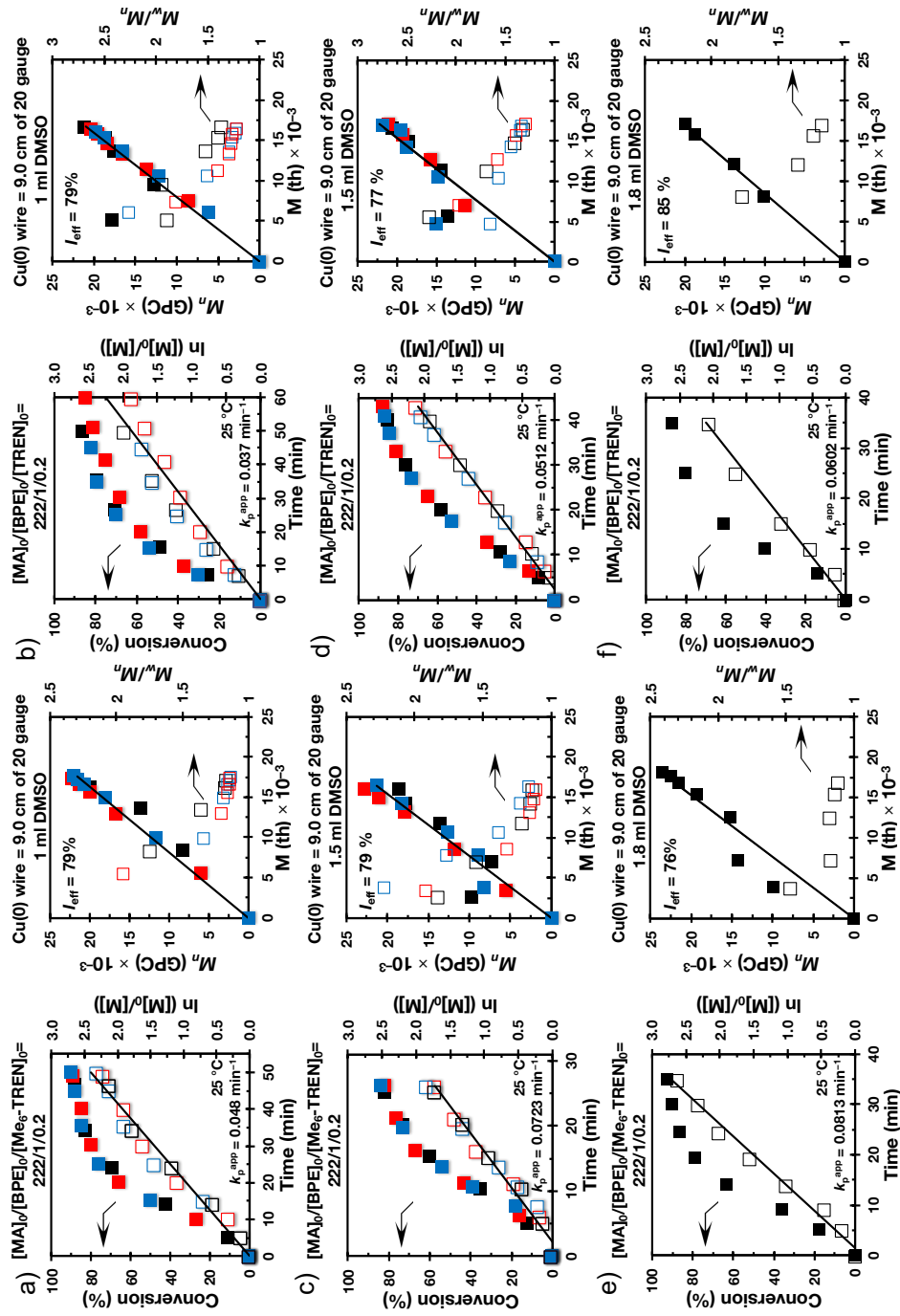
Figure 2.2. Kinetic plots, molecular weight and dispersity evolutions for the SET-LRP of MA in DMSO initiated with BPE and catalyzed with 9.0 cm nonactivated Cu(0) wire at 25 °C. Data in different colors were obtained from different kinetics, performed by different researchers. k_p^{app} and I_{eff} are the average values of three experiments. k_p^{app} vs $[DMSO]_0$ with DMSO varied from 1.0 mL (a) to 1.5 mL (c) to 1.8 mL (e) with 2 mL of MA for $[MA]_0/[BPE]_0/[Me_6\text{-}TREN]_0/[Cu(0)]_0 = 222/1/0.2/9$ cm. Identical experiments in which Me_6-TREN was replaced with TREN are in (b), (d), and (f).

35

In any organic or polymerization reaction the decrease in the reactants concentration generated by increasing the solvent concentration results in a decrease of the rate of reaction. This unexpected trend that consists of the increase in rate of polymerization with the decrease of the monomer concentration demonstrates the catalytic activity of DMSO in SET-LRP. This result is in agreement with the experiments reported with Cu(0) powder as catalyst.[12a] The determination of the external order of reaction in DMSO was calculated by plotting the $\ln(k_p^{app})$ vs $\ln([DMSO]_0)$ (**Figure 2.1a–c**). The slope of these dependencies provided the external order of reaction in DMSO for the different ligands used in these SET-LRP experiments. An external order of reaction in DMSO of 0.76 was obtained in the presence of Me$_6$-TREN, while in the presence of TREN and the mixed-ligand Me$_6$-TREN/TREN (1/1 molar ratio), the external orders of reaction in DMSO were 0.99 and 1.04, respectively.

Potential Mechanism for the Catalytic Activity of DMSO

In order to address the catalytic activity of DMSO, first it must be considered that SET-LRP experiments were performed in a mixture of two solvents, DMSO and the monomer, MA. Both DMSO and MA are good solvents that mediate the disproportionation of Cu(I)Br into Cu(0) and Cu(II)Br$_2$.[20a]

While both solvents MA and DMSO mediate the disproportionation in the presence of these two ligands, MA and DMSO, only DMSO is a good solvent for Cu(I)Br and Cu(II)Br$_2$ obtained during the activation and disproportionation and is also a better solvent that mediates this disproportionation. MA mediates disproportionation mostly by a surface effect. Therefore, it is expected that by increasing the ratio between DMSO and MA in the reaction mixture, the extent of disproportionation will increase. At the same time it has been demonstrated that DMSO stabilizes Cu(0) nanoparticles, while MA does not. **Figure 2.3** presents disproportionation experiments that support this hypothesis. An increase in the amount of Cu(0) obtained by disproportionation is observed at the transition from MA/DMSO = 3/1 to 2/1. This increase continues to the transition to MA/DMSO = 1/1. However, in addition to this trend, at a 1/1 ratio, the stabilization of Cu(0) nanoparticles by the higher concentration of DMSO is also visible (see left vial in **Figure 2.3**). Increasing the stability of nanoparticles decreases the crystallization process and provides smaller but more active Cu(0) nanoparticles of the catalyst.[20b] It is well established that faster SET-LRP is mediated in more disproportionating solvents and in their mixtures.[20c-e] In addition, mixtures of solvents can display also a cooperative and synergistic effect that was not yet investigated for the case of MA/DMSO.[19e] Last but not least, since DMSO is one of the best solvents for SET processes, an increased concentration of DMSO also is expected to increase the rate of SET-LRP.[19f] Therefore, all these factors, the extent of disproportionation that determines the concentration of Cu(0) produced by disproportionation, the Cu(0) particle size generated by disproportionation and their different reactivities, the solubility of Cu(I)Br and Cu(II)Br$_2$ compounds in the MA/DMSO solvent, and the quality of the MA/DMSO solvent for SET reactions, contribute to the catalytic effect of DMSO reported here, even if the most reactive Cu(0) species employed in the SET-LRP are atoms.[49]

[CuBr]/[Me$_6$-TREN] = 1/1   [CuBr] = 46.5 mM in 3 mL solution
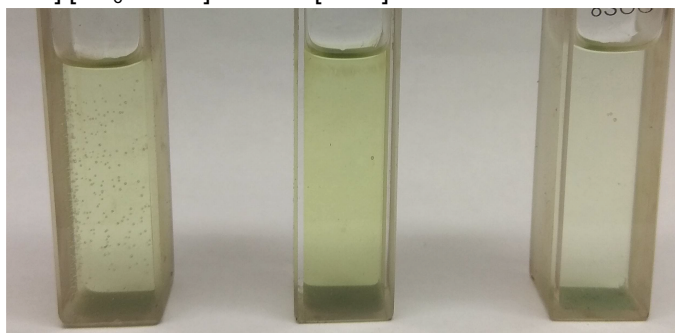
MA/DMSO = 1/1   MA/DMSO =2/1   MA/DMSO =3/1

Figure 2.3. Visual observation of CuBr/Me$_6$-TREN complex dissolved in DMSO/MA. Conditions: [CuBr] = 46.5 mM, solvent = 3.0 mL, [CuBr]$_0$/[Me$_6$-TREN]$_0$ = 1/1. Pictures were taken 60 min after mixing the reagents.

Mixed-Ligand Methodology During the SET-LRP of 2 mL of MA in 1 mL of DMSO Using Me$_6$-TREN, Me$_6$-TREN/TREN, and TREN as Ligands

The detection of the mixed-ligand effect for Me$_6$-TREN/TREN was first observed and reported for SET-LRP performed in water/organic solvents biphasic systems.[11] In the current series of experiments, the ratio between Me$_6$-TREN and TREN was changed from 1:0 to 0:1 while keeping the ratio of ligand to initiator constant at 10 mol %. The ratio between MA and DMSO was also kept constant (2 mL of MA to 1 mL of DMSO; **Scheme 2.1** and **Figure 2.4**)

Table 2.1. Dependence of k_p^{app} on the Dimension of the Cu(0) Wire in the SET-LRP of MA Initiated with BPE in DMSO at 25 °C[a]

entry	Wire length (cm) 20G	Reaction condition	k_p^{app} (min^{-1})	$k_p^{app}/$ k_p^{app}(TREN)	M_w/M_n	I_{eff}(%)
1	9.0	[MA]/[BPE]/[Me$_6$-TREN] 222/1/0.2	0.048	1.3	1.14	79
2	9.0	[MA]/[BPE]/[Me$_6$-TREN]/[TREN] 222/1/0.15/0.05	0.051	1.4	1.21	81
3	9.0	[MA]/[BPE]/[Me$_6$-TREN]/[TREN] 222/1/0.1/0.1	0.053	1.4	1.23	82
4	9.0	[MA]/[BPE]/[Me$_6$-TREN]/[TREN] 222/1/0.05/0.15	0.044	1.2	1.20	82
5	9.0	[[MA]/[BPE]/[TREN] 222/1/0.2	0.037	1.0	1.23	79

[a]Reaction conditions: monomer = 2 mL; solvent =1 mL.

37
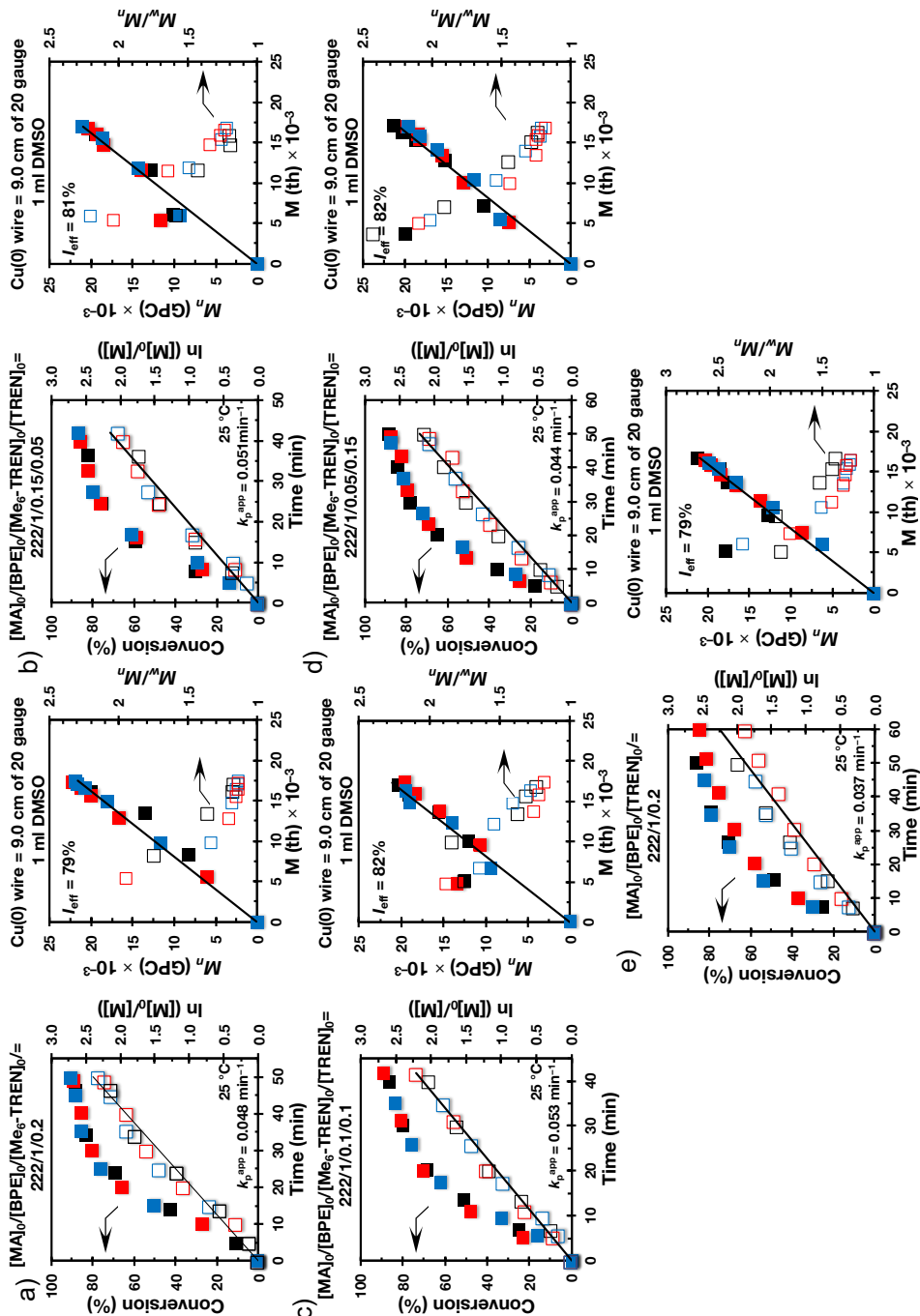
Figure 2.4. Kinetic plots, molecular weight, and dispersity evolutions for the SET-LRP of MA in DMSO initiated with BPE and catalyzed by the 9.0 cm nonactivated Cu(0) wire at 25 °C in the presence of (a) Me_6-TREN and (b–d) different ratios of Me_6-TREN/TREN and (e) TREN. Experimental data in different colors were obtained from different kinetics experiments, sometimes performed by different researchers. k_p^{app} and I_{eff} are the average values of three experiments. $[MA]_0/[BPE]_0/[ligand]_0/[Cu(0)]_0 = 222/1/0.2/9$ cm.
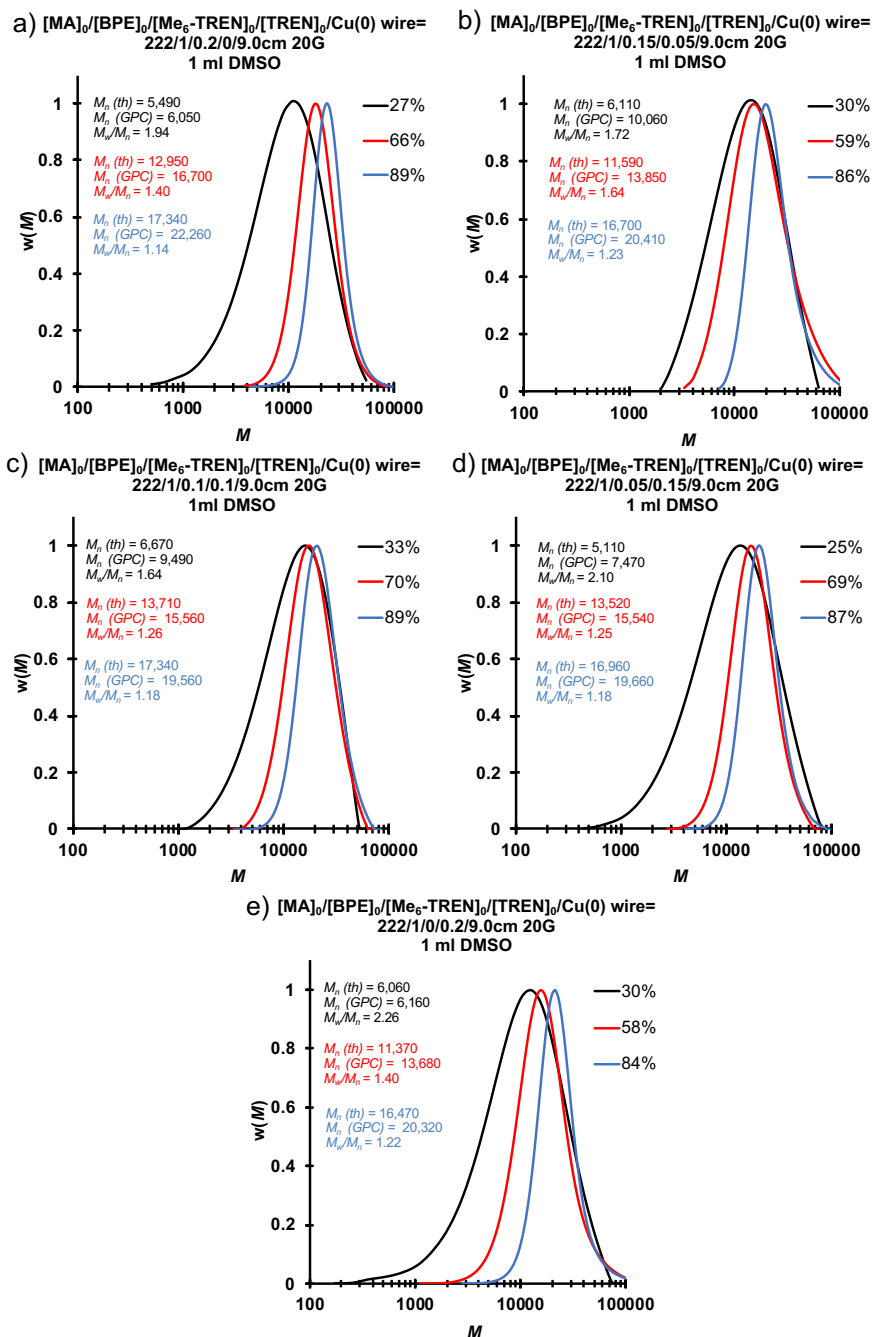
Figure 2.5. Representative GPC traces of the evolution of molecular weight as a function of conversion for the SET-LRP of MA in a mixture of 2 mL MA with 1 mL DMSO catalyzed by 9.0 cm nonactivated Cu(0) wire at 25 °C in the presence of various ligand compositions, as mentioned on top of the GPC curves. Reaction conditions: MA = 2 mL, DMSO = 1 mL, $[MA]_0/[BPE]_0/[L]_0 = 222/1/0.2$.
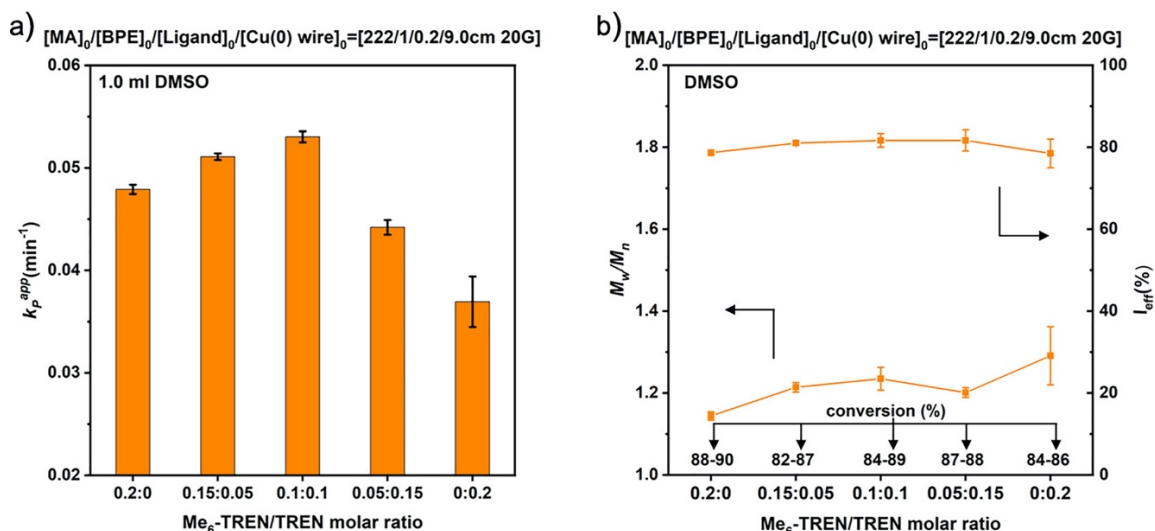
Figure 2.6. Evolution of k_p^{app} for the SET-LRP of MA (2 mL) initiated with BPE in DMSO (1 mL) mediated with different ratios between Me$_6$-TREN and TREN at 25 °C (a). Initiator efficiency (I_{eff} (%)) and dispersity (M_w/M_n) as a function of the ratio between Me$_6$-TREN and TREN.

Interestingly, all tested mixed-ligand compositions generated higher k_p^{app} values than those obtained in control experiments carried out in the presence of either Me$_6$-TREN or TREN. These results will be discussed later. The partial replacement of Me$_6$-TREN with TREN increased the k_p^{app} while retaining first-order kinetics (**Figure 2.4**). The best catalytic activity was observed at a 1:1 molar ratio of the two ligands (compare **Figure 2.4a, b, and c**), suggesting the H-bonded new ligand from **Scheme 2.1**. Under these conditions, the SET-LRP of MA proceeded faster than control experiments with Me$_6$-TREN (**Figure 2.4a**) and TREN (**Figure 2.4e**), respectively. This mixed-ligand methodology also provided the highest conversion and an improved control over molecular weight distribution (**Figures 2.5 and 2,6**). The summary of results is in **Table 2.1**.

Representative GPC data plotted in **Figure 2.5** illustrate the dependence of molecular weight vs conversion. GPC data show monomodal peak distributions shifting to higher molar mass at high conversion. The most relevant result was observed at the 1:1 molar ratio between the two ligands. In this case, the I_{eff} was found to be above 80%. These data demonstrate that the mixed-ligand catalyst consisting of nonactivated Cu(0) wire and Me$_6$-TREN/TREN is an effective new catalytic system for the SET-LRP of MA in DMSO.

Visualization of the Polymerization Reaction at High Conversion

The images in **Figure 2.7** reveal an almost undetectable increase in the blue color of the reaction mixture as the concentration of TREN increased. This trend most probably indicates a negligible increase in the extent of bimolecular termination that is too low to be detected by NMR and MALDI-TOF. A similar result was observed during the mixed-ligand effect observed in biphasic water–organic solvent systems.[11]
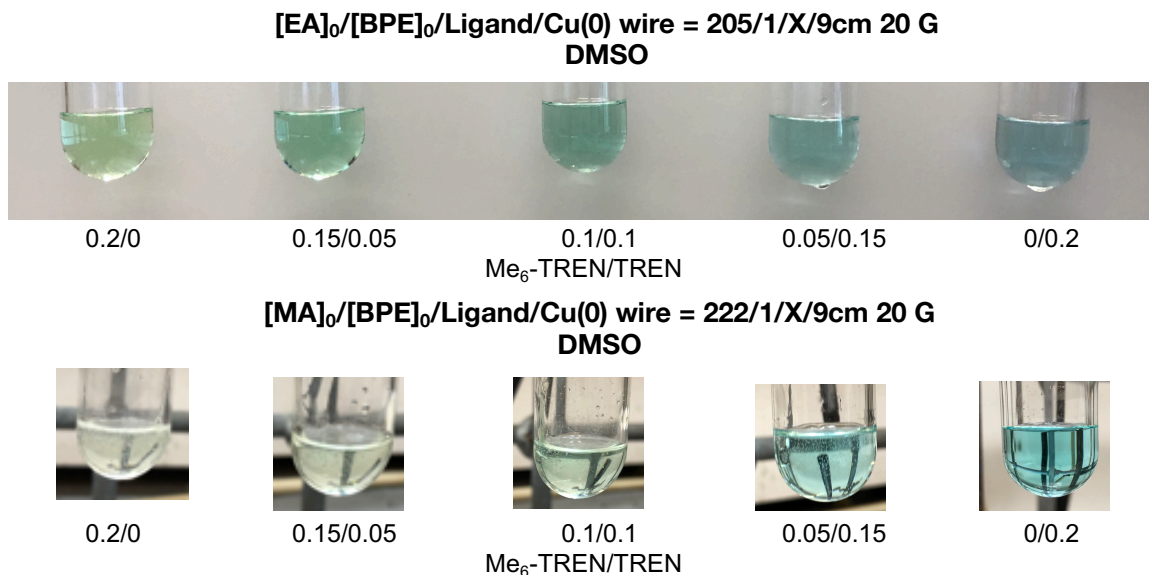
[EA]₀/[BPE]₀/Ligand/Cu(0) wire = 205/1/X/9cm 20 G

| 0.2/0 | 0.15/0.05 | 0.1/0.1 | 0.05/0.15 | 0/0.2 |

Me₆-TREN/TREN

[MA]₀/[BPE]₀/Ligand/Cu(0) wire = 222/1/X/9cm 20 G
DMSO

| 0.2/0 | 0.15/0.05 | 0.1/0.1 | 0.05/0.15 | 0/0.2 |

Me₆-TREN/TREN

Structural Analysis of PMA Before and After Thio-Bromo "Click"

A combination 400 MHz ^{1}H NMR and MALDI-TOF methods before and after reacting the -Br end-groups of PMA with thiophenol via thio-bromo "click" reaction[50] were employed to estimate the living character of SET-LRP performed at various molar ratios between Me₆-TREN and TREN and compare them with Me₆-TREN and TREN. Low molecular weight polymers were synthesized for these investigations. **Figures 2.8** and **2.9** show representative ^{1}H NMR spectra of PMA isolated at high conversion of SET-LRP in DMSO in the presence of Me₆-TREN (**Figures 2.8a and 2.9a**), Me₆-TREN/TREN (**Figures 2.8b and 2.9b**), and TREN (**Figures 2.8c, 2.9b**) before and after thio-bromo "click" reaction. Within experimental error, the chain end functionality (F^{Br}, F^{SPH}%) of all PMA samples is 100%. This is a remarkable result that demonstrates that the catalytic activity of DMSO increases the ligand activity of TREN and transforms it into an excellent ligand.
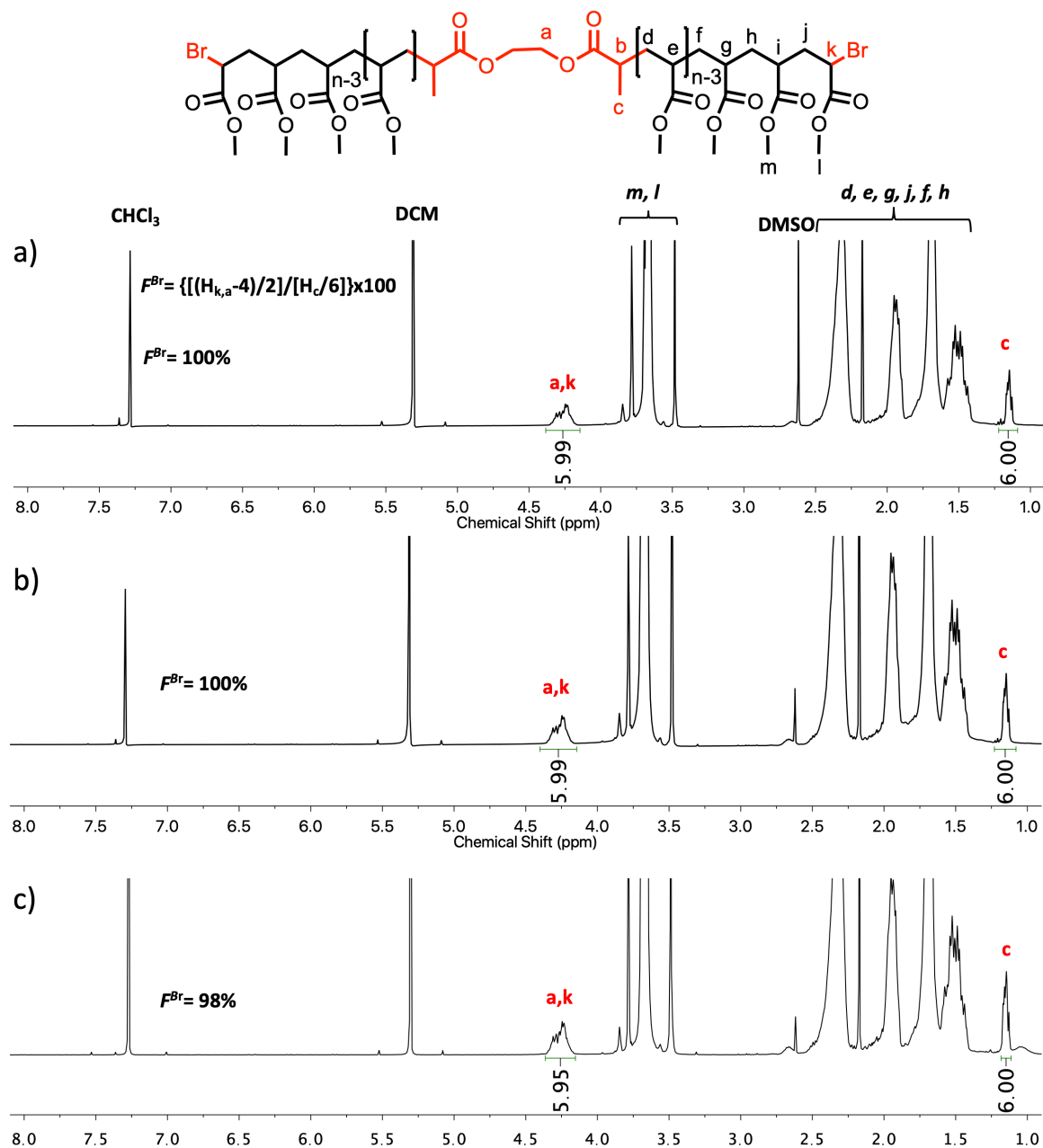
Figure 2.8. ^{1}H NMR spectra at 400 MHz of α,ω-di(bromo)PMA at (a) 94% conversion ($M_n = 8620$ and $M_w/M_n = 1.22$; [MA]$_0$/[BPE]$_0$/[Me$_6$-TREN]$_0$ = 60/1/0.2); (b) 90% conversion ($M_n = 9090$ and $M_w/M_n = 1.41$; [MA]$_0$/[BPE]$_0$/[Me$_6$-TREN]$_0$/[TREN]$_0$ = 60/1/0.1/0.1); (c) 96% conversion ($M_n = 7384$ and $M_w/M_n = 1.23$; [MA]$_0$/[BPE]$_0$/[TREN]$_0$ = 60/1/0.2); Polymerization conditions: MA = 2 mL, DMSO = 1.0 mL, and nonactivated 9 cm Cu(0) wire of 20 gauge. The signals at 7.26 and 5.30 ppm are due to partially nondeuterated residue of CDCl$_3$ and dichloromethane, respectively. F^{Br} values refer to chain-end functionality of PMA before thio-bromo "click" reaction (%).
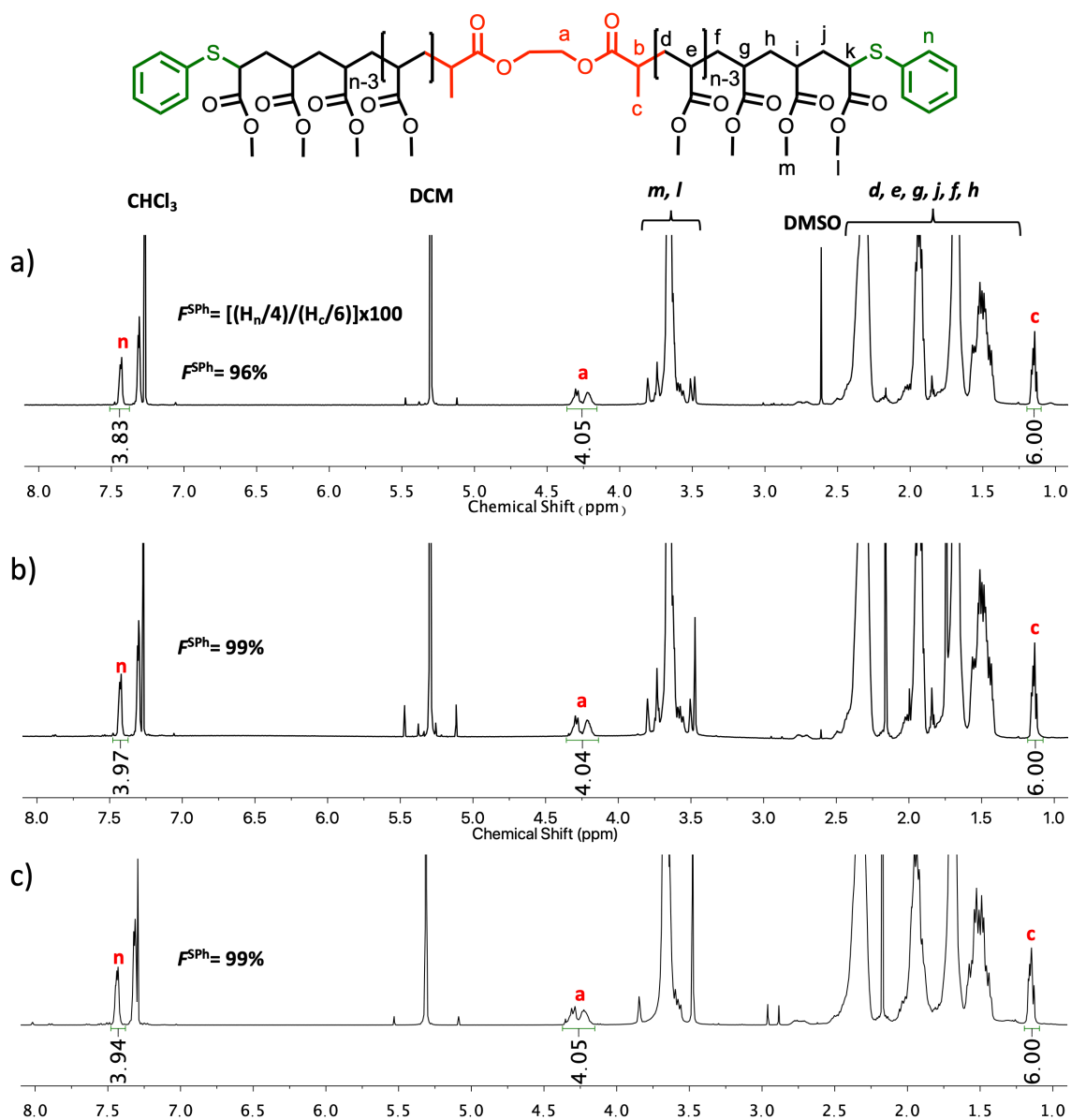
Figure 2.9 ¹H NMR spectra at 400 MHz of α,ω-di(phenylthio)PMA at (a) 94% conversion (M_n = 8620 and M_w/M_n = 1.22; [MA]₀/[BPE]₀/[Me₆-TREN]₀ = 60/1/0.2); (b) 90% conversion (M_n = 9090 and M_w/M_n = 1.41; [MA]₀/[BPE]₀/[Me₆-TREN]₀/[TREN]₀ = 60/1/0.1/0.1); (c) 96% conversion (M_n = 7380 and M_w/M_n = 1.23; [MA]₀/[BPE]₀/[TREN]₀ = 60/1/0.2);Conditions: MA = 2 mL, DMSO = 1.0 mL, and nonactivated 9 cm Cu(0) wire of 20 gauge wire. The signals at 7.26 and 5.30 ppm are due to a partially nondeuterated residue of CDCl₃ and dichloromethane, respectively. F^{SPh} values refer to chain-end functionality of PMA after a thio-bromo "click" reaction (%).
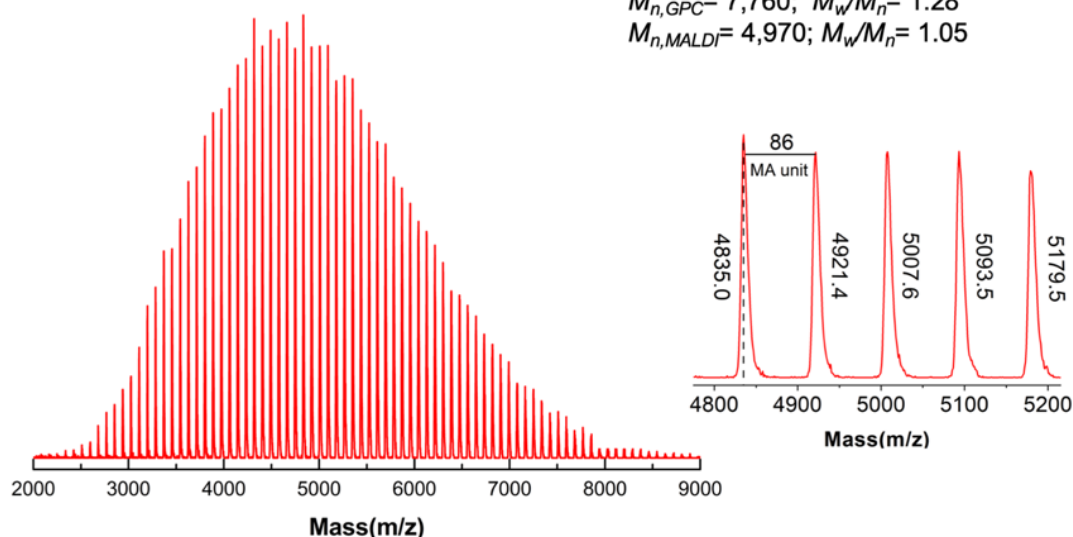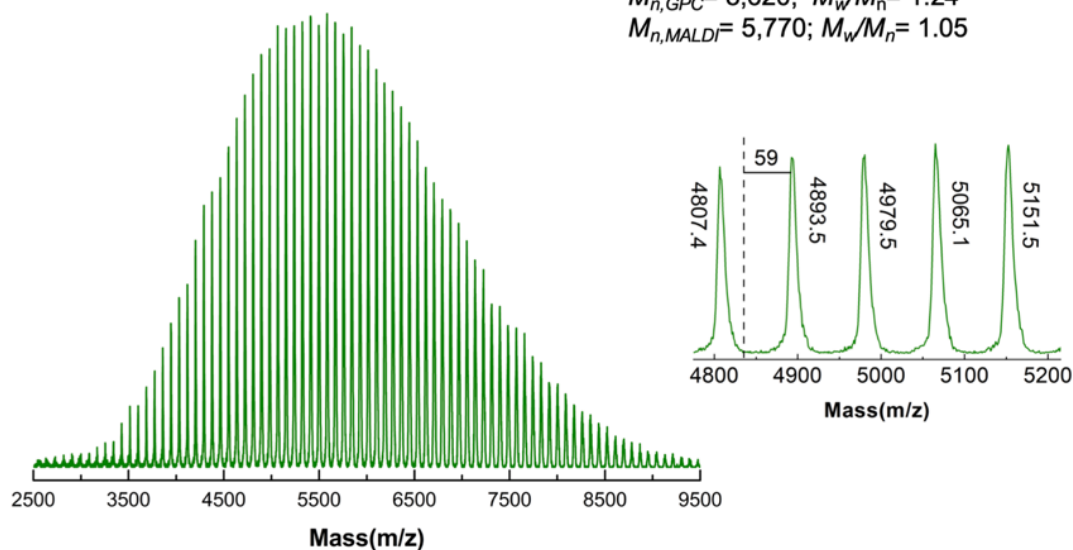
Figure 2.10. MALDI-TOF of PMA-Br isolated at 94% from SET-LRP of MA in DMSO solution initiated with BPE and catalyzed by nonactivated Cu(0) wire at 25 °C. (a) Before "thio-bromo click" reaction. (b) After "thio-bromo click" reaction. Reaction conditions: MA = 2 mL, DMSO = 1.0 mL, $[MA]_0/[BPE]_0/[Me_6\text{-}TREN]_0 = 60/1/0.2$, 9.0 cm of 20 gauge Cu(0) wire. The dotted line in expansion after thioeterification shows the original peak from before thioeterification, while 59 represents the increase in molar mass after thioeterification, that is, $2*[SC_6H_5 (109, 2)–Br (79, 9)] = 58.57$ for each chain-end.

a) PMA before thioetherification
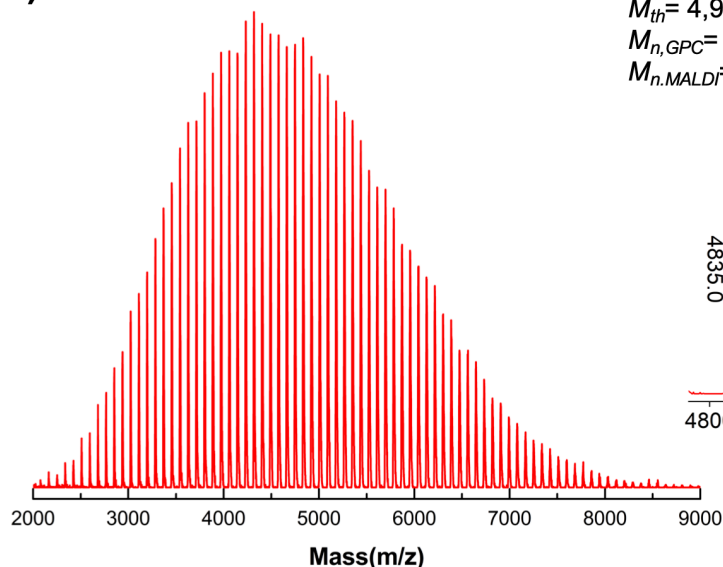
Conversion = 90%
M_{th} = 4,980
$M_{n,GPC}$ = 8,310; M_w/M_n = 1.44
$M_{n.MALDI}$ = 4,790; M_w/M_n = 1.06

86
MA unit

4835.0
4921.4
5007.6
5093.5
5179.5

Mass(m/z)

Mass(m/z)
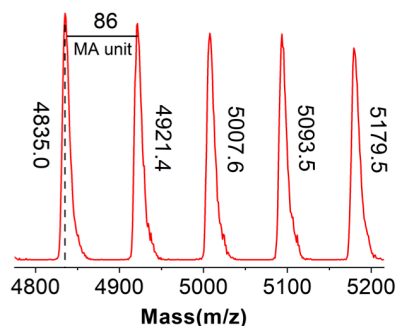
b) PMA after thioetherification
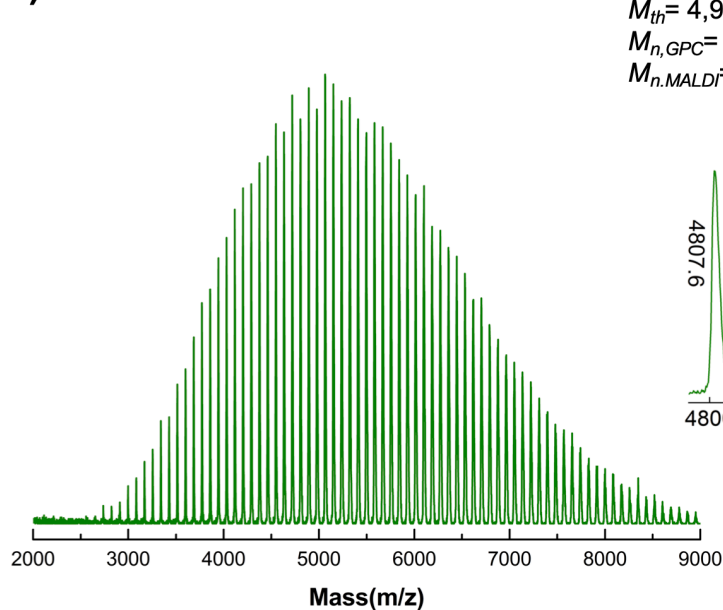
Conversion = 90%
M_{th} = 4,980
$M_{n,GPC}$ = 9,090; M_w/M_n = 1.41
$M_{n.MALDI}$ = 5,470; M_w/M_n = 1.05

59

4807.6
4893.5
4979.0
5065.1
5151.0

Mass(m/z)

Mass(m/z)
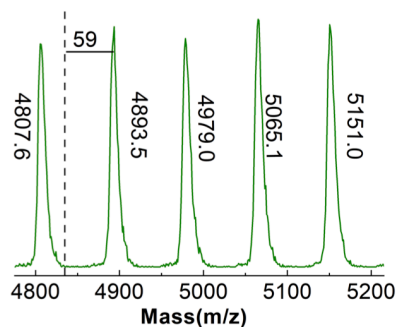
Figure 2.11. MALDI-TOF of PMA-Br isolated at 90% from SET-LRP of MA in DMSO solution initiated with BPE and catalyzed by a nonactivated Cu(0) wire at 25 °C: (a) Before the "thio-bromo click" reaction; (b) After the "thio-bromo click" reaction. Reaction conditions: MA = 2 mL, DMSO = 1.0 mL, $[MA]_0/[BPE]_0/[Me_6\text{-}TREN]_0/[TREN]_0$ = 60/1/0.1/0.1, 9.0 cm of 20 gauge Cu(0) wire. The dotted line in expansion after thioetherification shows the original peak from before thioetherification, while 59 represents the increase in molar mass after thioetherification, that is, $2*[SC_6H_5 (109, 2)–Br (79, 9)]$ = 58.57 for each chain end.

a) PMA before thioetherification

Conversion = 96%
M_{th}= 5,290
$M_{n,GPC}$= 6,830; M_w/M_n= 1.23
$M_{n,MALDI}$= 4,790; M_w/M_n= 1.06

86
MA unit

4835.4
4921.6
5007.6
5094.7

b) PMA after thioetherification

Conversion = 96%
M_{th}= 5,290
$M_{n,GPC}$= 7,380; M_w/M_n= 1.18
$M_{n,MALDI}$= 5,220; M_w/M_n= 1.05

59

4809.3
4895.4
4981.4
5069.2
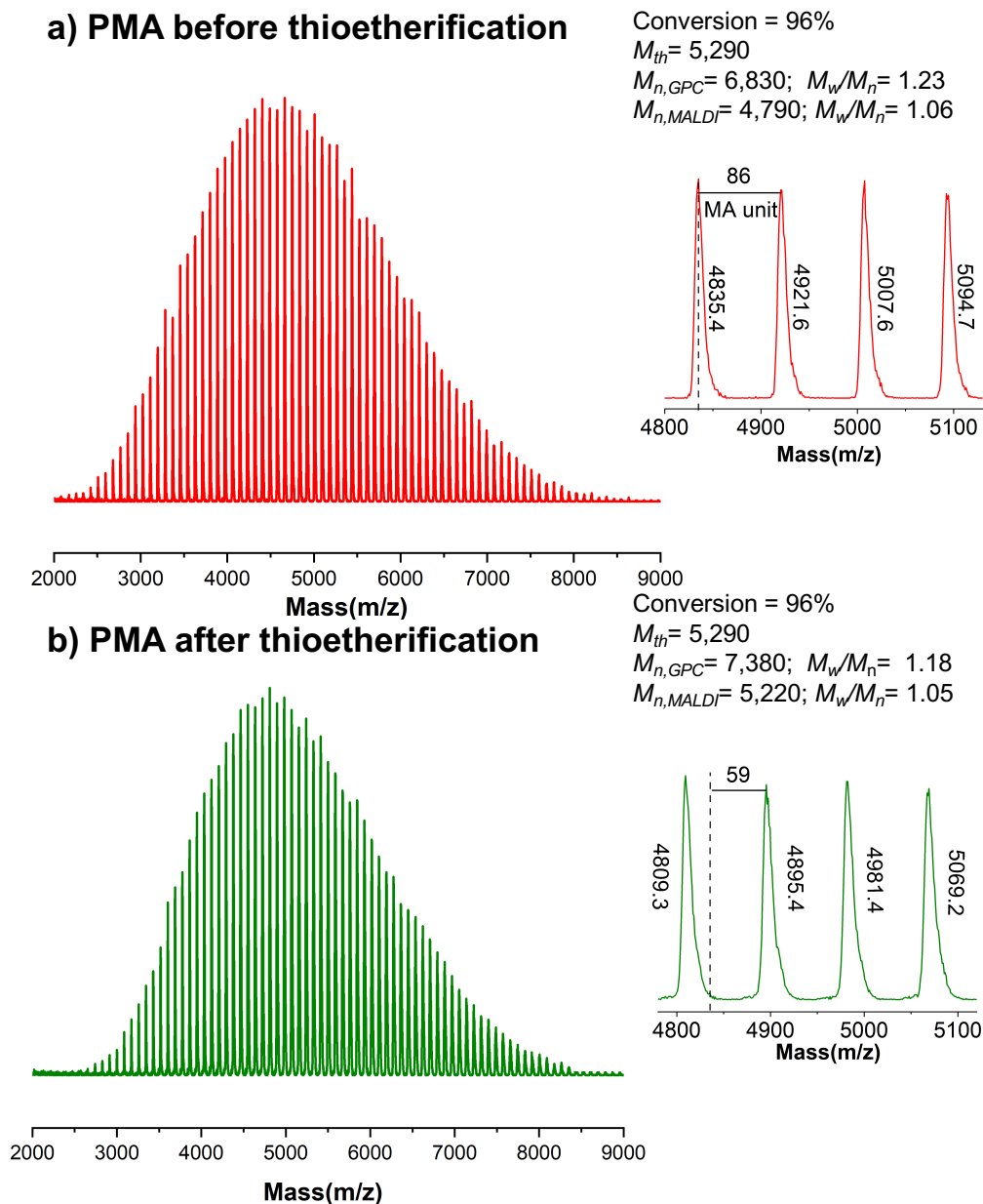
Figure 2.12. MALDI-TOF of PMA-Br isolated at 96% from SET-LRP of MA in DMSO solution initiated with BPE and catalyzed by nonactivated Cu(0) wire at 25 °C: (a) Before the "thio-bromo click" reaction; (b) After the "thio-bromo click" reaction. Reaction conditions: MA = 2 mL, DMSO = 1.0 mL, $[MA]_0/[BPE]_0/[TREN]_0$ = 60/1/0.2, 9.0 cm of 20 gauge Cu(0) wire. The dotted line in expansion after thioetherification shows the original peak from before thioetherification, while 59 represents the increase in molar mass after thioetherification, that is, $2*[SC_6H_5$ (109, 2)–Br (79, 9)] = 58.57 for each chain end.

Structural Analysis by MALDI-TOF Before and After Thio-Bromo "Click" Reaction

Representative MALDI-TOF spectra of PMA synthesized using Me$_6$-TREN, TREN, and equimolar amounts of Me$_6$-TREN and TREN isolated in between 90% and 96% conversion were analyzed before and after thioetherification (**Figures 2.10, 2.11, and 2.12**). The polymers isolated after SET-LRP at very high conversions showed one molecular weight distribution that was assigned to the bromine-terminated PMA ionized with Na$^+$.

After thioetherification, the original peaks disappeared and reappeared at 59 mass units higher mass values. This is the expected mass difference value for the replacement of −Br atoms (2×79.9) by −SPh moieties (2×109.2) at both polymer chain-ends.

MALDI-TOF analysis of PMA prepared using Me$_6$-TREN and TREN showed also high levels of chain-end functionality (**Figures 2.10, 2.11, and 2.12**, respectively). This demonstrates again the role of the catalytic activity of DMSO in transforming the neglected TREN into an excellent ligand for SET-LRP

Mixed-Ligand Effect Observed During SET-LRP of 2 mL of MA in 1.5 mL of DMSO Using Me$_6$-TREN, Me$_6$-TREN/TREN, and TREN as Ligands

Kinetic experiments for the SET-LRP of 2 mL of MA in 1.5 mL of DMSO performed with the mixed-ligand Me$_6$-TREN/TREN under similar reaction conditions to the experiments performed with 2 mL of MA in 1 mL of DMSO from **Figure 2.4** are reported in **Figure 2.13**.

The freeze-though process was identical in both series of experiments, and therefore, due to the larger scale of the experiments reported in **Figure 2.13**, a small induction period was observed in a few cases. All experiments from **Figure 2.13** were performed as triplicates. A comparison of the k_p^{app} values from **Figure 2.4** with the data from **Figure 2.13** indicates an increase in the k_p^{app} values by increasing the concentration of DMSO. An increase in the concentration of DMSO corresponds to a decrease in the concentration of MA and is expected to provide, under normal kinetic conditions, a decrease in the rate of polymerization. Therefore, the increased k_p^{app} values correspond to the catalytic effect of DMSO. Representative GPC experiments for the kinetics from **Figure 2.13** are reported in **Figure 2.14**.

The GPC traces from **Figure 2.14** provide the same trend with the corresponding data from **Figure 2.6**. Control experiments for the kinetic data reported in **Figure 2.13** are reported in **Figure 2.15**. Their GPC data are shown in **Figure 2.16**, while the summary of all results is reported in **Table 2.2**.

Figure 2.17 illustrates the results of the mixed-ligand effect performed with 2 mL of MA and 1.5 mL of DMSO. The control experiment data are also included in **Figure 2.17** to support the mixed-ligand effect. The most remarkable series of results comes from the comparison of the data from the mixed-ligand effect carried out with 2.0 mL of MA and

1.0 mL of DMSO versus 2.0 mL of MA and 1.5 mL of DMSO (compare **Figure 4** with **Figure 2.13** and **Figure 2.6 a** with **Figure 2.17**). This comparison is also made in **Table 2.3**. The most representative result from this comparison is that, while the k_p^{app} value for Me$_6$-TREN at 1 mL of DMSO is 1.30, the value of k_p^{app} for TREN at 1.5 mL of DMSO is 1.38. Therefore, TREN becomes at 1.5 mL of DMSO more efficient than Me$_6$-TREN at 1 mL of DMSO. This result explains the revitalization of TREN and its transformation into an excellent ligand by the catalytic effect of DMSO.

Structural Analysis of PMA Before and After Thio-Bromo "Click" Reaction

Structural analysis was performed by a combination of ^{1}H NMR and MALDI-TOF before and after thio-bromo "click" reaction (**Appendix 26–30**). The chain-end functionality of the PMA is 97% before thio-bromo "click" reaction and 98%, respectively, after thio-bromo "click" reaction, regardless of the structure of the ligand employed during SET-LRP (**Appendix 27 and 28**). These excellent results are confirmed by the MALDI-TOF analysis performed before and after thio-bromo "click" reactions (**Appendix 26, 29, and 30**).
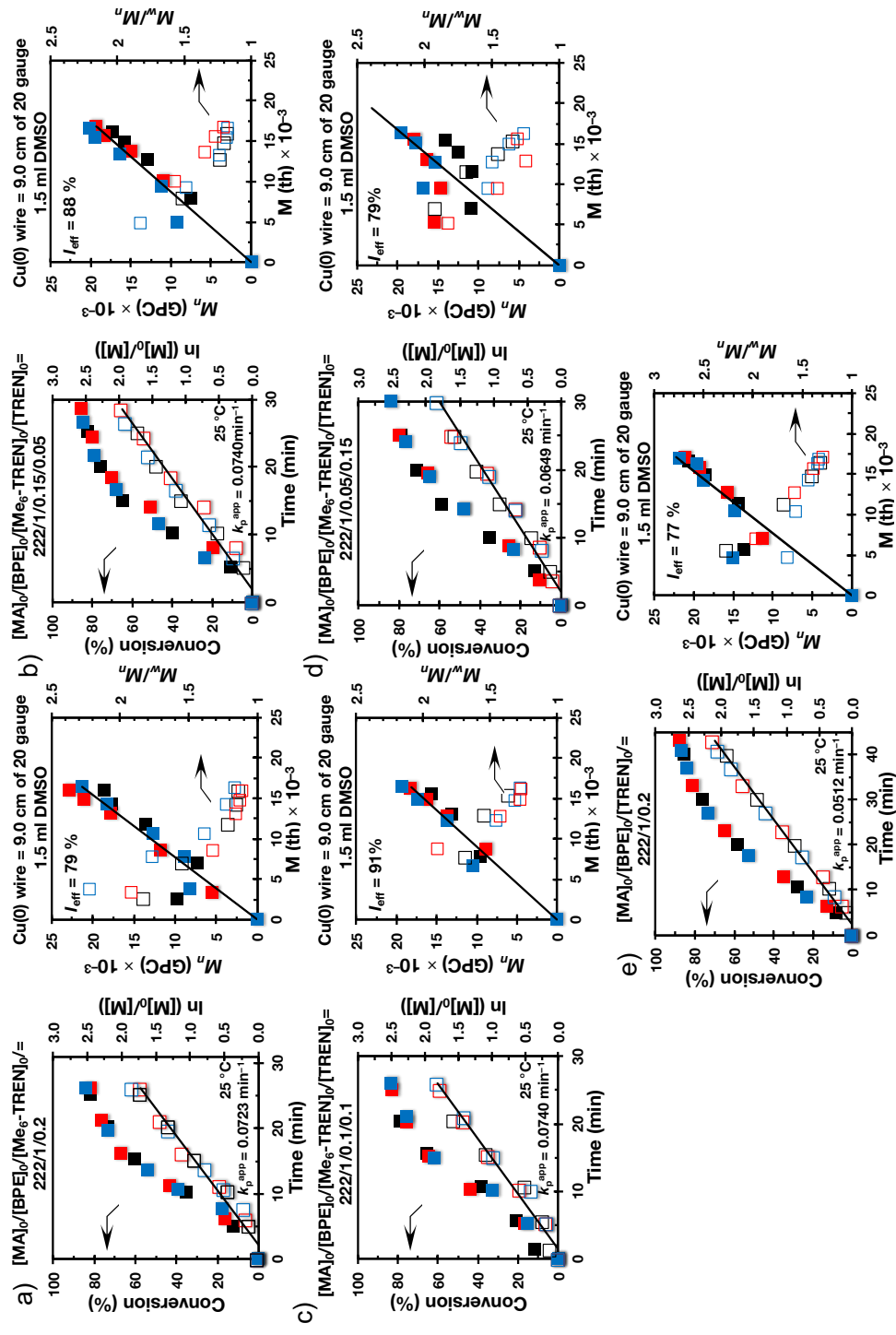
Figure 2.13. Kinetic plots, molecular weight, and dispersity evolutions for the SET-LRP of MA in DMSO, initiated with BPE and catalyzed by the 9.0 cm nonactivated Cu(0) wire at 25 °C. Experimental data in different colors were obtained from different kinetics experiments, carried out by different research. $k_p{}^{app}$ and I_{eff} are the average values of three experiments ([MA]$_0$/[BPE]$_0$/[ligand]$_0$/[Cu(0)]$_0$ = 222/1/0.2/9 cm); MA = 2 mL; DMSO = 1.5 mL.

49

a) [MA]$_0$/[BPE]$_0$/[Me$_6$-TREN]$_0$/[TREN]$_0$/Cu(0) wire= 222/1/0.2/0/9.0cm 20G 1.5 ml DMSO

M_n (th) = 3,390
M_n (GPC) = 5,590
M_w/M_n = 1.91

M_n (th) = 10,650
M_n (GPC) = 12,070
M_w/M_n = 1.40

M_n (th) = 16,000
M_n (GPC) = 22,850
M_w/M_n = 1.11

16%
54%
82%

b) [MA]$_0$/[BPE]$_0$/[Me$_6$-TREN]$_0$/[TREN]$_0$/Cu(0) wire= 222/1/0.15/0.05/9.0cm 20G 1.5 ml DMSO

M_n (th) = 4,920
M_n (GPC) = 9,280
M_w/M_n = 1.83

M_n (th) = 13,330
M_n (GPC) = 16,480
M_w/M_n = 1.24

M_n (th) = 16,580
M_n (GPC) = 20,260
M_w/M_n = 1.17

24%
68%
85%

c) [MA]$_0$/[BPE]$_0$/[Me$_6$-TREN]$_0$/[TREN]$_0$/Cu(0) wire= 222/1/0.1/0.1/9.0cm 20G 1.5 ml DMSO

M_n (th) = 6,670
M_n (GPC) = 10,410
M_w/M_n = 1.62

M_n (th) = 12,230
M_n (GPC) = 13,720
M_w/M_n = 1.45

M_n (th) = 16,330
M_n (GPC) = 19,270
M_w/M_n = 1.27

33%
62%
84%

d) [MA]$_0$/[BPE]$_0$/[Me$_6$-TREN]$_0$/[TREN]$_0$/Cu(0) wire= 222/1/0.05/0.15/9.0cm 20G 1.5 ml DMSO

M_n (th) = 5,300
M_n (GPC) = 15,460
M_w/M_n = 1.83

M_n (th) = 12,750
M_n (GPC) = 15,350
M_w/M_n = 1.50

M_n (th) = 16,390
M_n (GPC) = 19,670
M_w/M_n = 1.30

26%
65%
84%

e) [MA]$_0$/[BPE]$_0$/[Me$_6$-TREN]$_0$/[TREN]$_0$/Cu(0) wire= 222/1/0/0.2/9.0cm 20G 1.5 ml DMSO

M_n (th) = 5,680
M_n (GPC) = 13,610
M_w/M_n = 2.26

M_n (th) = 12,750
M_n (GPC) = 15,720
M_w/M_n = 1.58

M_n (th) = 17,150
M_n (GPC) = 21,210
M_w/M_n = 1.29

28%
65%
88%

Figure 2.14. Representative GPC traces of the evolution of molecular weight as a function of conversion for the SET-LRP of MA in a mixture of 1 mL of DMSO and catalyzed by the 9.0 cm nonactivated Cu(0) wire at 25 °C in the presence of various ligand compositions. Reaction conditions: MA = 2 mL, DMSO = 1.5 mL, [MA]$_0$/[BPE]$_0$/[L]$_0$ = 222/1/0.2.

Table 2.2. Dependence of k_p^{app} on the Dimension of the Cu(0) Wire in the SET-LRP of MA Initiated with BPE in 1.5 ml DMSO at 25 °C[a]

entry	Wire length (cm) 20G	Reaction condition	k_p^{app} (min^{-1})	M_w/M_n	I_{eff}(%)
1	9.0	[MA]/[BPE]/[Me$_6$-TREN] 222/1/0.2	0.0723	1.11	79
2	9.0	[MA]/[BPE]/[Me$_6$-TREN]/[TREN] 222/1/0.15/0.05	0.0740	1.17	88
3	9.0	[MA]/[BPE]/[Me$_6$-TREN]/[TREN] 222/1/0.1/0.1	0.0740	1.26	91
4	9.0	[MA]/[BPE]/[Me$_6$-TREN]/[TREN] 222/1/0.05/0.15	0.0649	1.26	79
5	9.0	[[MA]/[BPE]/[TREN] 222/1/0.2	0.0512	1.28	77
6	9.0	[MA]/[BPE]/[Me$_6$-TREN] 222/1/0.15	0.0679	1.13	78
7	9.0	[MA]/[BPE]/[Me$_6$-TREN] 222/1/0.10	0.0661	1.13	80
8	9.0	[MA]/[BPE]/[Me$_6$-TREN] 222/1/0.05	0.0547	1.10	76
9	9.0	[[MA]/[BPE]/[TREN] 222/1/0.15	0.0475	1.27	78
10	9.0	[[MA]/[BPE]/[TREN] 222/1/0.10	0.0415	1.27	78
11	9.0	[[MA]/[BPE]/[TREN] 222/1/0.05	0.0337	1.24	84

[a]Reaction conditions: monomer = 2 mL; solvent =1.5 mL.

Table 2.3. The Dependence of k_p^{app} on the 9cm 20 G of the Cu(0) Wire in the SET-LRP of MA Initiated with BPE in DMSO at 25 °C[a]

entry	Volume of DMSO (ml)	Reaction condition	k_p^{app} (min^{-1})	k_p^{app}/k_p^{app}(entry 10)	M_w/M_n	I_{eff}(%)
1	1.5	[MA]/[BPE]/[Me$_6$-TREN] 222/1/0.2	0.072	1.95	1.11	79
2	1.0	[MA]/[BPE]/[Me$_6$-TREN] 222/1/0.2	0.048	1.30	1.14	79
3	1.5	[MA]/[BPE]/[Me$_6$-TREN]/[TREN] 222/1/0.15/0.05	0.074	2.00	1.17	88
4	1.0	[MA]/[BPE]/[Me$_6$-TREN]/[TREN] 222/1/0.15/0.05	0.051	1.38	1.21	81
5	1.5	[MA]/[BPE]/[Me$_6$-TREN]/[TREN] 222/1/0.1/0.1	0.074	2.00	1.26	91
6	1.0	[MA]/[BPE]/[Me$_6$-TREN]/[TREN] 222/1/0.1/0.1	0.053	1.43	1.23	82
7	1.5	[MA]/[BPE]/[Me$_6$-TREN]/[TREN] 222/1/0.05/0.15	0.065	1.76	1.26	79
8	1.0	[MA]/[BPE]/[Me$_6$-TREN]/[TREN] 222/1/0.05/0.15	0.044	1.19	1.20	82
9	1.5	[[MA]/[BPE]/[TREN] 222/1/0.2	0.051	1.38	1.28	77
10	1.0	[[MA]/[BPE]/[TREN] 222/1/0.2	0.037	1.00	1.23	79

[a]Reaction conditions: MA = 2 mL.

51
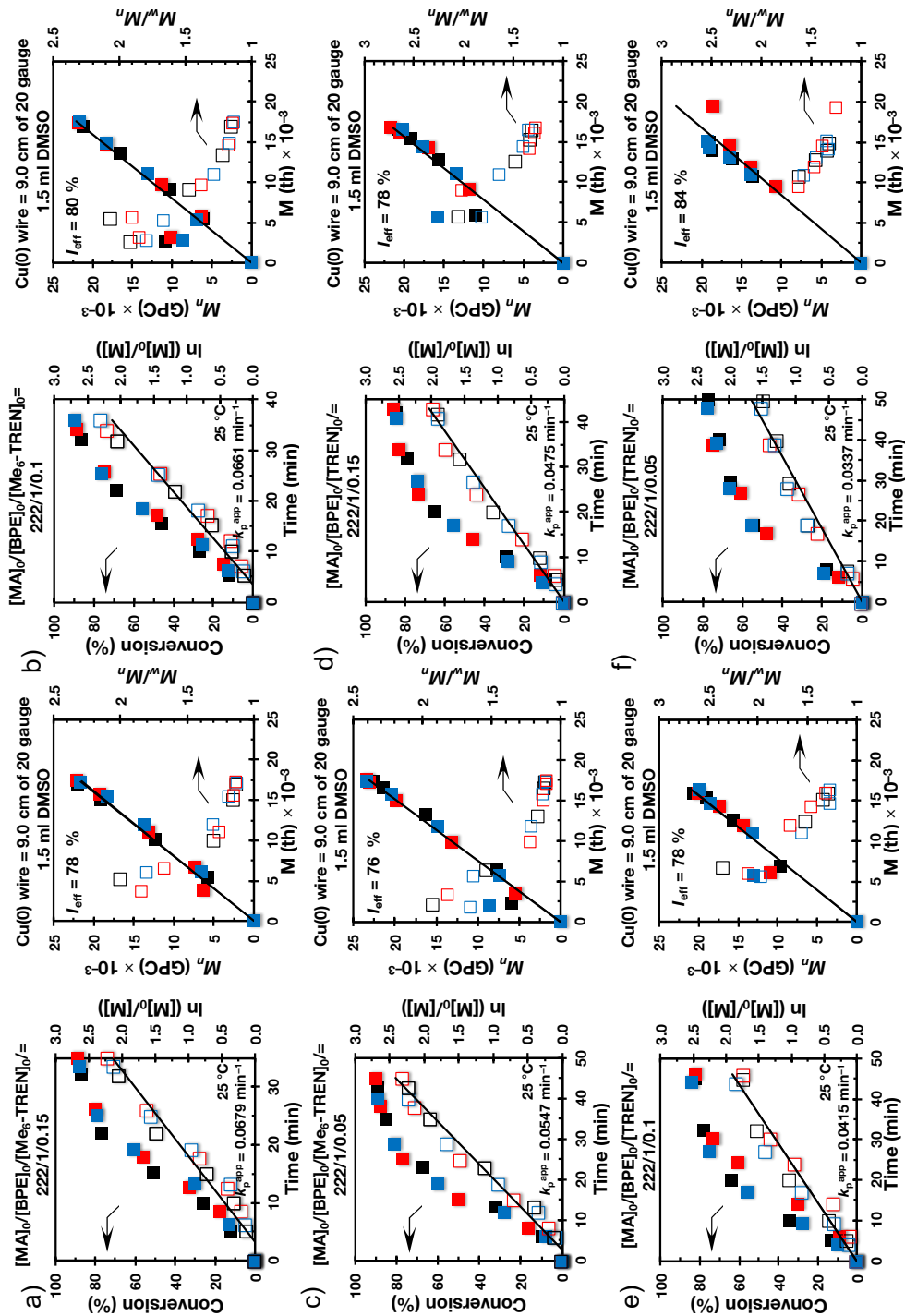
Figure 2.15. Control experiments: Kinetic plots, molecular weight, and dispersity evolutions for the SET-LRP of MA in DMSO, initiated with BPE and catalyzed by the 9.0 cm nonactivated Cu(0) wire at 25 °C. Experimental data in different colors were obtained from different kinetics experiments and generated by different research. k_p^{app} and I_{eff} is the average value of three experiment ($[MA]_0/[BPE]_0/[ligand]_0/[Cu(0)]_0 = 222/1/0.15$ to 0.05/9 cm); MA = 2 mL
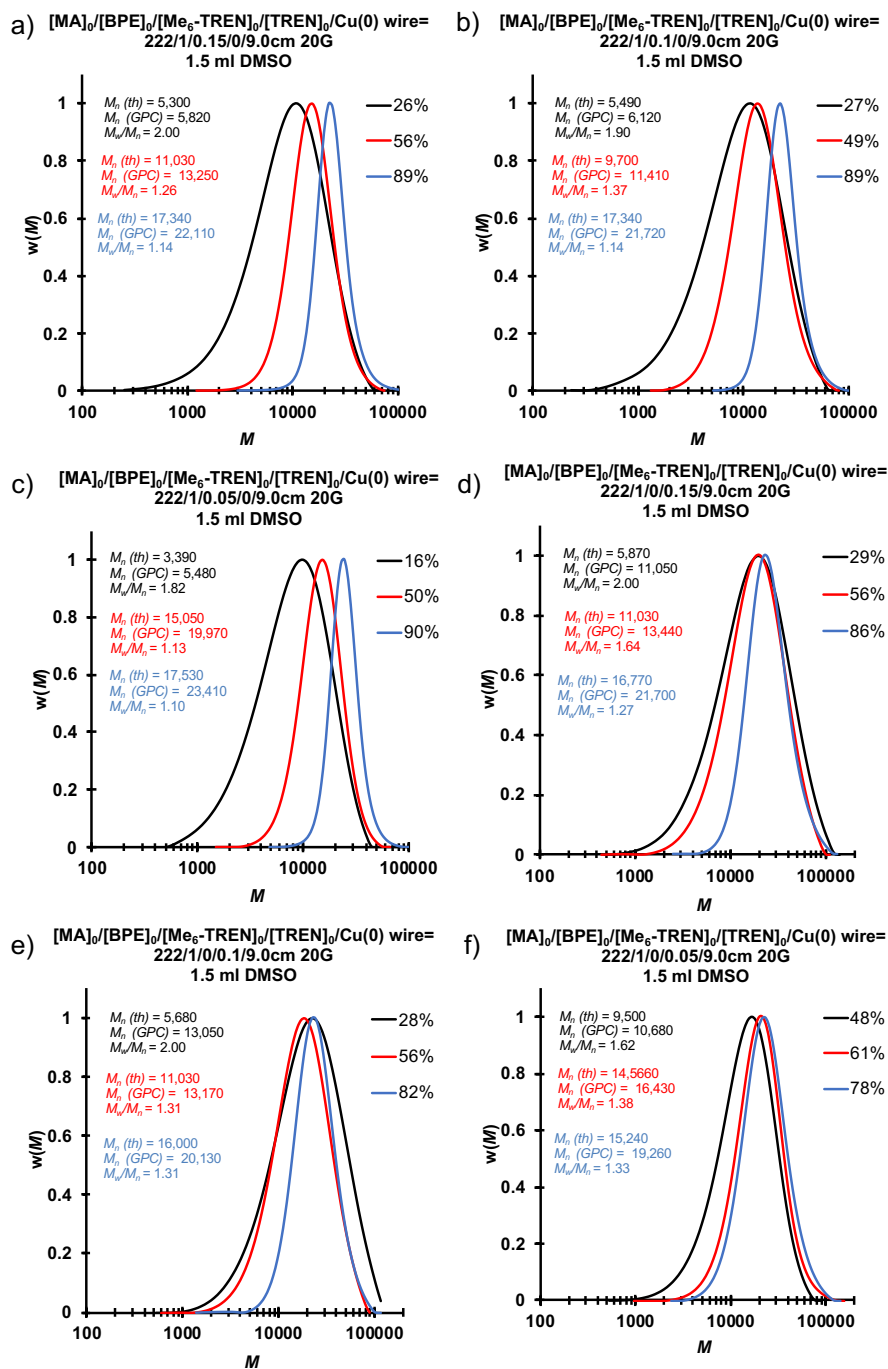
Figure 2.16. Representative GPC traces of the evolution of molecular weight as a function of conversion for the SET-LRP of MA in a mixture of 1 mL of DMSO and catalyzed by the 9.0 cm nonactivated Cu(0) wire at 25 °C in the presence of various ligand compositions. Conditions: MA = 2 mL, DMSO = 1.5 mL, ([MA]$_0$/[BPE]$_0$/[ligand]$_0$/[Cu(0)]$_0$ = 222/1/0.15 to 0.05/9 cm); MA = 2 mL.
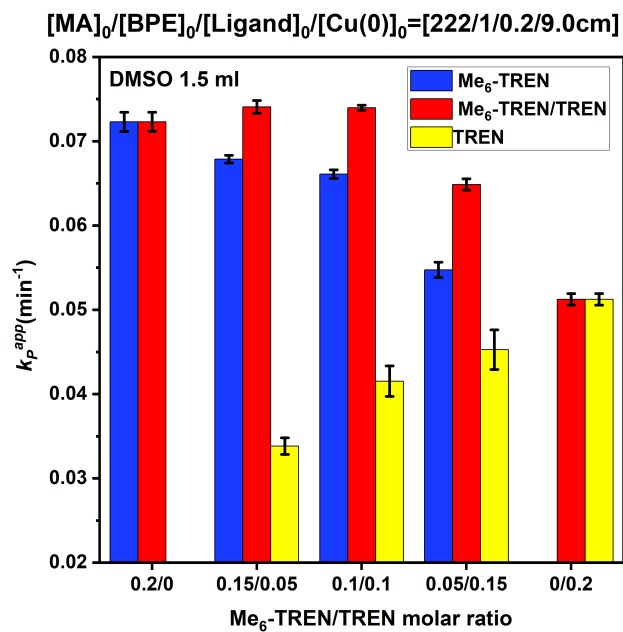
Figure 2.17. Evolution of k_p^{app} for the SET-LRP of MA (2 mL) initiated with BPE in DMSO (1.5 mL) mediated with different ratios between Me_6-TREN and TREN at 25 °C (in red). Control experiments performed only with Me_6-TREN (in blue) and only with TREN (in yellow) are also incorporated.

Conclusion

DMSO exhibits a catalytic effect when used as solvent during SET-LRP of MA initiated with BPE and catalyzed with nonactivated Cu(0) wire both in the presence of Me_6-TREN and TREN and in mixtures of Me_6-TREN with TREN. A mixed-ligand effect was observed when mixtures of Me_6-TREN with TREN were used as ligands. The catalytic activity of DMSO can be exploited, as demonstrated here, to enhance the reactivity of TREN and of its 1/1 mixture with Me_6-TREN, while decreasing the basicity of the ligand and eliminating side reactions mediated by it. The most fundamental question related to this topic that must be addressed is the following: do all disproportionating solvents display a catalytic effect in SET-LRP or only DMSO? Research to address this question is in progress.

References

(1) Maurya, D. S.; Malik, A.; Feng, X.; Bensabeh, N.; Lligadas, G.; Percec, V. The Me_6-TREN/TREN Mixed-Ligand Effect During SET-LRP in the Catalytically Active DMSO Revitalizes TREN into an Excellent Ligand. *Biomacromolecules* **2020**, *21,* 1902-1919

(2) Reetz, M. T.; Sell, T.; Meiswinkel, A.; Mehler, G. A New Principle in Combinatorial Asymmetric Transition-Metal Catalysis: Mixtures of Chiral Monodentate P Ligands. *Angew. Chem., Int. Ed.* **2003**, *42*, 790– 793.

(3) Duursma, A.; Hoen, R.; Schuppan, J.; Hulst, R.; Minnaard, A. J.; Feringa, B. L. First Examples of Improved Catalytic Asymmetric C-C Bond Formation Using the Monodentate Ligand Combination Approach. *Org. Lett.* **2003**, *5*, 3111– 3113.

(4) Fors, B. P.; Buchwald, S. L. A Multiligand Based Pd Catalyst for C-N Cross-Coupling Reactions. *J. Am. Chem. Soc.* **2010**, *132*, 15914– 15917.

(5) Fan, Y.; Xia, Y.; Tang, J.; Ziarelli, F.; Qu, F.; Rocchi, P.; Iovanna, J. L.; Peng, L. An Efficient Mixed-Ligand Pd Catalytic System to Promote C-N Coupling for the Synthesis of N-Arylaminotriazole Nucleosides. *Chem. - Eur. J.* **2012**, *18*, 2221– 2225.

(6) Cong, M.; Fan, Y.; Raimundo, J. M.; Xia, Y.; Liu, Y.; Quéléver, G.; Qu, F.; Peng, L. C-S Coupling Using a Mixed-Ligand Pd Catalyst: A Highly Effective Strategy for Synthesizing Arylthio-Substituted Heterocycles. *Chem. - Eur. J.* **2013**, *19*, 17267– 17272.

(7) (a) Percec, V.; Golding, G. M.; Smidrkal, J.; Weichold, O. $NiCl_2$(dppe)-Catalyzed Cross-Coupling of Aryl Mesylates, Arenesulfonates, and Halides with Arylboronic Acids. *J. Org. Chem.* **2004**, *69*, 3447– 3452. (b) Wilson, D. A.; Wilson, C. J.; Rosen, B. M.; Percec, V. Two-Step, One-Pot Ni-Catalyzed Neopentylglycolborylation and Complementary Pd/Ni-Catalyzed Cross-Coupling with Aryl Halides, Mesylates, and Tosylates. *Org. Lett.* **2008**, *10*, 4879– 4882. (c) Moldoveanu, C.; Wilson, D. A.; Wilson, C. J.; Corcoran, P.; Rosen, B. M.; Percec, V. Neopentylglycolborylation of Aryl Chlorides Catalyzed by the Mixed Ligand System $NiCl_2$(dppp)/dppf. *Org. Lett.* **2009**, *11*, 4974– 4977. (d) Wilson, D. A.; Wilson, C. J.; Moldoveanu, C.; Resmerita, A. M.; Corcoran, P.; Hoang, L. M.; Rosen, B. M.; Percec, V. Neopentylglycolborylation of Aryl Mesylates and Tosylates Catalyzed by Ni-Based Mixed-Ligand Systems Activated with Zn. *J. Am. Chem. Soc.* **2010**, *132*, 1800– 1801. (e) Leowanawat, P.; Resmerita, A. M.; Moldoveanu, C.; Liu, C.; Zhang, N.; Wilson, D. A.; Hoang, L. M.; Rosen, B. M.; Percec, V. Zero-Valent Metals Accelerate the Neopentylglycolborylation of Aryl Halides Catalyzed by $NiCl_2$-Based Mixed-Ligand Systems. *J. Org. Chem.* **2010**, *75*, 7822– 7828. (f) Moldoveanu, C.; Wilson, D. A.; Wilson, C. J.; Leowanawat, P.; Resmerita, A. M.; Liu, C.; Rosen, B. M.; Percec, V. *J. Org. Chem.* **2010**, *75*, 5438– 5452. (g) Leowanawat, P.; Zhang, N.; Resmerita, A.-M.; Rosen, B. M.; Percec, V. $Ni(COD)_2$/PCy_3 Catalyzed Cross-Coupling of Aryl and Heteroaryl Neopentylglycolboronates with Aryl and Heteroaryl Mesylates and Sulfamates in THF at Room Temperature. *J. Org. Chem.* **2011**, *76*, 9946– 9955. (h) Leowanawat, P.; Zhang, N.; Safi, M.; Hoffman, D. J.; Fryberger, M. C.; George, A.; Percec, V. trans-Chloro(1-Naphthyl)bis(triphenylphosphine)nickel(II)/PCy_3 Catalyzed Cross-Coupling of Aryl and Heteroaryl Neopentylglycolboronates with Aryl and Heteroaryl Mesylates and Sulfamates at Room Temperature. *J. Org. Chem.* **2012**, *77,*

2885– 2892. (i) Leowanawat, P.; Zhang, N.; Percec, V. Nickel Catalyzed Cross-Coupling of Aryl C-O Based Electrophiles with Aryl Neopentylglycolboronates. *J. Org. Chem.* **2012**, *77*, 1018– 1025. j) Zhang, N.; Hoffman, D. J.; Gutsche, N.; Gupta, J.; Percec, V. Comparison of Arylboron-Based Nucleophiles in Ni-Catalyzed Suzuki-Miyaura Cross-Coupling with Aryl Mesylates and Sulfamates. *J. Org. Chem.* **2012**, *77*, 5956– 5964. (k) Leowanawat, P.; Zhang, N.; Safi, M.; Hoffman, D. J.; Fryberger, M. C.; George, A.; Percec, V. trans-Chloro(1-Naphthyl)bis(triphenylphosphine) nickel(II)/PCy$_3$ Catalyzed Cross-Coupling of Aryl and Heteroaryl Neopentylglycolboronates with Aryl and Heteroaryl Mesylates and Sulfamates at Room Temperature. *J. Org. Chem.* **2012**, *77*, 2885– 2892.(l) Malineni, J.; Jezorek, R. L.; Zhang, N.; Percec, V. An Indefinitely Air-Stable σ-Ni^{II} Precatalyst for Quantitative Cross-Coupling of Unreactive Aryl Halides and Mesylates with Aryl Neopentylglycolboronates. *Synthesis* **2016**, *48*, 2795– 2807.m) Malineni, J.; Jezorek, R. L.; Zhang, N.; Percec, V. Ni^{II}Cl(1-Naphthyl)(PCy$_3$)$_2$, An Air-Stable σ-Ni^{II}Precatalyst for Quantitative Cross-Coupling of Aryl C-O Electrophiles with Aryl Neopentylglycolboronates. *Synthesis* **2016**, *48*, 2808– 2815,.

(8) Li, K.-T.; Shieh, D. C. Polymerization of 2,6-Dimethylphenol with Mixed-Ligand Copper Complexes. *Ind. Eng. Chem. Res.* **1994**, *33*, 1107– 1112.

(9) Matyjaszewski, K.; Wei, M.; Xia, J.; McDermott, N. E. Controlled/"Living" Radical Polymerization of Styrene and Methyl Methacrylate Catalyzed by Iron Complexes. *Macromolecules* **1997**, *30*, 8161– 8164.

(10) Iizuka, E.; Wakioka, M.; Ozawa, F. Mixed-Ligand Approach to Palladium-Catalyzed Direct Arylation Polymerization: Synthesis of Donor-Acceptor Polymers with Dithienosilole (DTS) and Thienopyrroledione (TPD) Units. *Macromolecules* **2015**, *48* (9), 2989– 2993.

(11) Feng, X.; Maurya, D. S.; Bensabeh, N.; Moreno, A.; Oh, T.; Luo, Y.; Lejnieks, J.; Galià, M.; Miura, Y.; Monteiro, M. J.; Lligadas, G.; Percec, V. Replacing Cu(II)Br$_2$ with Me$_6$-TREN in Biphasic Cu(0)/TREN Catalyzed SET-LRP Reveals the Mixed-Ligand Effect. *Biomacromolecules* **2020**, *21*, 250– 261.

(12) (a) Percec, V.; Guliashvili, T.; Ladislaw, J. S.; Wistrand, A.; Stjerndahl, A.; Sienkowska, M. J.; Monteiro, M. J.; Sahoo, S. Ultrafast Synthesis of Ultrahigh Molar Mass Polymers by Metal-Catalyzed Living Radical Polymerization of Acrylates, Methacrylates, and Vinyl Chloride Mediated by SET at 25 °C. *J. Am. Chem. Soc.* **2006**, *128*, 14156– 14165. (b) Percec, V.; Popov, A. V.; Ramirez-Castillo, E.; Monteiro, M.; Barboiu, B.; Weichold, O.; Asandei, A. D.; Mitchell, C. M. Aqueous Room Temperature Metal-Catalyzed Radical Polymerization of Vinyl Chloride. *J. Am. Chem. Soc.* **2002**, *124*, 4940– 4941.

(13) Rosen, B. M.; Percec, V. Single-Electron Transfer and Single-Electron Transfer Degenerative Chain Transfer Living Radical Polymerization. *Chem. Rev.* **2009**, *109*, 5069– 5119.

(14) Zhang, N.; Samanta, S. R.; Rosen, B. M.; Percec, V. Single Electron Transfer in Radical Ion and Radical-Mediated Organic, Materials and Polymer Synthesis. *Chem. Rev.* **2014**, *114*, 5848– 5958.

(15) Lligadas, G.; Grama, S.; Percec, V. Single-Electron Transfer Living Radical Polymerization Platform to Practice, Develop and Invent. *Biomacromolecules* **2017**, *18*, 2981– 3008.

(16)   Boyer, C.; Corrigan, N. A.; Jung, K.; Nguyen, D.; Nguyen, T. K.; Adnan, N. N.; Oliver, S.; Shanmugam, S.; Yeow, J. Copper-Mediated Living Radical Polymerization (Atom Transfer Polymerization and Copper(0) Mediated Polymerization): From Fundamentals to Bioapplications. *Chem. Rev.* **2016**, *116*, 1803– 1949.

(17)   Anastasaki, A.; Nikolaou, V.; Nurumbetov, G.; Wilson, O.; Kempe, K.; Quinn, J. F.; Davis, T. P.; Whittaker, M. R.; Haddleton, D. M. Cu(0)-Mediated Living Radical Polymerization: a Versatile Tool for Materials Synthesis. *Chem. Rev.* **2016**, *116*, 835– 877.

(18)   Anastasaki, A.; Nikolaou, V.; Haddleton, D. M. Cu(0)-Mediated Living Radical Polymerization: Recent Highlights and Applications: a Perspective. *Polym. Chem.* **2016**, *7*, 1002– 1026,.

(19)   Rosen, B. M.; Jiang, X.; Wilson, C. J.; Nguyen, N. H.; Monteiro, M. J.; Percec, V. The Disproportionation of Cu(I)X Mediated by Ligand and Solvent Into Cu(0) and Cu(II)X$_2$ and Its Implications for SET-LRP. *J. Polym. Sci., Part A: Polym. Chem.* **2009**, *47*, 5606– 5628,.

(20)   (a) Levere, M. E.; Nguyen, N. H.; Leng, X.; Percec, V. Visualization of the Crucial Step in SET-LRP. *Polym. Chem.* **2013**, *4*, 1635– 1647. (b) Jiang, X.; Rosen, B. M.; Percec, V. Mimicking "Nascent" Cu(0) Mediated SET-LRP of Methyl Acrylate in DMSO Leads to Complete Conversion in Several Minutes. *J. Polym. Sci., Part A: Polym. Chem.* **2010**, *48*, 403– 409. (c) Lligadas, G.; Percec, V. A Comparative Analysis of SET-LRP of MA in Solvents Mediating Different Degrees of Disproportionation of Cu(I)Br. *J. Polym. Sci., Part A: Polym. Chem.* **2008**, *46*, 6880– 6895. d) Nguyen, N. H.; Kulis, J.; Sun, H.-J.; Jia, Z.; van Beusekom, B.; Levere, M. E.; Wilson, D. A.; Monteiro, M. J.; Percec, V. A Comparative Study of the SET-LRP of Oligo(Ethylene Oxide) Methyl Ether Acrylate in DMSO and in H$_2$O. *Polym. Chem.* **2013**, *4*, 144– 155.(e) Jiang, X.; Fleischmann, S.; Nguyen, N. H.; Rosen, B. M.; Percec, V. Cooperative and Synergistic Solvent Effects in SET-LRP of MA. *J. Polym. Sci., Part A: Polym. Chem.* **2009**, *47*, 5591– 5605.(f) Bunnett, J. F.; Scamehorn, R. G.; Traber, R. P. Solvents for Aromatic SRN1 Reactions. *J. Org. Chem.* **1976**, *41*, 3677– 3682,.

(21)   Rosen, B. M.; Percec, V. A Density Functional Theory Computational Study of the Role of Ligand on the Stability of Cu(I) and Cu(II) Species Associated with ATRP and SET-LRP. *J. Polym. Sci., Part A: Polym. Chem.* **2007**, *45*, 4950– 4964.

(22)   Sienkowska, M. J.; Rosen, B. M.; Percec, V. SET-LRP of Vinyl Chloride Initiated with CHBr$_3$ in DMSO at 25 °C. *J. Polym. Sci., Part A: Polym. Chem.* **2009**, *47*, 4130– 4140.

(23)   Hatano, T.; Rosen, B. M.; Percec, V. SET-LRP of Vinyl Chloride Initiated with CHBr$_3$ and Catalyzed by Cu(0)-Wire/TREN in DMSO at 25 °C. *J. Polym. Sci., Part A: Polym. Chem.* **2010**, *48*, 164– 172.

(24)   Percec, V.; Popov, A. V.; Ramirez-Castillo, E.; Weichold, O. Living Radical Polymerization of Vinyl Chloride Initiated with Iodoform and Catalyzed by Nascent Cu(0)/Tris(2-aminoethyl)amine or Polyethyleneimine in Water at 25 °C Proceeds by a New Competing Pathways Mechanism. *J. Polym. Sci., Part A: Polym. Chem.* **2003**, *41*, 3283– 3299,.

(25)   Nguyen, N. H.; Levere, M. E.; Percec, V. TREN versus Me$_6$-TREN as Ligands in SET-LRP of Methyl Acrylate. *J. Polym. Sci., Part A: Polym. Chem.* **2012**, *50*, 35– 46.

(26)   Nicol, E.; Derouineau, T.; Puaud, F.; Zaitsev, A. Synthesis of Double Hydrophilic Poly(ethylene oxide)-*b*-poly(2-hydroxyethyl acrylate) by Single-Electron Transfer-Living Radical Polymerization. *J. Polym. Sci., Part A: Polym. Chem.* **2012**, *50*, 3885–3894.

(27)   Nguyen, N. H.; Levere, M. E.; Percec, V. SET-LRP of Methyl Acrylate to Complete Conversion with Zero Termination. *J. Polym. Sci., Part A: Polym. Chem.* **2012**, *50*, 860– 873.

(28)   Voorhaar, L.; Wallyn, S.; Du Prez, F. E.; Hoogenboom, R. Cu(0)-Mediated Polymerization of Hydrophobic Acrylates Using High-Throughput Experimentation. *Polym. Chem.* **2014**, *5*, 4268– 4276,.

(29)   Simula, A.; Nikolaou, V.; Alsubaie, F.; Anastasaki, A.; Haddleton, D. M. The Effect of Ligand, Solvent and Cu(0) Source on the Efficient Polymerization of Polyether Acrylates and Methacrylates in Aqueous and Organic Media. *Polym. Chem.* **2015**, *6*, 5940– 5950.

(30)   Moreno, A.; Grama, S.; Liu, T.; Galià, M.; Lligadas, G.; Percec, V. SET-LRP Mediated by TREN in Biphasic Water-Organic Solvent Mixtures Provides the Most Economical and Efficient Process. *Polym. Chem.* **2017**, *8*, 7559– 7574.

(31)   Moreno, A.; Galià, M.; Lligadas, G.; Percec, V. SET-LRP in Biphasic Mixtures of the Nondisproportionating Solvent Hexafluoroisopropanol with Water. *Biomacromolecules* **2018**, *19*, 4480– 4491, DOI.

(32)   Moreno, A.; Liu, T.; Galià, M.; Lligadas, G.; Percec, V. Acrylate-Macromonomers and Telechelics of PBA by Merging Biphasic SET-LRP of BA, Chain Extension with MA and Biphasic Esterification. *Polym. Chem.* **2018**, *9*, 1961– 1971.

(33)   Moreno, A.; Jezorek, R. L.; Liu, T.; Galià, M.; Lligadas, G.; Percec, V. Macromonomers, Telechelics and More Complex Architectures of PMA by a Combination of Biphasic SET-LRP and Biphasic Esterification. *Polym. Chem.* **2018**, *9*, 1885– 1899.

(34)   Moreno, A.; Liu, T.; Ding, L.; Buzzacchera, I.; Galià, M.; Möller, M.; Wilson, C. J.; Lligadas, G.; Percec, V. SET-LRP in Biphasic Mixtures of Fluorinated Alcohols with Water. *Polym. Chem.* **2018**, *9*, 2313– 2327.

(35)   Jezorek, R. L.; Enayati, M.; Smail, R. B.; Lejnieks, J.; Grama, S.; Monteiro, M. J.; Percec, V. The Stirring Rate Provides a Dramatic Acceleration of the Ultrafast Interfacial SET-LRP in Biphasic Acetonitrile-Water Mixtures. *Polym. Chem.* **2017**, *8*, 3405– 3424.

(36)   Smail, R. B.; Jezorek, R. L.; Lejnieks, J.; Enayati, M.; Grama, S.; Monteiro, M. J.; Percec, V. Acetone-Water Biphasic Mixtures as Solvents for Ultrafast SET-LRP of Hydrophobic Acrylates. *Polym. Chem.* **2017**, *8*, 3102– 3123.

(37)   Enayati, M.; Jezorek, R. L.; Smail, R. B.; Monteiro, M. J.; Percec, V. Ultrafast SET-LRP in Biphasic Mixtures of the Non-Disproportionating Solvent Acetonitrile with Water. *Polym. Chem.* **2016**, *7*, 5930– 5942.

(38)   Enayati, M.; Smail, R. B.; Grama, S.; Jezorek, R. L.; Monteiro, M. J.; Percec, V. The Synergistic Effect During Biphasic SET-LRP in Ethanol-Nonpolar Solvent-Water Mixtures. *Polym. Chem.* **2016**, *7*, 7230– 7241.

(39)   Enayati, M.; Jezorek, R. L.; Monteiro, M. J.; Percec, V. Ultrafast SET-LRP of Hydrophobic Acrylates in Multiphase Alcohol-Water Mixtures. *Polym. Chem.* **2016**, *7*, 3608– 3621.

(40)   Grama, S.; Lejnieks, J.; Enayati, M.; Smail, R. B.; Ding, L.; Lligadas, G.; Monteiro, M. J.; Percec, V. Searching for Efficient SET-LRP Systems *via* Biphasic Mixtures of Water with Carbonates, Ethers and Dipolar Aprotic Solvents. *Polym. Chem.* **2017**, *8*, 5865– 5874.

(41)   Lligadas, G.; Percec, V. Synthesis of Perfectly Bifunctional Polyacrylates by Single-Electron-Transfer Living Radical Polymerization. *J. Polym. Sci., Part A: Polym. Chem.* **2007**, *45*, 4684– 4695.

(42)   Ciampolini, M.; Nardi, N. Five-Coordinated High-Spin Complexes of Bivalent Cobalt, Nickel, and Copper with Tris(2-dimethylaminoethyl)amine. *Inorg. Chem.* **1966**, *5*, 41– 44.

(43)   Nguyen, N. H.; Rosen, B. M.; Jiang, X.; Fleischmann, S.; Percec, V. New Efficient Reaction Media for SET-LRP Produced from Binary Mixtures of Organic Solvents and H_2O. *J. Polym. Sci., Part A: Polym. Chem.* **2009**, *47*, 5577– 5590.

(44)   Lligadas, G.; Rosen, B. M.; Bell, C. A.; Monteiro, M. J.; Percec, V. Effect of Cu(0) Particle Size on The Kinetics of SET-LRP in DMSO and Cu-Mediated Radical Polymerization in MeCN at 25°C. *Macromolecules* **2008**, *41*, 8365– 8371,.

(45)   Nguyen, N. H.; Rosen, B. M.; Lligadas, G.; Percec, V. Surface-Dependent Kinetics of Cu(0)-Wire-Catalyzed Single-Electron Transfer Living Radical Polymerization of Methyl Acrylate in DMSO at 25°C. *Macromolecules* **2009**, *42*, 2379– 2386.

(46)   Ahrland, S.; Rawsthorne, J.; Haaland, A.; Jerslev, B.; Schaffer, C. E.; Sunde, E.; Sørensen, N. A. The Stability of Metal Halide Complexes in Aqueous Solution. VII. The Chloride Complexes of Copper(I). *Acta Chem. Scand.* **1970**, *24*, 157– 172.

(47)   Ciavatta, L.; Ferri, D.; Palombari, R. On the equilibrium $Cu^{2+} + Cu(s) \rightleftarrows 2Cu^+$. *J. Inorg. Nucl. Chem.* **1980**, *42*, 593– 598.

(48)   Nguyen, N. H.; Sun, H.-J.; Levere, M. E.; Fleischmann, S.; Percec, V. Where is Cu(0) Generated by Disproportionation During SET-LRP?. *Polym. Chem.* **2013**, *4*, 1328– 1332.

(49)   (a) Negrel, J. C.; Gony, M.; Chanon, M.; Lai, R. Reactivity of Copper Metal Vapours with Substituted Bromobenzenes. Formation and Molecular Structure of $Cu(PMe_3)_3Br$. *Inorg. Chim. Acta* **1993**, *207*, 59– 63. (b) Julliard, M.; Chanon, M. Photoelectron Transfer Catalyst. *Chem. Scr.* **1894**, *4*, 11– 21 (c) Timms, P. L. Review Lecture: The Use of Free Atoms of Transition Metals in Chemical Synthesis. *Proc. R. Soc. London, Ser. A* **1984**, *396*, 1– 19. (d) Klabunde, K. J. Organic Chemistry of Metal Vapors. *Acc. Chem. Res.* **1975**, *8*, 393– 399.(e) Klabunde, K. J.; Li, Y. X.; Tan, B. J. Solvated Metal Atom Dispersed Catalyst. *Chem. Mater.* **1991**, *3*, 30– 39.

(50)   (a) Rosen, B. M.; Lligadas, G.; Hahn, C.; Percec, V. Synthesis of Dendrimers Through Divergent Iterative Thio-Bromo "Click" Chemistry. *J. Polym. Sci., Part A: Polym. Chem.* **2009**, *47*, 3931– 3939. (b) Rosen, B. M.; Lligadas, G.; Hahn, C.; Percec, V. Synthesis of Dendritic Macromolecules Through Divergent Iterative Thio-Bromo "Click" Chemistry and SET-LRP. *J. Polym. Sci., Part A: Polym. Chem.* **2009**, *47*, 3940– 3948

Appendices

Appendix 1. Evolution of M_w/M_n and I_{eff} for the SET-LRP of MA initiated with BPE in various "programmed" biphasic reaction mixtures at 25 °C. (a) NMP/water mixture (8/2, v/v) using 9.0 cm nonactivated Cu(0) wire as catalyst. (b) DMF/water mixture (8/2, v/v) using 9.0 cm of nonactivated Cu(0) wire as catalyst. (c) DMF/water mixture (8/2, v/v) using 4.0 cm of nonactivated Cu(0) wire as catalyst. (d) DMF/water mixture (8/2, v/v) using 12.5 cm of nonactivated Cu(0) wire as catalyst. (e) DMAc/water mixture (8/2, v/v) using 9.0 cm of nonactivated Cu(0) wire as catalyst. Reaction conditions: MA = 1 mL, organic solvent = 0.4 mL, water = 0.1 mL, and $[MA]_0/[BPE]_0/[L]_0 = 222/1/0.1$.
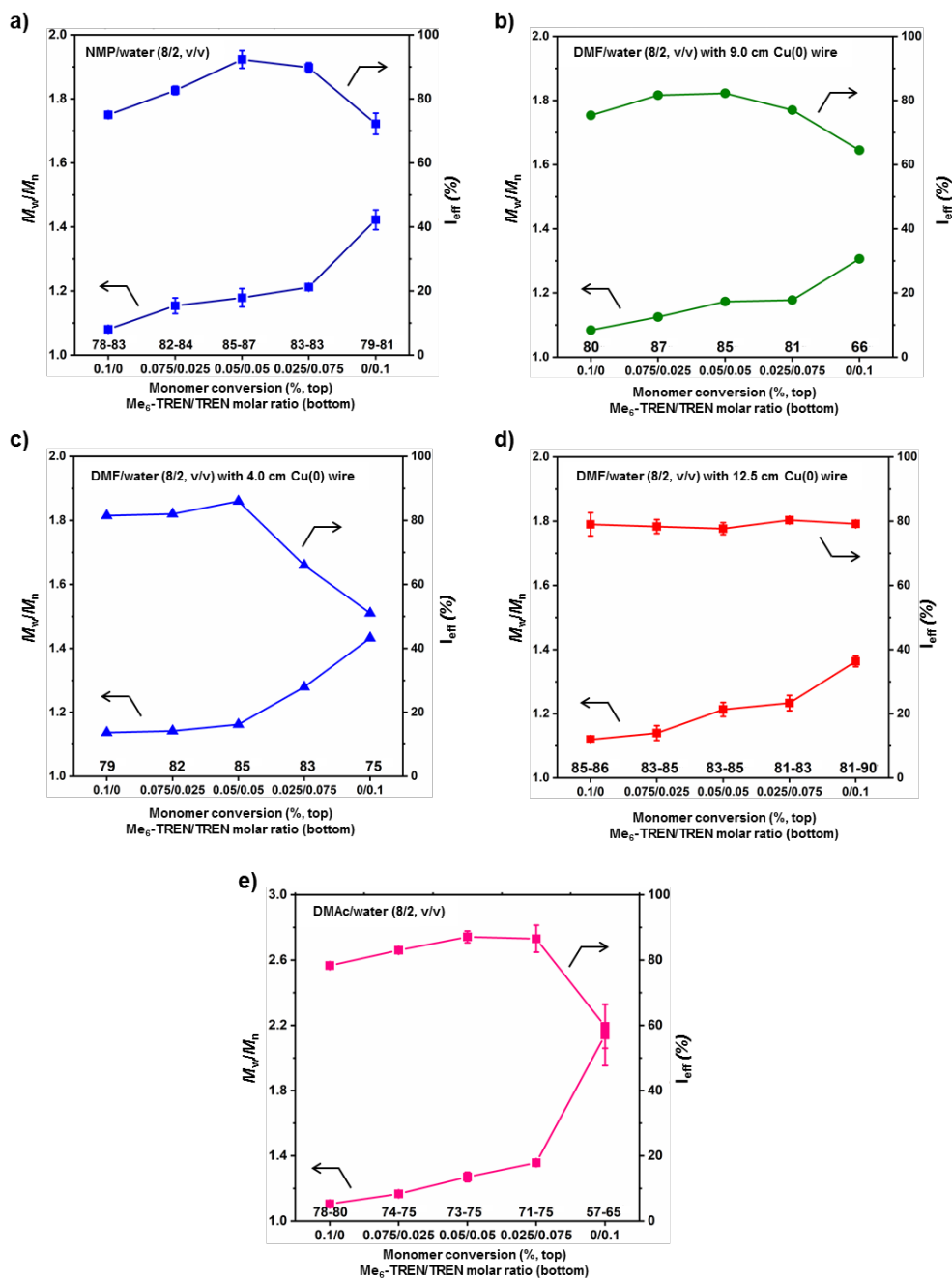
Appendix 2. Kinetic plots, molecular weight and polydispersity evolution for the SET-LRP of MA in DMF/water mixture (8/2, v/v) initiated with BPE and catalyzed by 9.0 cm nonactivated Cu(0) wire at 25 °C. Experimental data in different colors were obtained from different kinetics experiments sometimes performed by different researches. k_p^{app} and I_{eff} are the average values of three experiments. Reaction conditions: MA = 1 mL, DMF = 0.4 mL, water = 0.1 mL, $[MA]_0/[BPE]_0/[L]_0 = 222/1/0.1$.
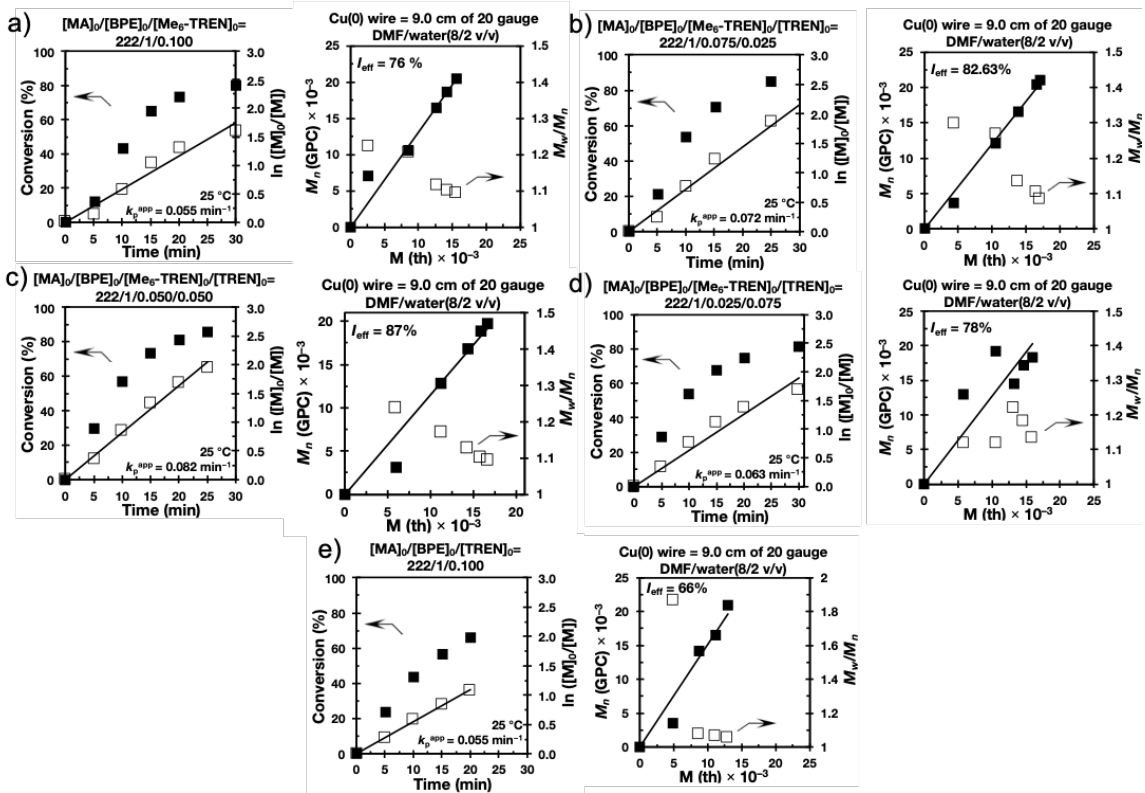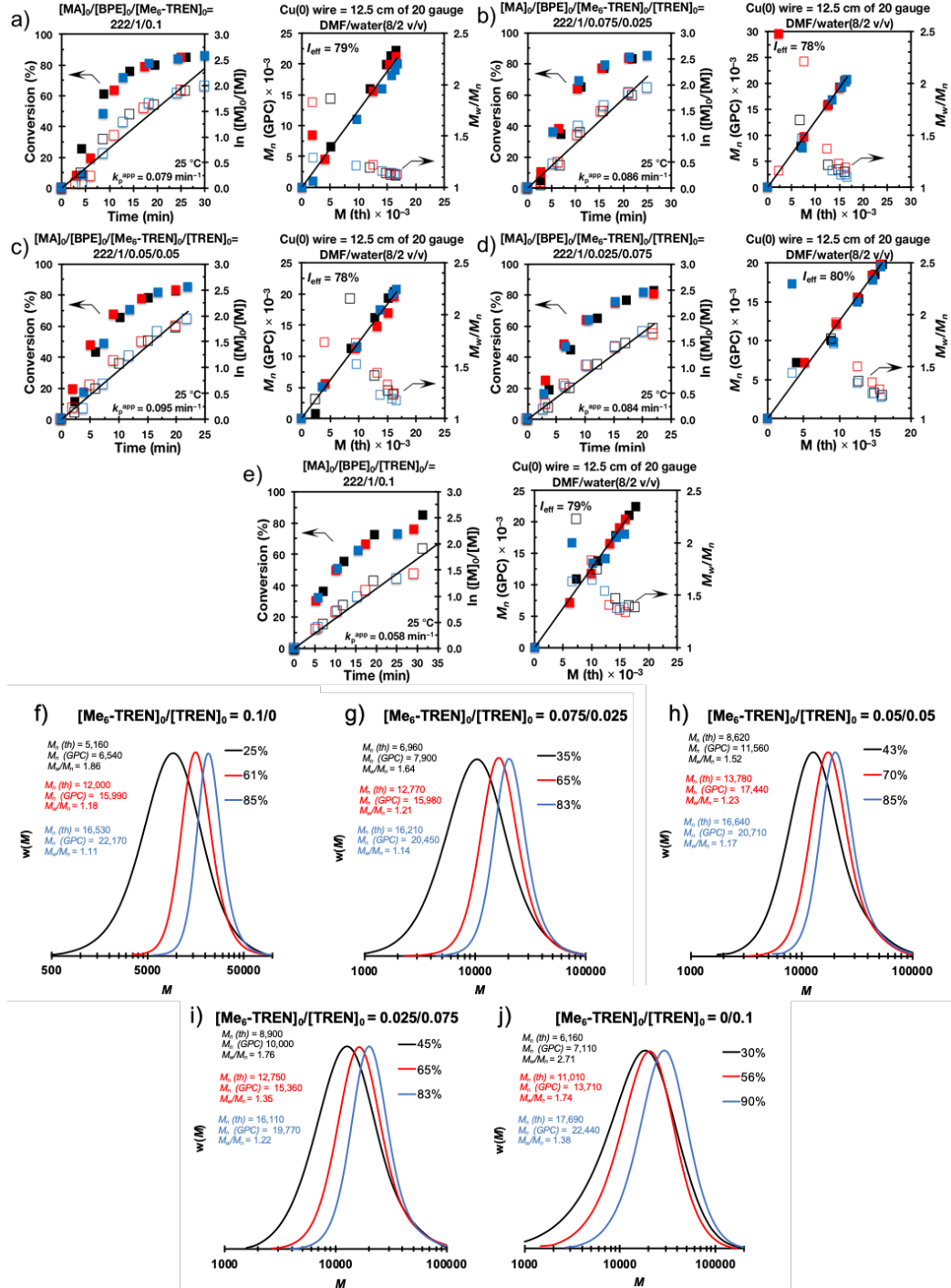
Appendix 3. Kinetic plots, molecular weight and polydispersity evolution for the SET-LRP of MA in DMF/water mixture (8/2, v/v) initiated with BPE and catalyzed by 4.0 cm nonactivated Cu(0) wire at 25 °C. Experimental data in different colors were obtained from different kinetics experiments sometimes performed by different researches. k_p^{app} and I_{eff} are the average values of three experiments. Reaction conditions: MA = 1 mL, DMF = 0.4 mL, water = 0.1 mL, $[MA]_0/[BPE]_0/[L]_0 = 222/1/0.1$.
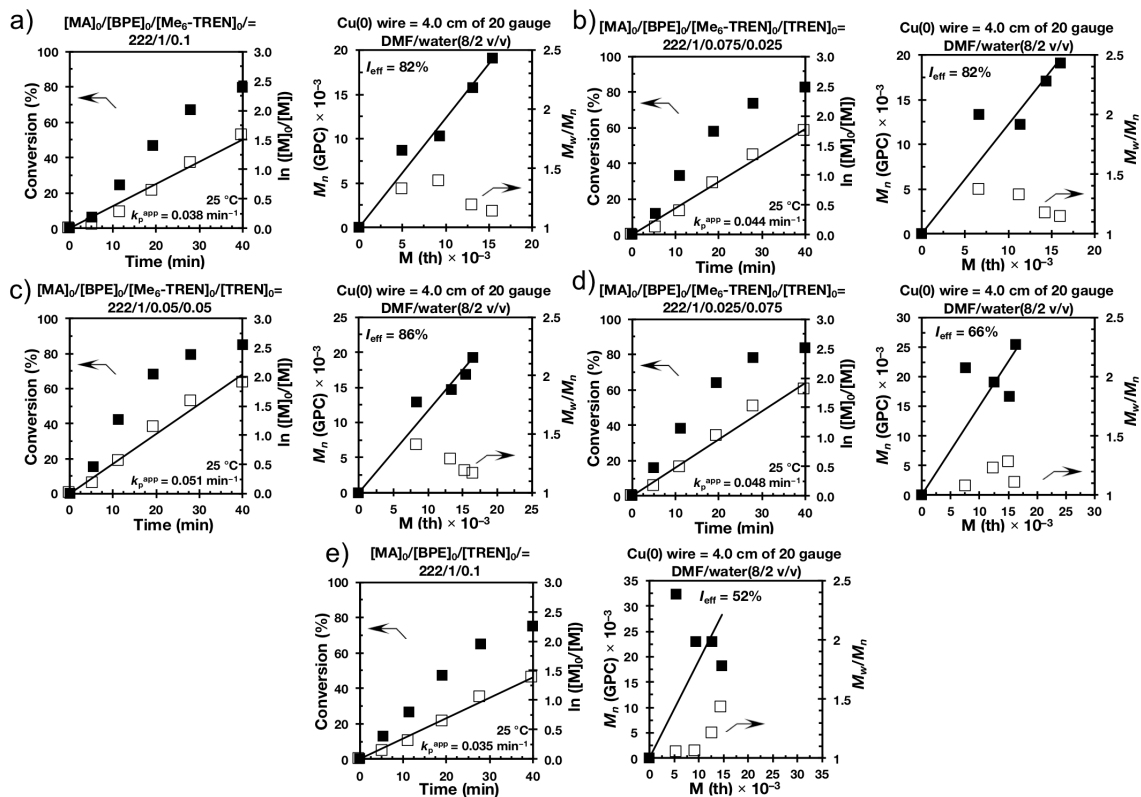
Appendix 4. Kinetic plots, molecular weight, polydispersity evolution and representative GPC traces of the evolution of molecular weight as a function of conversion for the SET-LRP of MA in DMF/water mixture (8/2, v/v) initiated with BPE and catalyzed by 12.5 cm nonactivated Cu(0) wire at 25 °C. Experimental data in different colors were obtained from different kinetics experiments sometimes performed by different researches. . k_p^{app} and I_{eff} are the average values of three experiments. Reaction conditions: MA = 1 mL, DMF = 0.4 mL, water = 0.1 mL, $[MA]_0/[BPE]_0/[L]_0 = 222/1/0.1$.
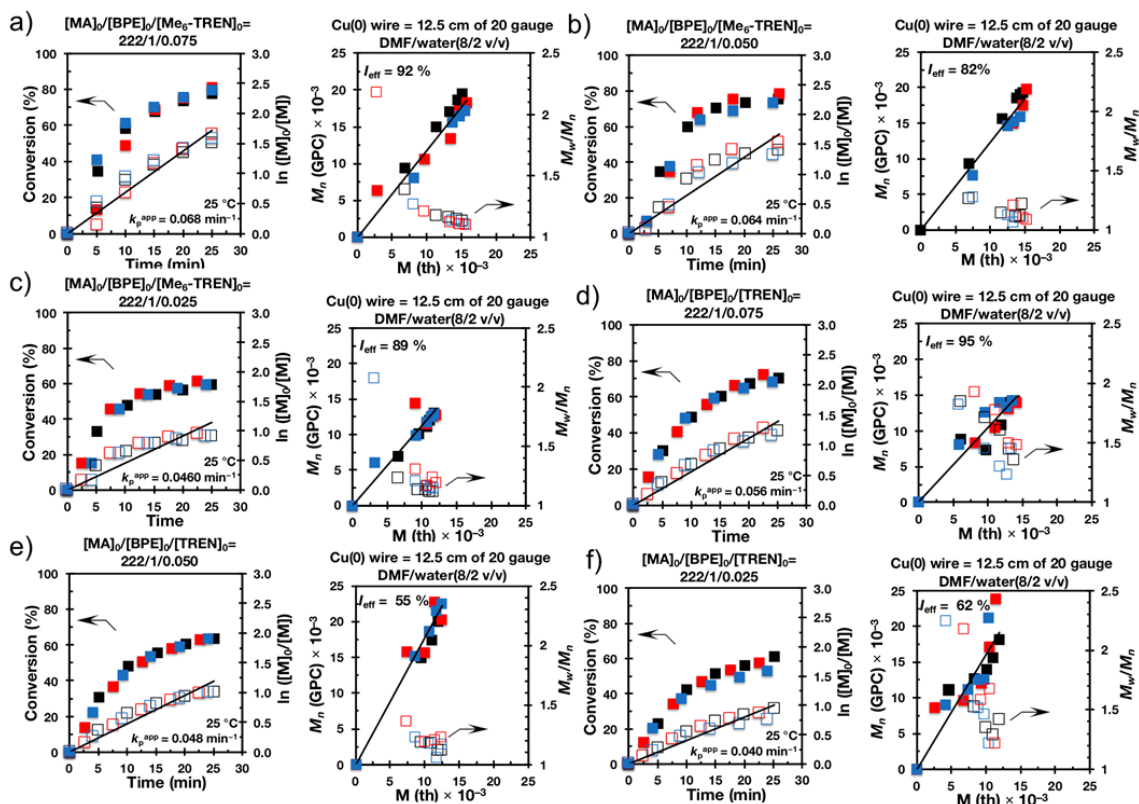
Appendix 5. Kinetic plots, molecular weight and polydispersity evolution for the SET-LRP of MA in DMF/water mixture (8/2, v/v) initiated with BPE and catalyzed by the 12.5 cm nonactivated Cu(0) wire at 25 °C. Experimental data in different colors were obtained from different kinetics experiments sometimes performed by different researches. . k_p^{app} and I_{eff} are the average values of three experiments. Reaction conditions: MA = 1 mL, DMF = 0.4 mL, water = 0.1 mL, $[MA]_0/[BPE]_0/[L]_0$ = 222/1/0.075 (panels a,d), $[MA]_0/[BPE]_0/[L]_0$ = 222/1/0.05 (panels b,e), $[MA]_0/[BPE]_0/[L]_0$ = 222/1/0.025 (panels c,f).

Appendix 6. Kinetic plots, molecular weight, polydispersity evolution and representative GPC traces of the evolution of molecular weight as a function of conversion for the SET-LRP of MA in DMAc/water mixture (8/2, v/v) initiated with BPE and catalyzed by 9.0 cm nonactivated Cu(0) wire at 25 °C. Experimental data in different colors were obtained from different kinetics experiments sometimes performed by different researches. . k_p^{app} and I_{eff} are the average values of three experiments. Reaction conditions: MA = 1 mL, DMAc = 0.4 mL, water = 0.1 mL, $[MA]_0/[BPE]_0/[L]_0 = 222/1/0.1$.
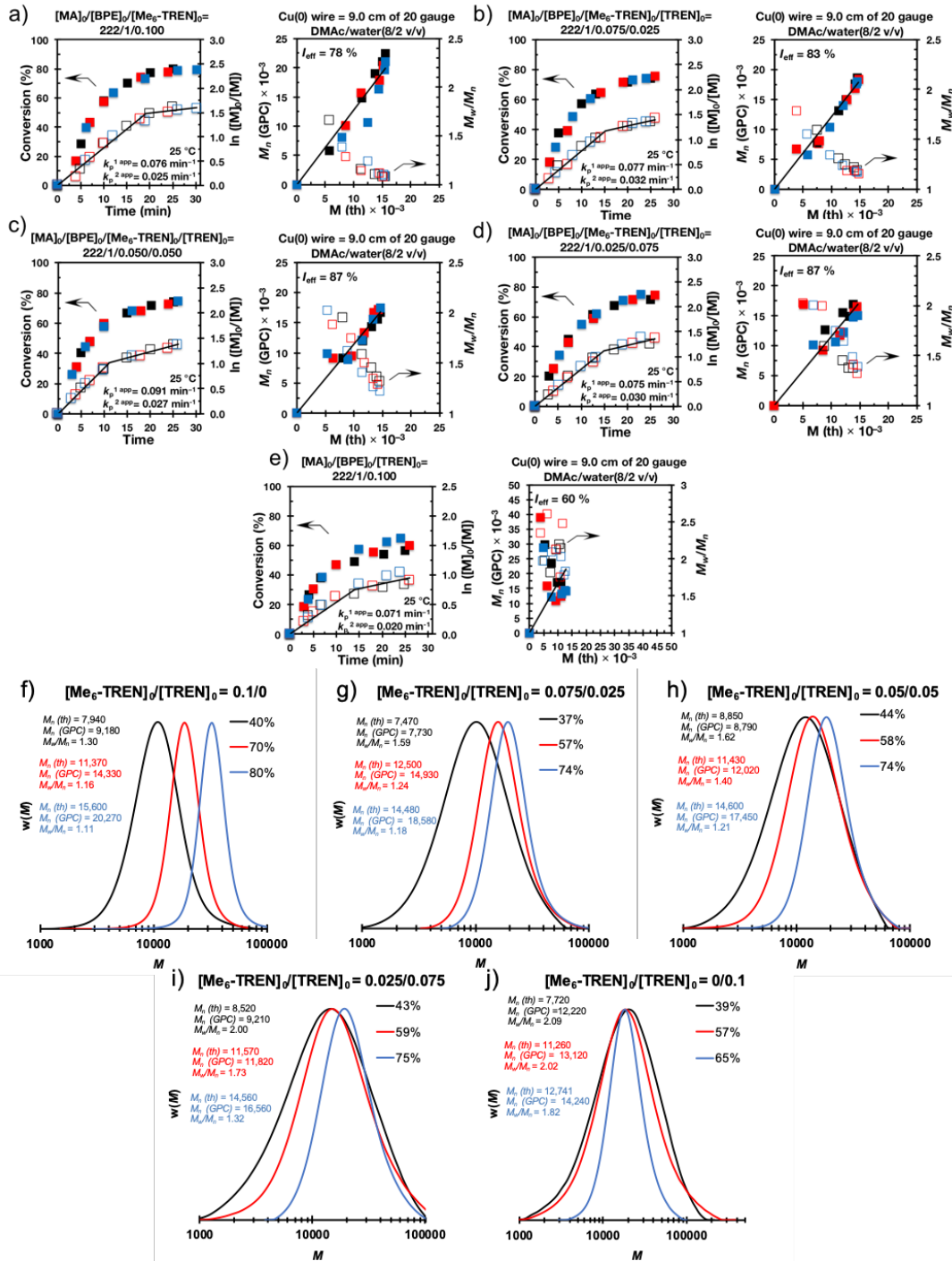
Appendix 7. Visualization of the reaction mixture for the control experiments performed under the conditions placed at the top of each series of experiments. EA is the short name used for ethyl acetate employed to mimic an inert compound resembling methyl acrylate (MA).

a)

$[EA]_0/[BPE]_0/Ligand/Cu(0)$ wire = 205/1/X/12.5cm 20G
DMF/water(8/2 v/v)

0.1/0	0.075/0.025	0.05/0.05	0.025/0.075	0/0.1

Me_6-TREN/TREN

b)

$[EA]_0/[BPE]_0/Ligand/Cu(0)$ wire = 205/1/X/9.0cm 20G
NMP/water(8/2 v/v)

0.1/0	0.075/0.025	0.05/0.05	0.025/0.075	0/0.1

Me_6-TREN/TREN

c)

$[EA]_0/[BPE]_0/Ligand/Cu(0)$ wire = 205/1/X/9.0cm 20G
DMAc/water(8/2 v/v)

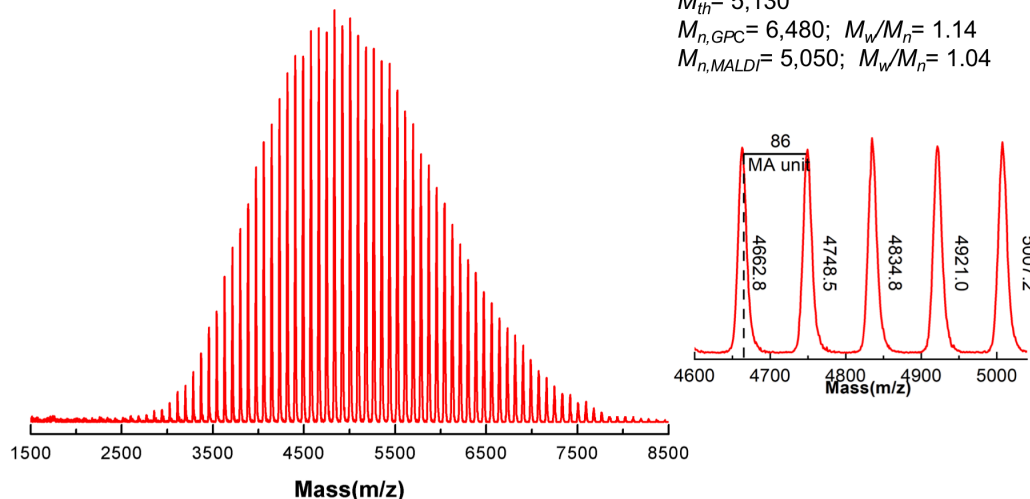| 0.1/0	0.075/0.025	0.05/0.05	0.025/0.075	0/0.1

Me_6-TREN/TREN

Appendix 8. ^{1}H NMR spectra at 400 MHz of α,ω-di(phenylthio)PMA at (a) 93% monomer conversion (M_n= 7,420 and M_w/M_n= 1.15) ([MA]$_0$/[BPE]$_0$/[Me$_6$-TREN]$_0$ = 60/1/0.1); (b) 91% monomer conversion (M_n = 8,260 and M_w/M_n= 1.17) ([MA]$_0$/[BPE]$_0$/[Me$_6$-TREN]$_0$/[TREN]$_0$ = 60/1/0.05/0.05); (c) 94% monomer conversion (M_n= 6,090 and M_w/M_n =1.34) ([MA]$_0$/[BPE]$_0$/[TREN]$_0$ = 60/1/0.1). Polymerization conditions: MA = 1 mL, DMF = 0.4 mL, water = 0.1 ml using 12.5 cm of nonactivated Cu(0) wire 20-gauge wire. The signals at 7.26 ppm and 5.30 ppm are due to partially nondeuterated residue of CDCl$_3$ and dichloromethane, respectively.
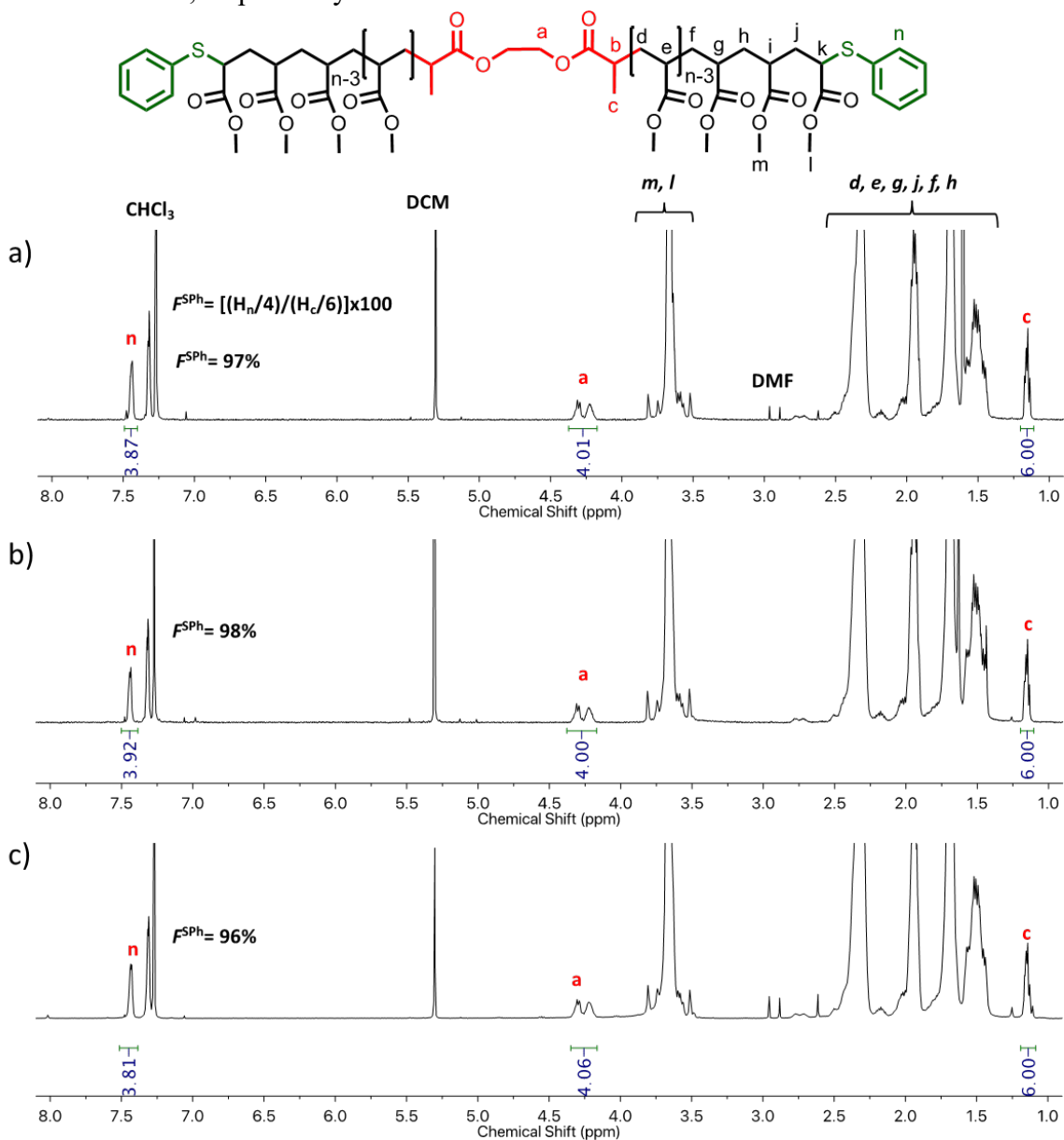
Appendix 9. MALDI-TOF of α,ω-di(bromo)PMA isolated at 93% monomer convesion from SET-LRP of MA in DMF/water (8/2, v/v) mixture initiated with BPE and catalyzed by nonactivated Cu(0) wire at 25 °C: (a) before and (b) after "thio-bromo "click". Polymerization conditions: MA = 1 mL, DMF = 0.4 mL, water = 0.1 mL using 12.5 cm of nonactivated Cu(0) wire 20-gauge wire ($[MA]_0/[BPE]_0/[Me_6-TREN]_0 = 60/1/0.1$). The dotted line in expansion after thioetherification shows the original peak from before thioetherification, while 58 represents the increase in molar mass after thioetherification i.e., $2 \times [SPh (109.2) - Br (79.9)] = 58.57$ for each chain end.
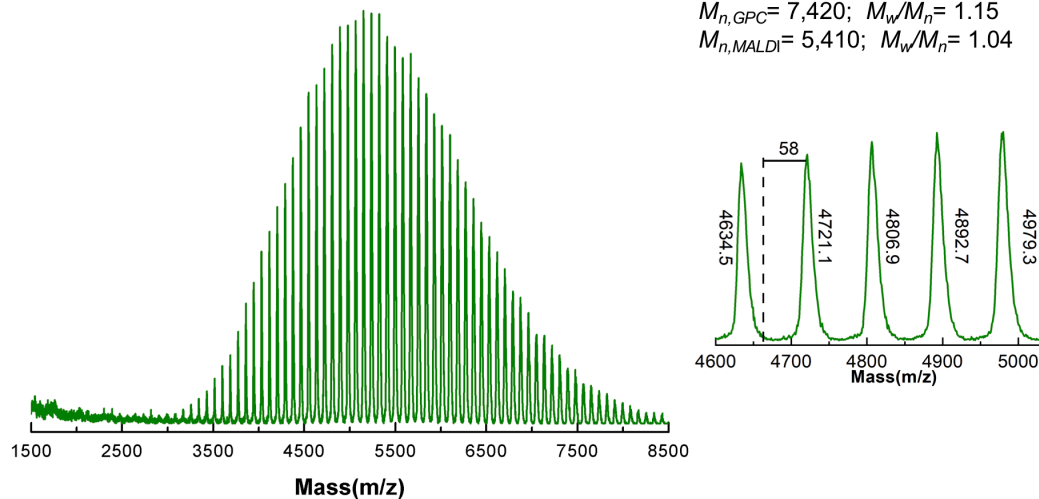
a) PMA before thioetherification

Conversion = 93%
M_{th}= 5,130
$M_{n,GPC}$= 6,480; M_w/M_n= 1.14
$M_{n,MALDI}$= 5,050; M_w/M_n= 1.04

86
MA unit

4662.8
4748.5
4834.8
4921.0
5007.2

4600   4700   4800   4900   5000
Mass(m/z)

1500   2500   3500   4500   5500   6500   7500   8500
Mass(m/z)

b) PMA after thioetherification

Conversion = 93%
M_{th}= 5,130
$M_{n,GPC}$= 7,420; M_w/M_n= 1.15
$M_{n,MALDI}$= 5,410; M_w/M_n= 1.04

58

4634.5
4721.1
4806.9
4892.7
4979.3

4600   4700   4800   4900   5000
Mass(m/z)

1500   2500   3500   4500   5500   6500   7500   8500
Mass(m/z)

Appendix 10. MALDI-TOF of α,ω-di(bromo)PMA isolated at 94% monomer conversion from SET-LRP of MA in DMF/water (8/2, v/v) mixture initiated with BPE and catalyzed by nonactivated Cu(0) wire at 25 °C: (a) before and (b) after "thio-bromo "click". Polymerization conditions: MA = 1 mL, DMF = 0.4 mL, water = 0.1 ml using 12.5 cm of nonactivated Cu(0) wire 20-gauge wire ($[MA]_0/[BPE]_0/[TREN]_0 = 60/1/0.1$). The dotted line in expansion after thioetherification shows the original peak from before thioetherification, while 58 represents the increase in molar mass after thioetherification i.e., 2x[SPh (109. 2) - Br (79.9)] = 58.57 for each chain end.
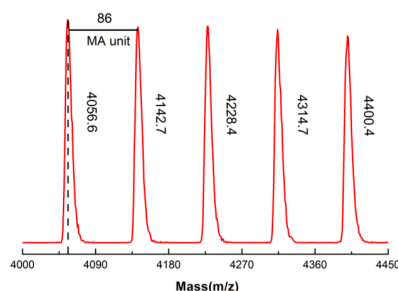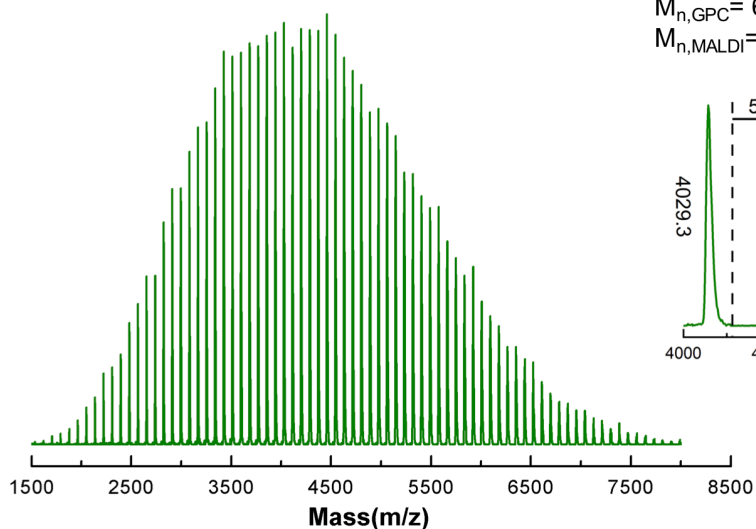
a) PMA before thioetherification
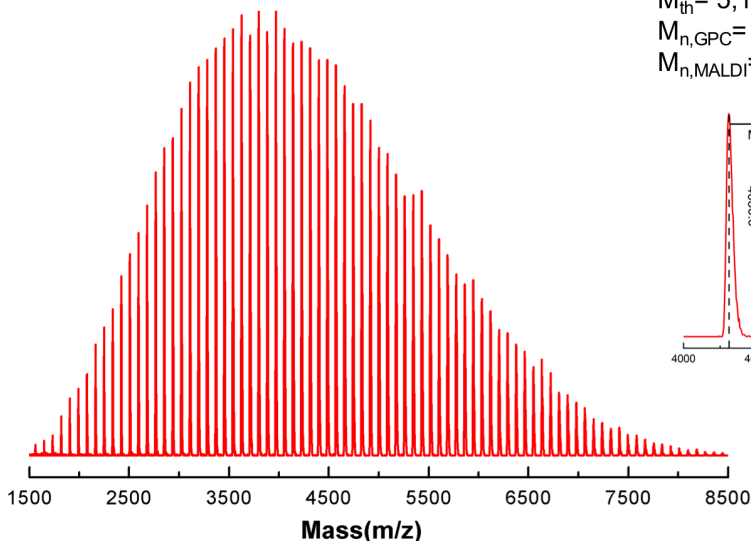
Conversion = 94%
M_{th}= 5,180
$M_{n,GPC}$= 5,990; M_w/M_n= 1.25
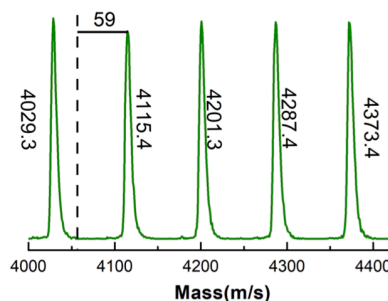$M_{n,MALDI}$= 4,290; M_w/M_n= 1.08


b) PMA after thioetherification

Conversion = 94%
M_{th}= 5,180
$M_{n,GPC}$= 6,090; M_w/M_n= 1.34
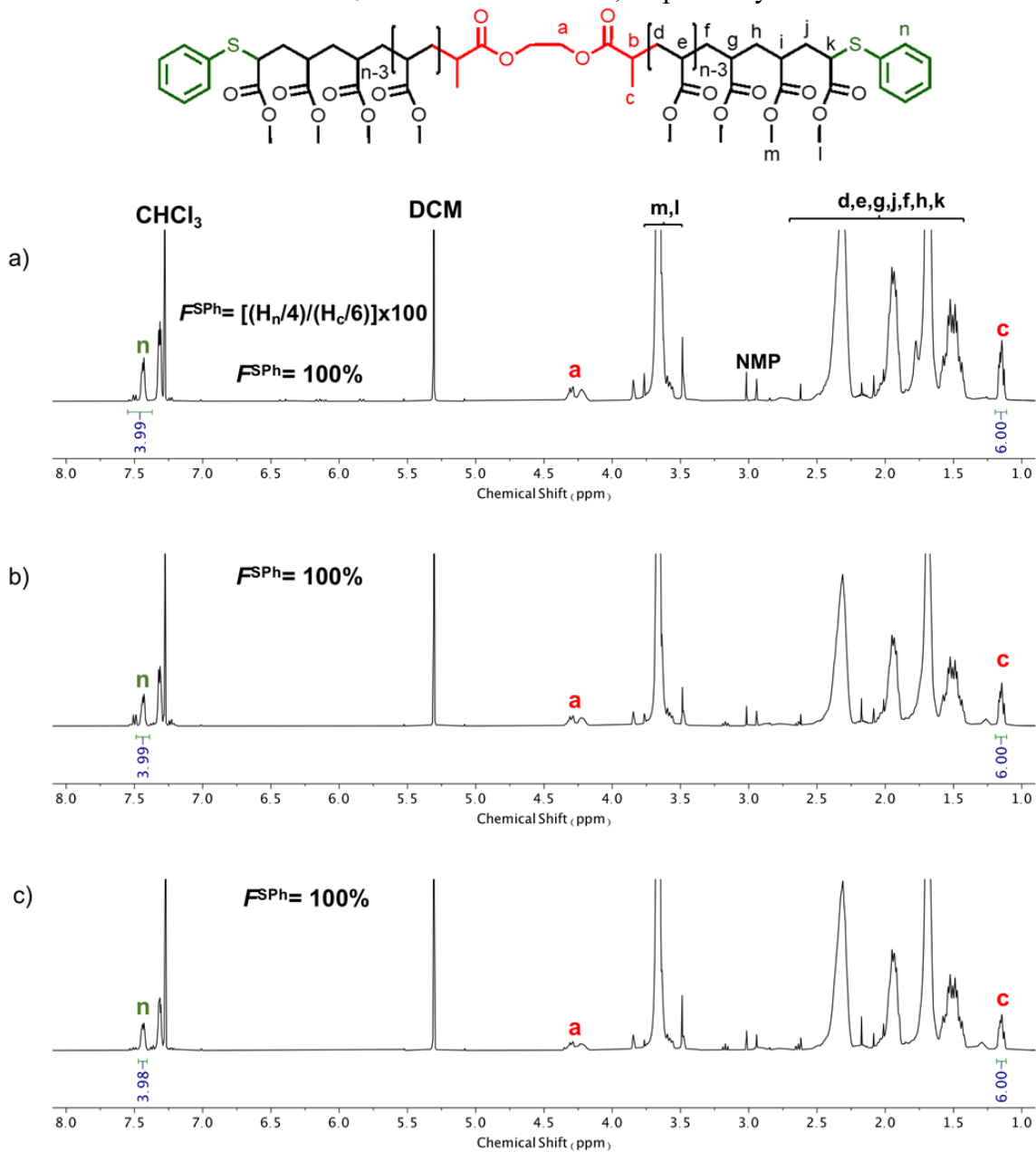$M_{n,MALDI}$= 4,120; M_w/M_n= 1.08

Appendix 11. ^{1}H NMR spectra at 400 MHz of α,ω-di(bromo)PMA at (a) 98% monomer conversion (M_n= 6,850 and M_w/M_n= 1.17) ([MA]$_0$/[BPE]$_0$/[Me$_6$-TREN]$_0$ = 60/1/0.1); (b) 98% monomer conversion (M_n = 4,750 and M_w/M_n= 1.25) ([MA]$_0$/[BPE]$_0$/[Me$_6$-TREN]$_0$/[TREN]$_0$ = 60/1/0.05/0.05); (c) 99% monomer conversion (M_n= 6,470 and M_w/M_n =1.33) ([MA]$_0$/[BPE]$_0$/[TREN]$_0$ = 60/1/0.1). Polymerization conditions: MA = 1 mL, NMP = 0.4 mL, water = 0.1 ml using 9.0 cm of nonactivated Cu(0) wire 20-gauge wire. The signals at 7.26 ppm and 5.30 ppm are due to partially nondeuterated residue of CDCl$_3$ and dichloromethane, respectively.

71
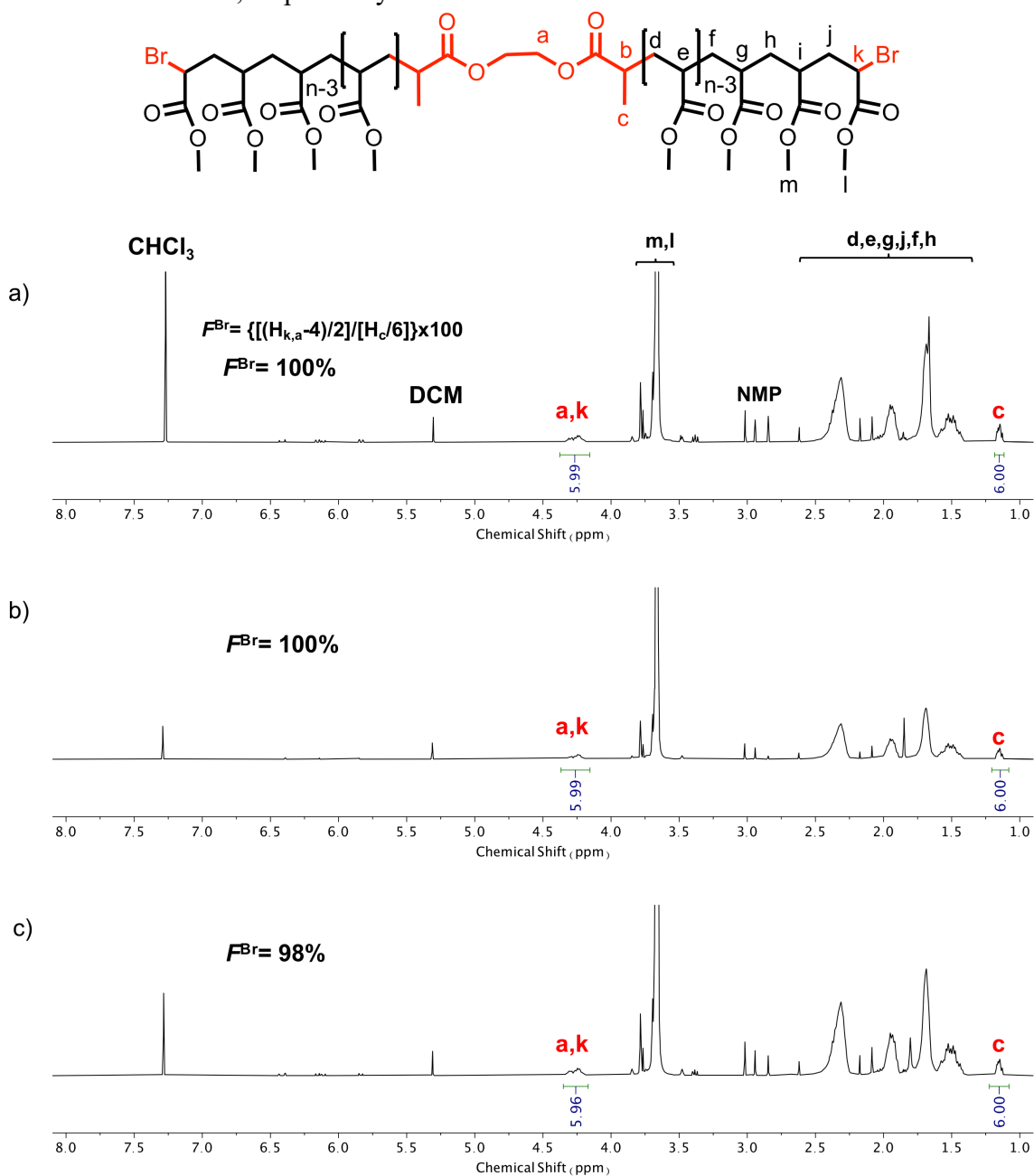
Appendix 12. ^{1}H NMR spectra at 400 MHz of α,ω-di(phenylthio)PMA at (a) 98% monomer conversion (M_n = 7,340 and M_w/M_n = 1.17) ([MA]$_0$/[BPE]$_0$/[Me$_6$-TREN]$_0$ = 60/1/0.1); (b) 98% monomer conversion (M_n = 5,890 and M_w/M_n = 1.29) ([MA]$_0$/[BPE]$_0$/[Me$_6$-TREN]$_0$/[TREN]$_0$ = 60/1/0.05/0.05); (c) 99% monomer conversion (M_n = 7,400 and M_w/M_n = 1.35) ([MA]$_0$/[BPE]$_0$/[TREN]$_0$ = 60/1/0.1). Polymerization conditions: MA = 1 mL, NMP = 0.4 mL, water = 0.1 ml using 9.0 cm of nonactivated Cu(0) wire 20-gauge wire. The signals at 7.26 ppm and 5.30 ppm are due to partially nondeuterated residue of CDCl$_3$ and dichloromethane, respectively.
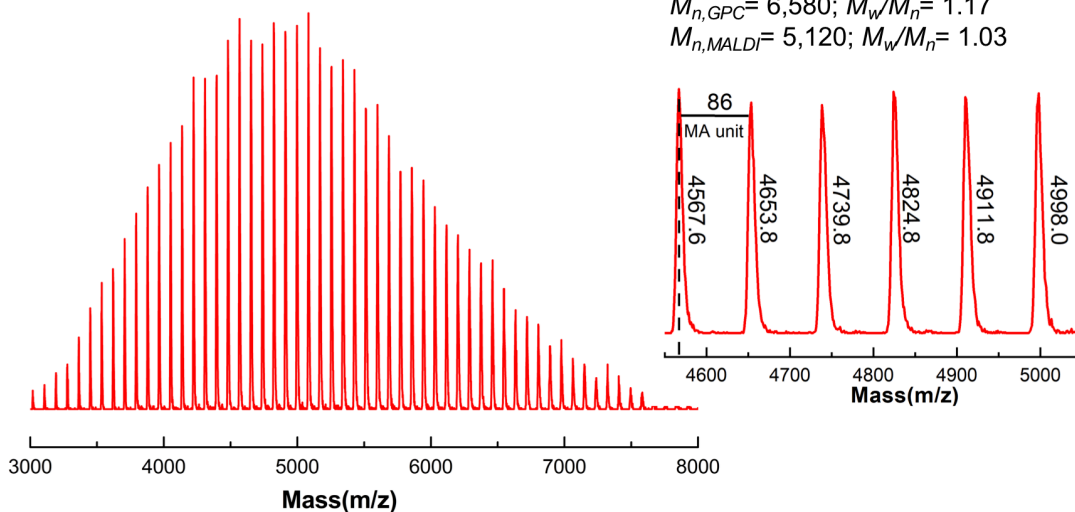
Appendix 13. MALDI-TOF of α,ω-di(bromo)PMA isolated at 98% monomer conversion from SET-LRP of MA in NMP/water (8/2, v/v) mixture initiated with BPE and catalyzed by nonactivated Cu(0) wire at 25 °C: (a) before and (b) after "thio-bromo "click". Polymerization conditions: MA = 1 mL, NMP = 0.4 mL, water = 0.1 ml using 9.0 cm of nonactivated Cu(0) wire 20-gauge wire ($[MA]_0/[BPE]_0/[Me_6\text{-TREN}]_0$ = 60/1/0.1). The dotted line in expansion after thioetherification shows the original peak from before thioetherification, while 58 represents the increase in molar mass after thioetherification i.e., 2x[SPh (109. 2) - Br (79.9)] = 58.57 for each chain end.

a) PMA before thioetherification

Conversion = 98%
M_{th}= 5,390
$M_{n,GPC}$= 6,580; M_w/M_n= 1.17
$M_{n,MALDI}$= 5,120; M_w/M_n= 1.03

b) PMA after thioetherification

Conversion =98 %
M_{th}= 5,390
$M_{n,GPC}$= 7,340; M_w/M_n= 1.17
$M_{n,MALDI}$= 5,390; M_w/M_n= 1.03

Appendix 14. MALDI-TOF of α,ω-di(bromo)PMA isolated at 98% monomer conversion from SET-LRP of MA in NMP/water (8/2, v/v) mixture initiated with BPE and catalyzed by nonactivated Cu(0) wire at 25 °C: (a) before and (b) after "thio-bromo "click". Polymerization conditions: MA = 1 mL, NMP = 0.4 mL, water = 0.1 ml using 9.0 cm of nonactivated Cu(0) wire 20-gauge wire ([MA]$_0$/[BPE]$_0$/[Me$_6$-TREN]$_0$/[TREN]$_0$ = 60/1/0.05/0.05). The dotted line in expansion after thioetherification shows the original peak from before thioetherification, while 58 represents the increase in molar mass after thioetherification i.e., 2x[SPh (109. 2) - Br (79.9)] = 58.57 for each chain end.
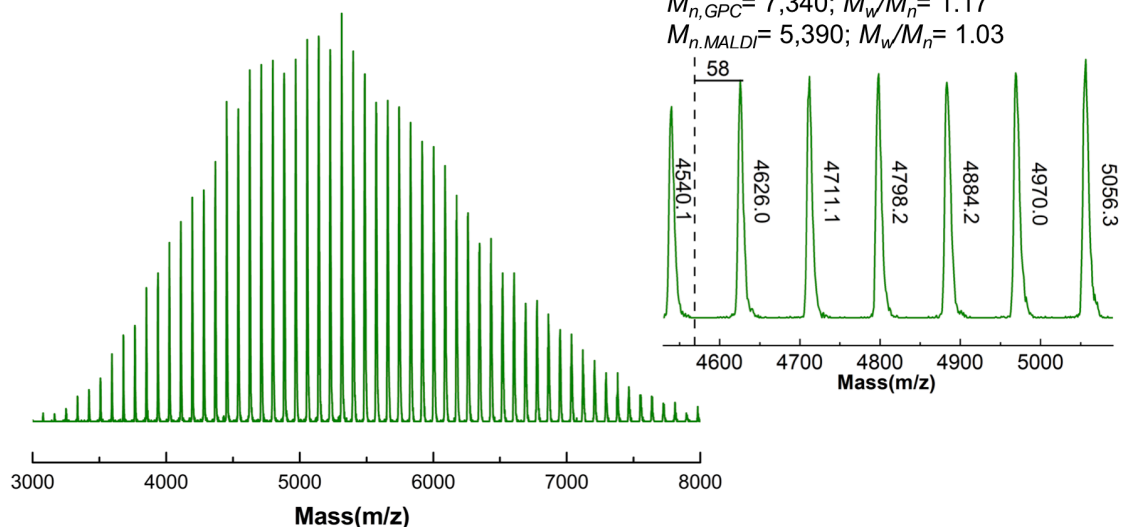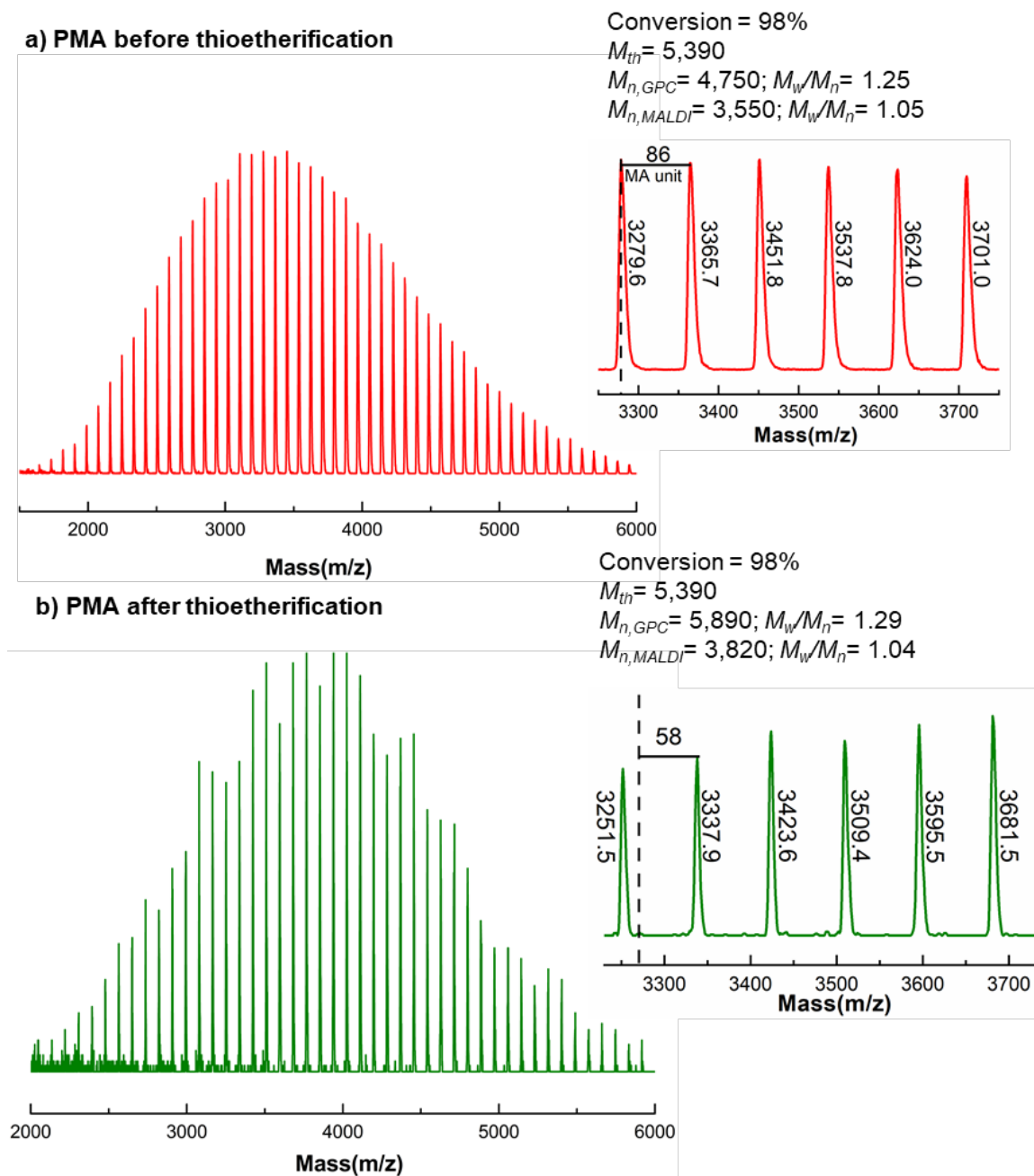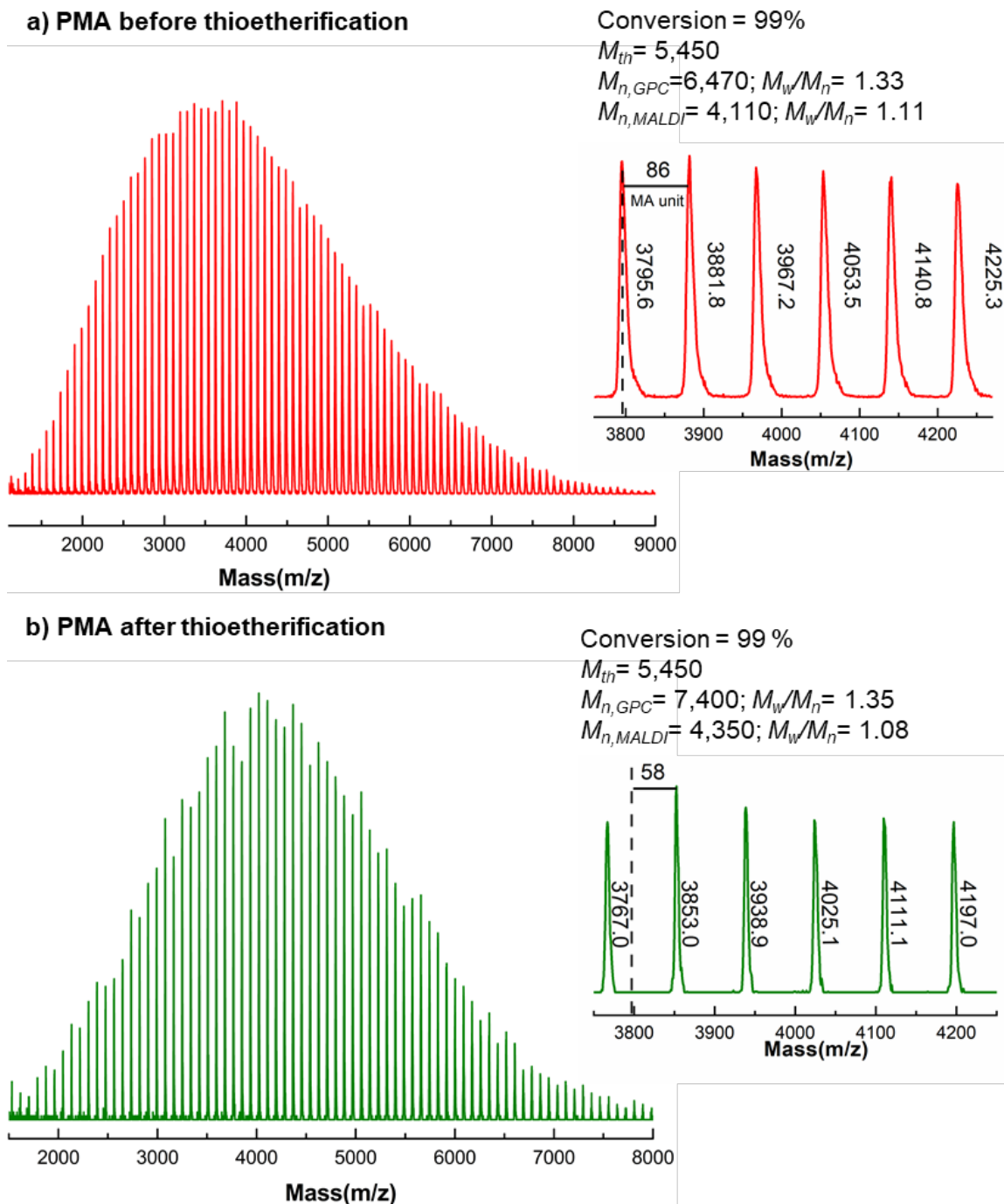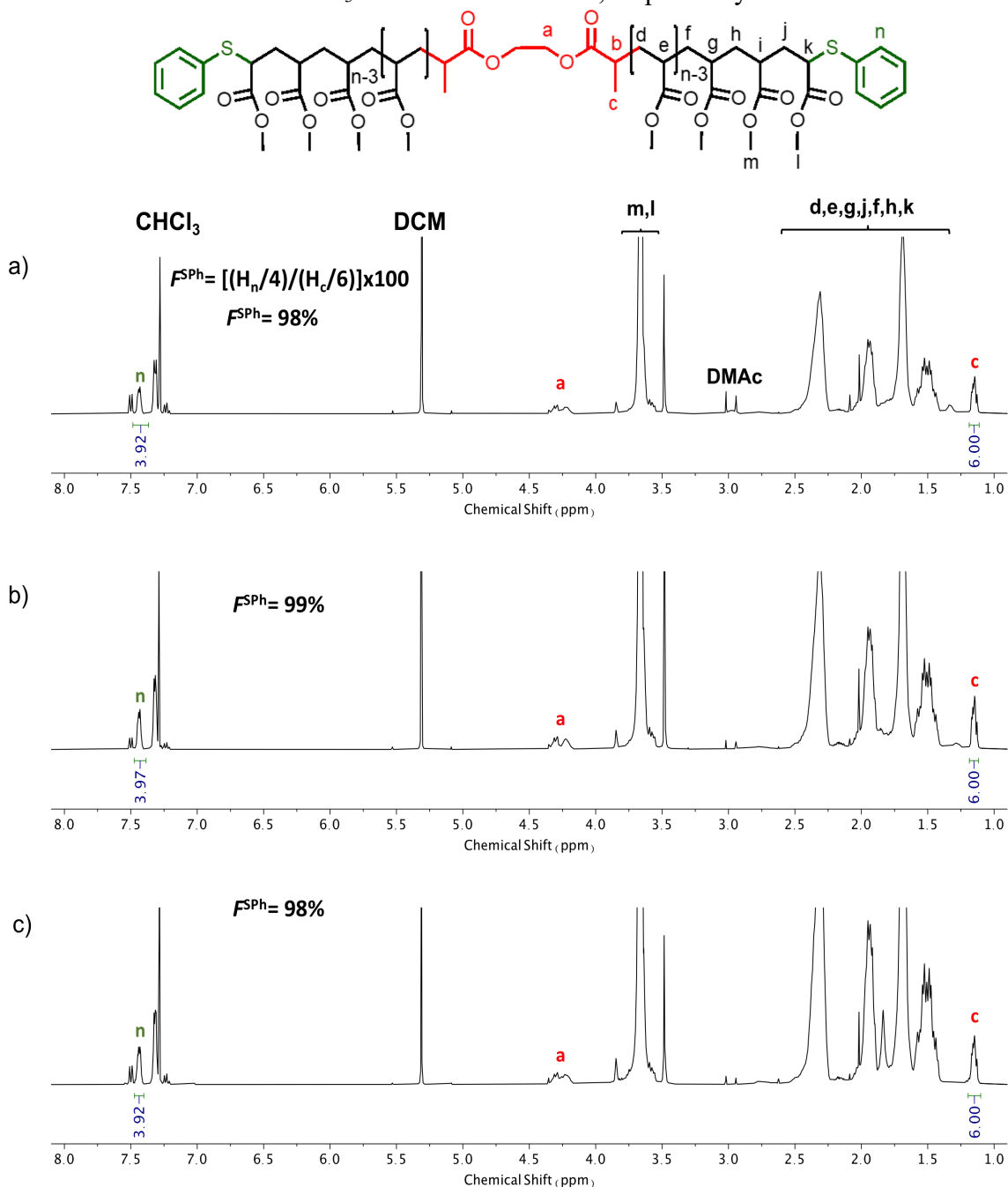
Appendix 15. MALDI-TOF of α,ω-di(bromo)PMA isolated at 99% monomer conversion from SET-LRP of MA in NMP/water (8/2, v/v) mixture initiated with BPE and catalyzed by nonactivated Cu(0) wire at 25 °C: (a) before and (b) after "thio-bromo "click". Polymerization conditions: MA = 1 mL, NMP = 0.4 mL, water = 0.1 ml using 9.0 cm of nonactivated Cu(0) wire 20-gauge wire ([MA]$_0$/[BPE]$_0$/[TREN]$_0$ = 60/1/0.1). The dotted line in expansion after thioetherification shows the original peak from before thioetherification, while 58 represents the increase in molar mass after thioetherification i.e., 2x[SPh (109. 2) - Br (79.9)] = 58.57 for each chain end.

a) PMA before thioetherification

Conversion = 99%
M_{th}= 5,450
$M_{n,GPC}$=6,470; M_w/M_n= 1.33
$M_{n,MALDI}$= 4,110; M_w/M_n= 1.11

b) PMA after thioetherification

Conversion = 99 %
M_{th}= 5,450
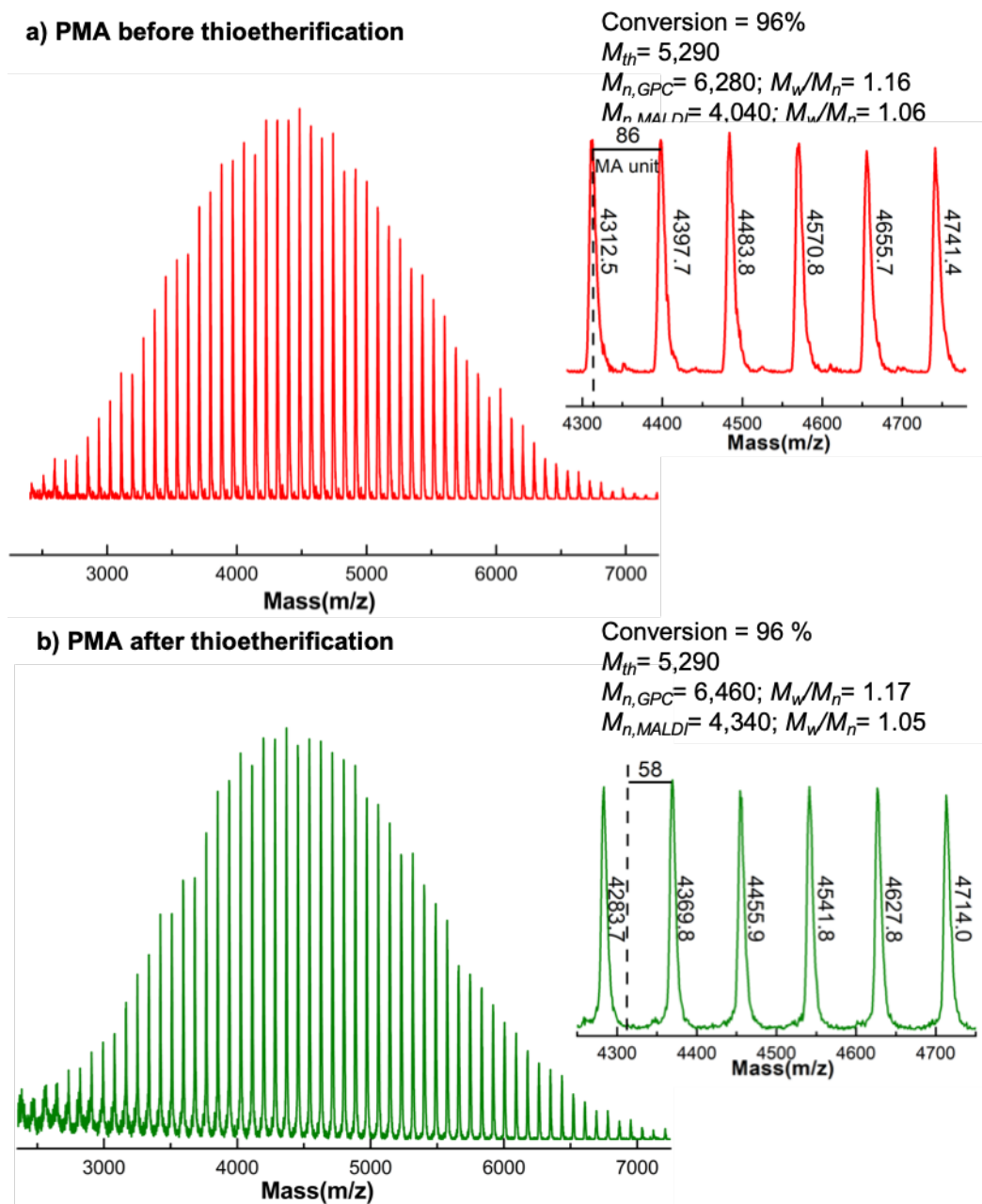$M_{n,GPC}$= 7,400; M_w/M_n= 1.35
$M_{n,MALDI}$= 4,350; M_w/M_n= 1.08

Appendix 16. ^{1}H NMR spectra at 400 MHz of α,ω-di(bromo)PMA at (a) 96% monomer conversion (M_n= 6,280 and M_w/M_n= 1.16) ([MA]$_0$/[BPE]$_0$/[Me$_6$-TREN]$_0$ = 60/1/0.1); (b) 98% monomer conversion (M_n = 6,150 and M_w/M_n= 1.29) ([MA]$_0$/[BPE]$_0$/[Me$_6$-TREN]$_0$/[TREN]$_0$ = 60/1/0.05/0.05); (c) 83% monomer conversion (M_n= 4,870 and M_w/M_n =1.95) ([MA]$_0$/[BPE]$_0$/[TREN]$_0$ = 60/1/0.1). Polymerization conditions: MA = 1 mL, DMAc = 0.4 mL, water = 0.1 ml using 9.0 cm of nonactivated Cu(0) wire 20-gauge wire. The signals at 7.26 ppm and 5.30 ppm are due to partially nondeuterated residue of CDCl$_3$ and dichloromethane, respectively.
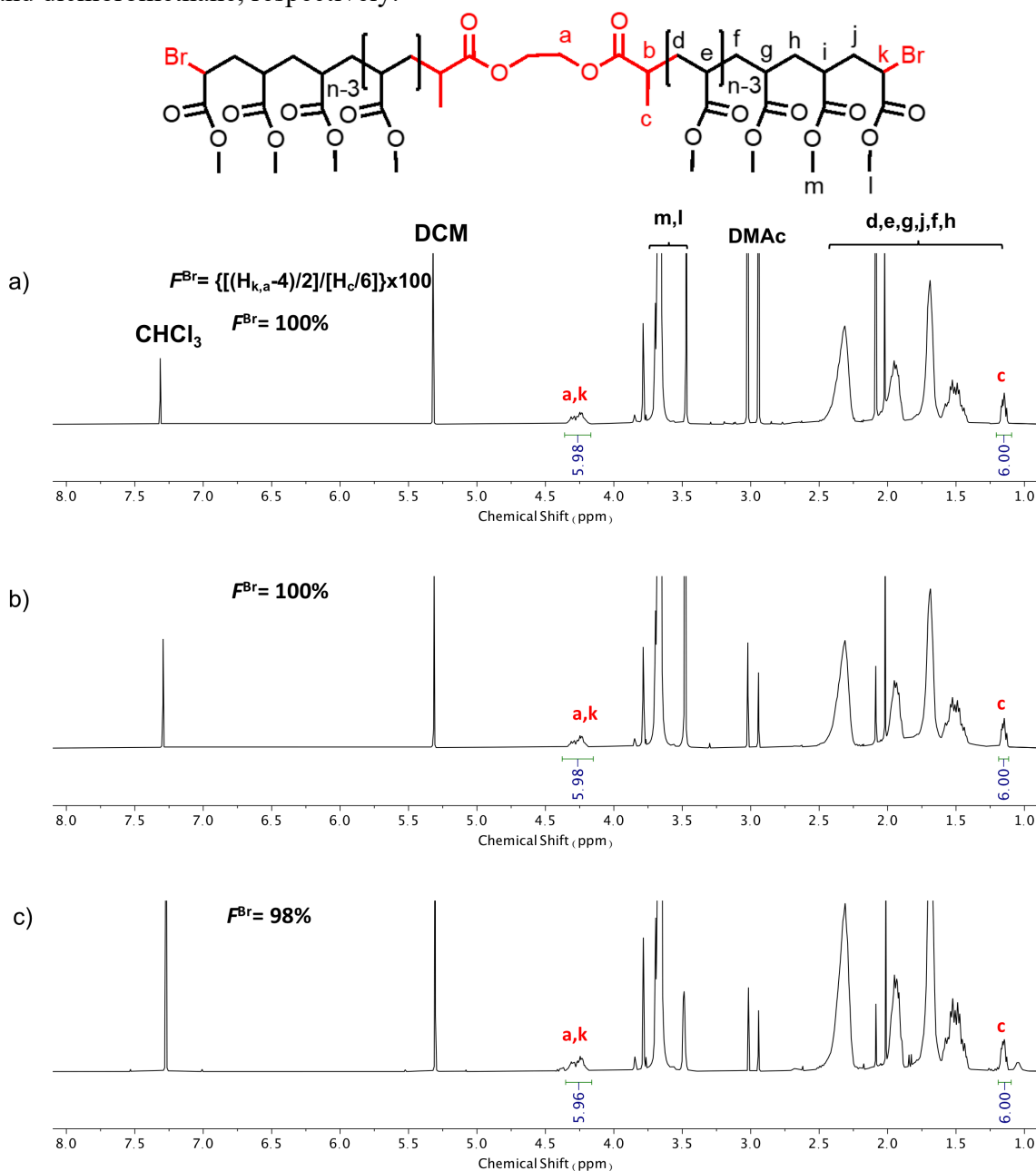
Appendix 17. ^1H NMR spectra at 400 MHz of α,ω-di(phenylthio)PMA at (a) 96% monomer conversion (M_n= 6,460 and M_w/M_n= 1.17) ([MA]$_0$/[BPE]$_0$/[Me$_6$-TREN]$_0$ = 60/1/0.1); (b) 98% monomer conversion (M_n = 6,560 and M_w/M_n= 1.30) ([MA]$_0$/[BPE]$_0$/[Me$_6$-TREN]$_0$/[TREN]$_0$ = 60/1/0.05/0.05); (c) 83% monomer conversion (M_n= 7,380 and M_w/M_n =1.69) ([MA]$_0$/[BPE]$_0$/[TREN]$_0$ = 60/1/0.1). Polymerization conditions: MA = 1 mL, DMAc = 0.4 mL, water = 0.1 ml using 9.0 cm of nonactivated Cu(0) wire 20-gauge wire. The signals at 7.26 ppm and 5.30 ppm are due to partially nondeuterated residue of CDCl$_3$ and dichloromethane, respectively.
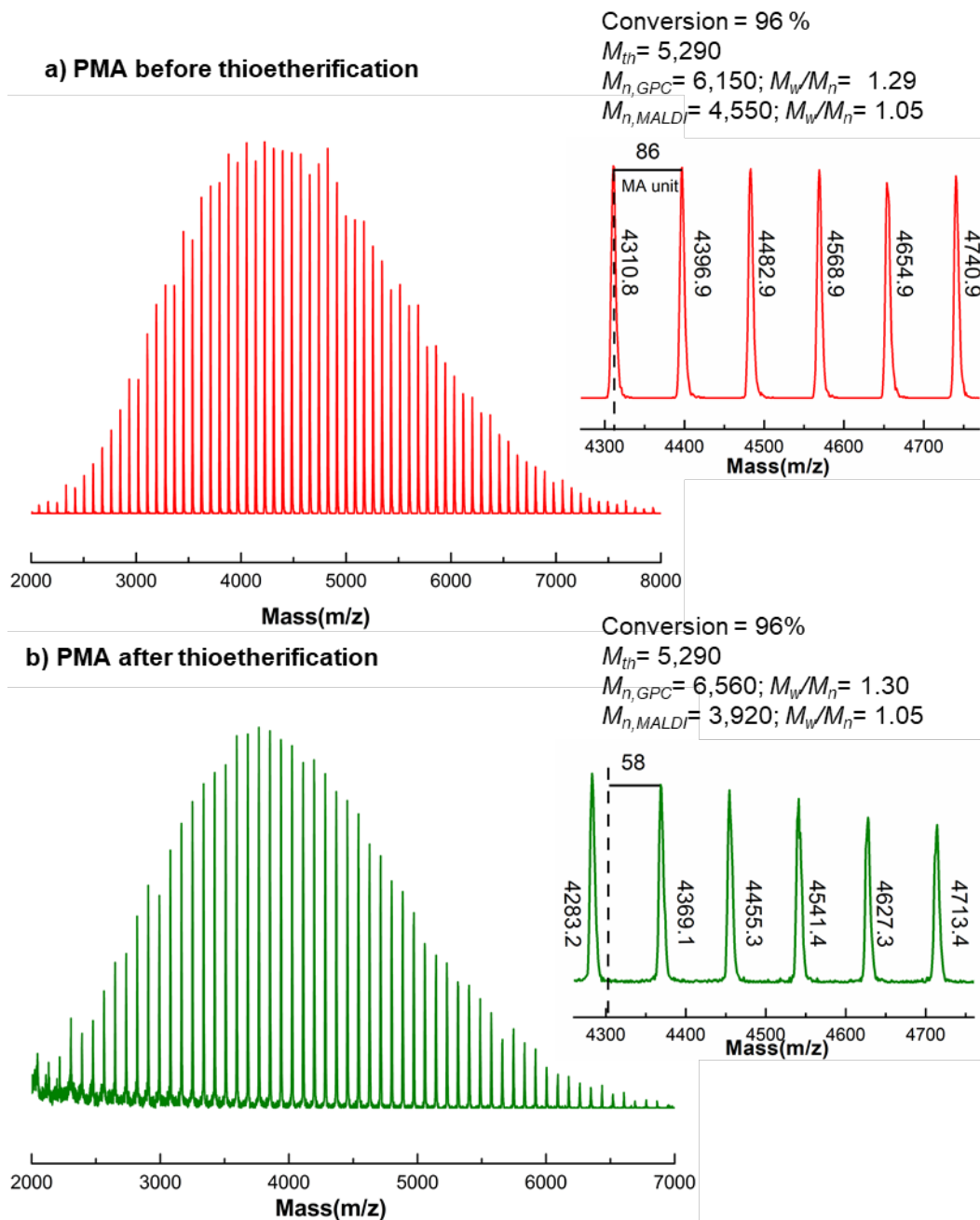
Appendix 18. MALDI-TOF of α,ω-di(bromo)PMA isolated at 96% monomer conversion from SET-LRP of MA in DMAc/water (8/2, v/v) mixture initiated with BPE and catalyzed by nonactivated Cu(0) wire at 25 °C: (a) before and (b) after "thio-bromo "click". Polymerization conditions: MA = 1 mL, DMAc = 0.4 mL, water = 0.1 ml using 9.0 cm of nonactivated Cu(0) wire 20-gauge wire ($[MA]_0/[BPE]_0/[Me_6\text{-}TREN]_0 = 60/1/0.1$). The dotted line in expansion after thioetherification shows the original peak from before thioetherification, while 58 represents the increase in molar mass after thioetherification i.e., 2x[SPh (109. 2) - Br (79.9)] = 58.57 for each chain end.

a) PMA before thioetherification

Conversion = 96%
M_{th}= 5,290
$M_{n,GPC}$= 6,280; M_w/M_n= 1.16
$M_{n,MALDI}$= 4,040; M_w/M_n= 1.06

b) PMA after thioetherification

Conversion = 96 %
M_{th}= 5,290
$M_{n,GPC}$= 6,460; M_w/M_n= 1.17
$M_{n,MALDI}$= 4,340; M_w/M_n= 1.05

Appendix 19. MALDI-TOF of α,ω-di(bromo)PMA isolated at 96% monomer conversion from SET-LRP of MA in DMAc/water (8/2, v/v) mixture initiated with BPE and catalyzed by nonactivated Cu(0) wire at 25 °C: (a) before and (b) after "thio-bromo "click". Polymerization conditions: MA = 1 mL, DMAc = 0.4 mL, water = 0.1 ml using 9.0 cm of nonactivated Cu(0) wire 20-gauge wire ($[MA]_0/[BPE]_0/[Me_6\text{-}TREN]_0/[TREN]_0$ = 60/1/0.05/0.05). The dotted line in expansion after thioetherification shows the original peak from before thioetherification, while 58 represents the increase in molar mass after thioetherification i.e., 2x[SPh (109. 2) - Br (79.9)] = 58.57 for each chain end.

a) PMA before thioetherification

Conversion = 96 %
M_{th}= 5,290
$M_{n,GPC}$= 6,150; M_w/M_n= 1.29
$M_{n,MALDI}$= 4,550; M_w/M_n= 1.05

86
MA unit
4310.8 4396.9 4482.9 4568.9 4654.9 4740.9

b) PMA after thioetherification

Conversion = 96%
M_{th}= 5,290
$M_{n,GPC}$= 6,560; M_w/M_n= 1.30
$M_{n,MALDI}$= 3,920; M_w/M_n= 1.05

58
4283.2 4369.1 4455.3 4541.4 4627.3 4713.4

Appendix 20. MALDI-TOF of α,ω-di(bromo)PMA isolated at 83% monomer conversion from SET-LRP of MA in DMAc/water (8/2, v/v) mixture initiated with BPE and catalyzed by nonactivated Cu(0) wire at 25 °C: (a) before and (b) after "thio-bromo "click". Polymerization conditions: MA = 1 mL, DMAc = 0.4 mL, water = 0.1 ml using 9.0 cm of nonactivated Cu(0) wire 20-gauge wire ($[MA]_0/[BPE]_0/[Me_6\text{-}TREN]_0 = 60/1/0.1$). The dotted line in expansion after thioetherification shows the original peak from before thioetherification, while 58 represents the increase in molar mass after thioetherification i.e., 2x[SPh (109. 2) - Br (79.9)] = 58.57 for each chain end.

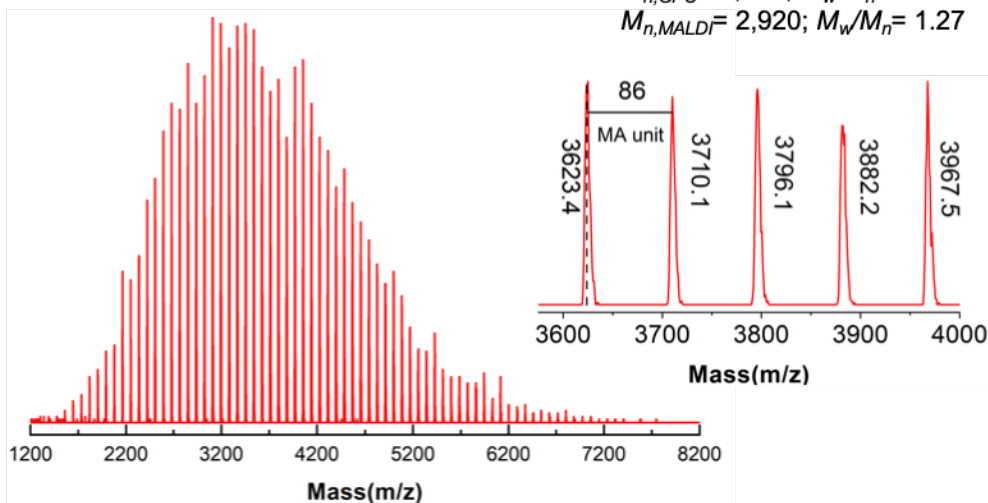a) PMA before thioetherification

Conversion = 83%
M_{th}= 4,620
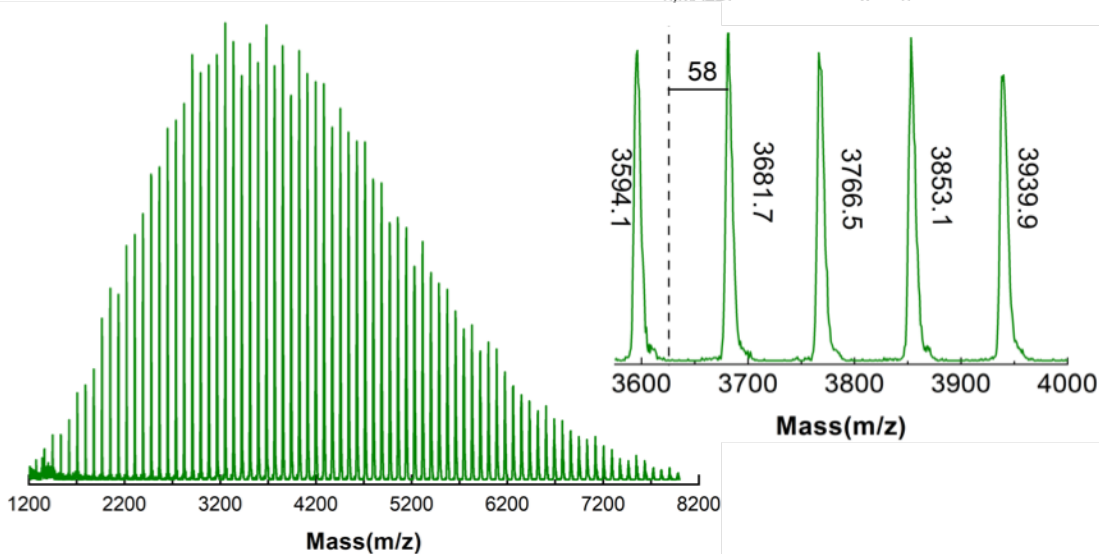$M_{n,GPC}$= 4,870; M_w/M_n= 1.95
$M_{n,MALDI}$= 2,920; M_w/M_n= 1.27

b) PMA after thioetherification

Conversion = 83%
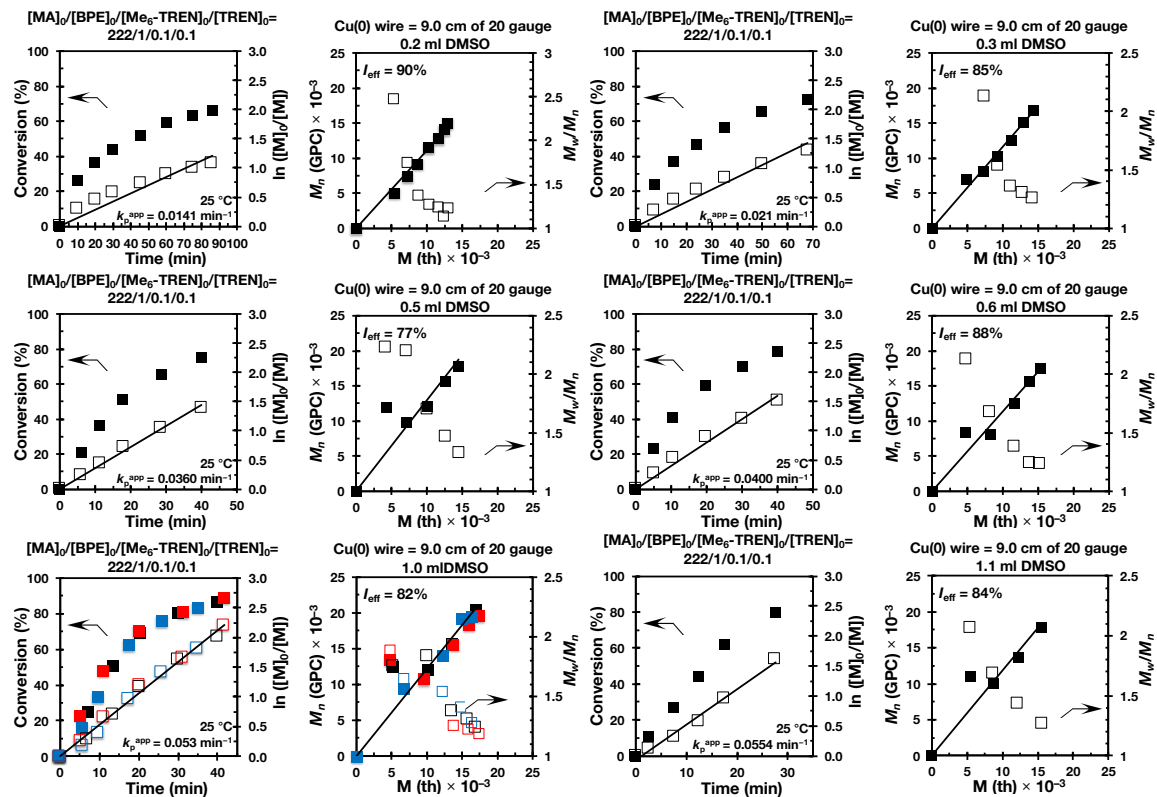M_{th}= 4,620
$M_{n,GPC}$= 7,380; M_w/M_n= 1.69
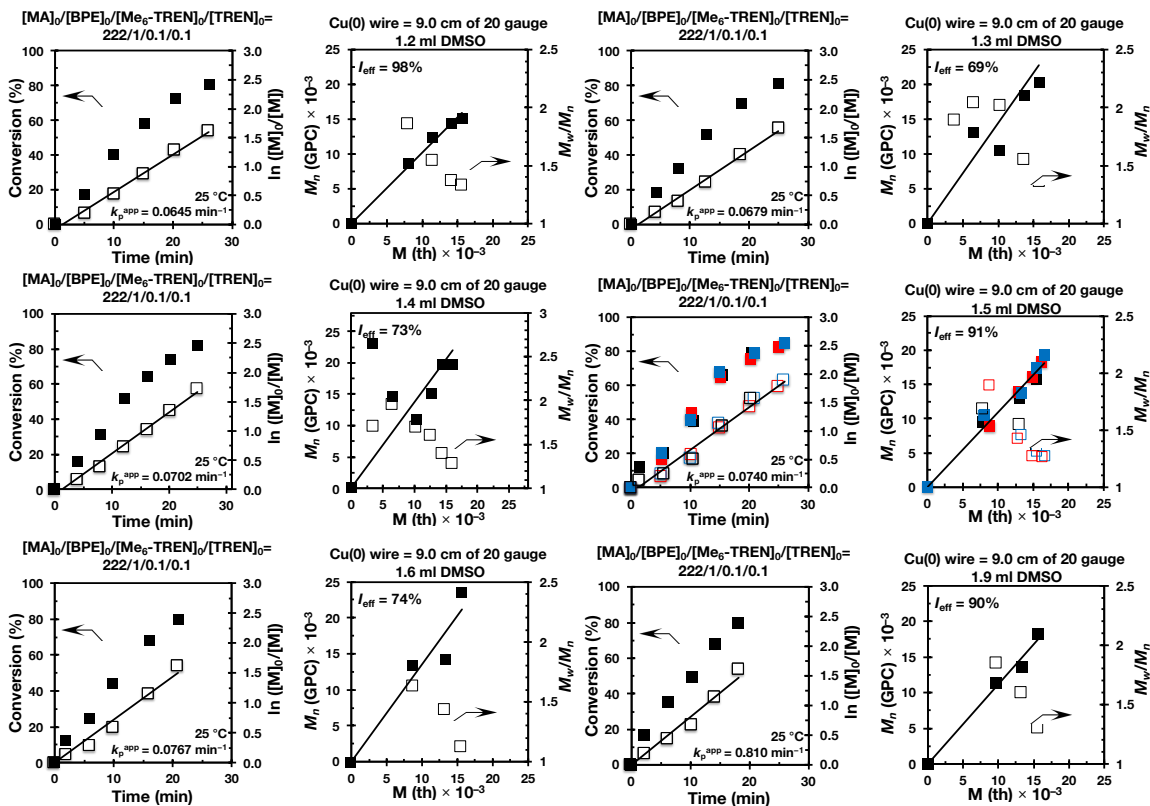$M_{n,MALDI}$= 3,310; M_w/M_n= 1.12

Appendix 21. Kinetic plots, molecular weight and dispersity evolutions for the SET-LRP of MA in DMSO, initiated with BPE and catalyzed by 9.0 cm non-activated Cu(0) wire at 25 °C. Experimental data in different colors were obtained from different kinetics experiments, sometimes performed by different researchers k_p^{app} and I_{eff} are the average values of three experiments. $\ln(k_p^{app})$ *vs* $\ln([DMSO]_0)$, DMSO was varied from 1 to 1.8 mL with 2 mL of MA. $[MA]_0/[BPE]_0/[Me_6\text{-}TREN]_0/[Cu(0)]_0 = 222/1/0.2/9cm$.
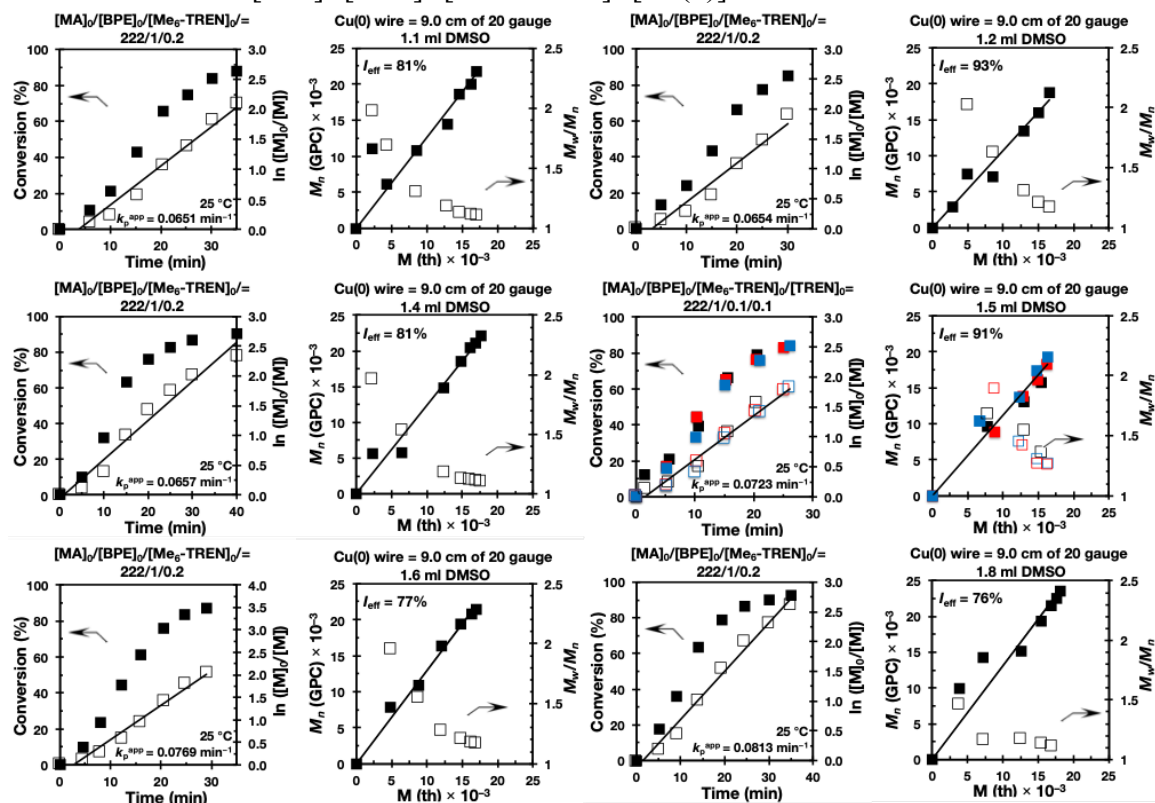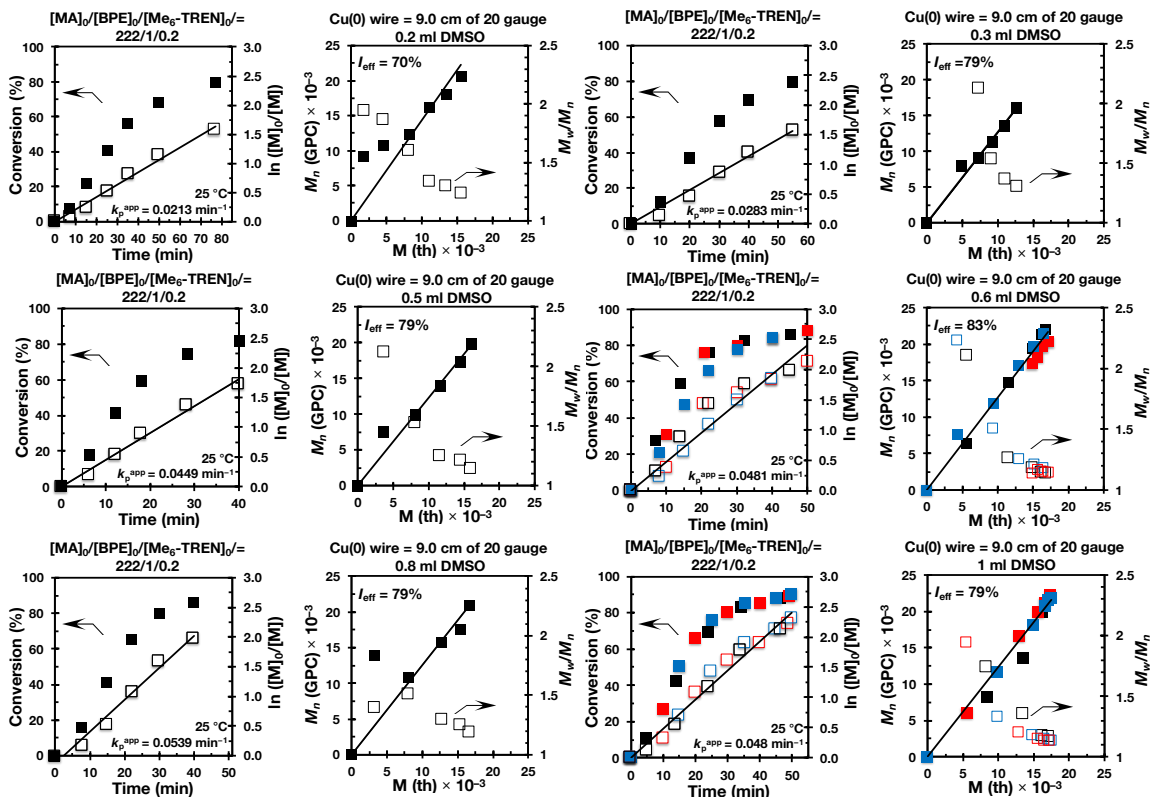
Appendix 22. Kinetic plots, molecular weight and dispersity evolutions for the SET-LRP of MA in DMSO, initiated with BPE and catalyzed by 9.0 cm non-activated Cu(0) wire at 25 °C. Experimental data in different colors were obtained from different kinetics experiments, sometimes performed by different researchers k_p^{app} and I_{eff} are the average values of three experiments. $\ln(k_p^{app})$ *vs* $\ln([DMSO]_0)$, DMSO was varied from 0.2 to 1.1 mL with 2 mL of MA. $[MA]_0/[BPE]_0/[Me_6\text{-}TREN]_0/[TREN]_0/[Cu(0)]_0 = 222/1/0.1/0.1/9$ cm.

Appendix 23. Kinetic plots, molecular weight and dispersity evolutions for the SET-LRP of MA in DMSO, initiated with BPE and catalyzed by 9.0 cm non-activated Cu(0) wire at 25 °C. Experimental data in different colors were obtained from different kinetics experiments, sometimes performed by different researchers. k_p^{app} and I_{eff} are the average value of three experiments. $\ln(k_p^{app})$ *vs* $\ln([DMSO]_0)$, DMSO was varied from 1.2 to 1.9 mL with 2 mL of MA. $[MA]_0/[BPE]_0/[Me_6\text{-}TREN]_0/[TREN]_0/[Cu(0)]_0 = 222/1/0.1/0.1/9cm$.

Appendix 24. Kinetic plots, molecular weight and dispersity evolutions for the SET-LRP of MA in DMSO initiated with BPE and catalyzed with 9.0 cm non-activated Cu(0) wire at 25 °C. Experimental data in different colors were obtained from different kinetics experiments, sometimes performed by different researchers. k_p^{app} and I_{eff} are the average values of three experiments. k_p^{app} vs [DMSO]$_0$ with DMSO varied from 0.2 to 1 mL with 2 mL of MA. [MA]$_0$/[BPE]$_0$/[Me$_6$-TREN]$_0$/[Cu(0)]$_0$ = 222/1/0.2/ 9cm.

Appendix 25. Kinetic plots, molecular weight and dispersity evolutions for the SET-LRP of MA in DMSO initiated with BPE and catalyzed with 9.0 cm non-activated Cu(0) wire at 25 °C. Experimental data in different colors were obtained from different kinetics experiments, sometimes performed by different researchers. k_p^{app} and I_{eff} are the average values of three experiments. k_p^{app} vs $[DMSO]_0$ with DMSO varied from 0.2 to 1.8 mL with 2 mL of MA. $[MA]_0/[BPE]_0/[TREN]_0/[Cu(0)]_0 = 222/1/0.2/9cm$.
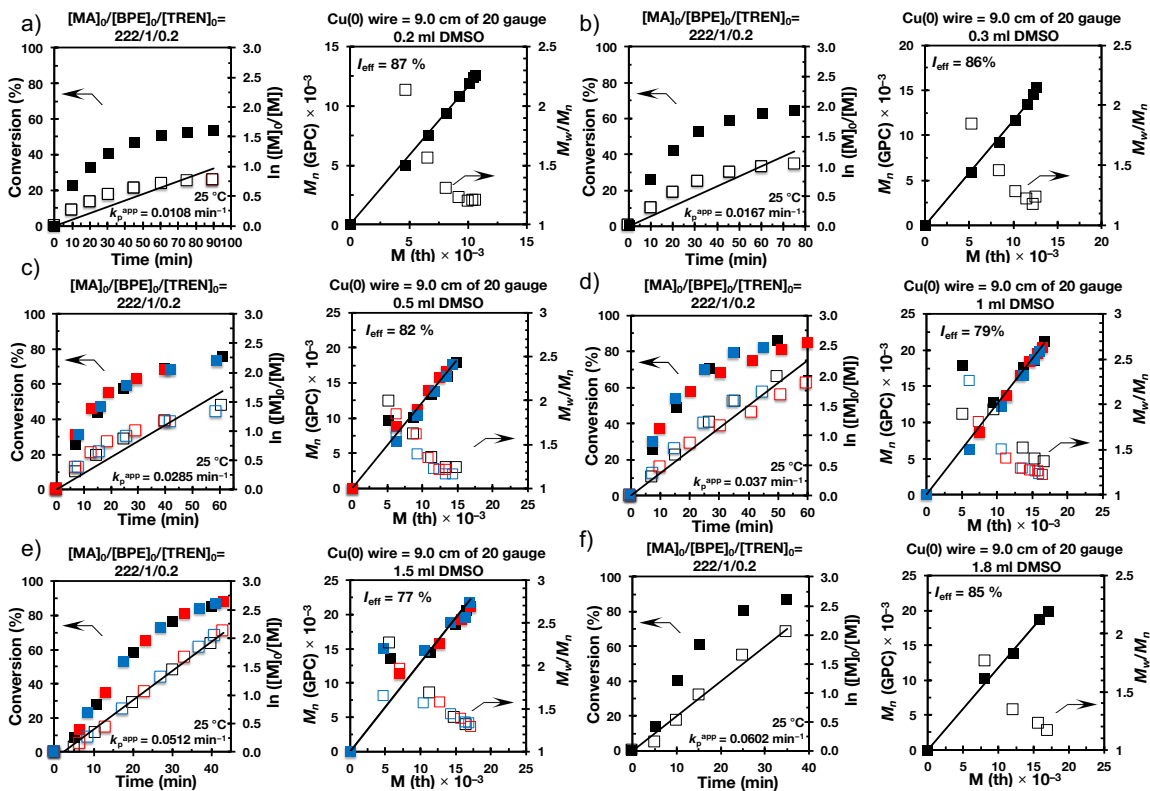
Appendix 26. MALDI-TOF of PMA-Br isolated at 83 % from SET-LRP of MA in DMSO solution initiated with BPE and catalyzed by non-activated Cu(0) wire at 25 °C; (a) before thio-bromo "click" reaction; (b) after thio-bromo "click" reaction. Reaction conditions: MA = 2 mL, DMSO = 1.50 mL, $[MA]_0/[BPE]_0/[Me_6\text{-}TREN]_0$ = 60/1/0.2, 9.0 cm of 20 gauge Cu(0) wire. The dotted line in expansion after thioeterification shows the original peak from before thioeterification, while 59 represents the increase in molar mass after thioeterification i.e., $2*[SC_6H_5 (109, 2)–Br (79, 9)]$ = 58.57 for each chain end.
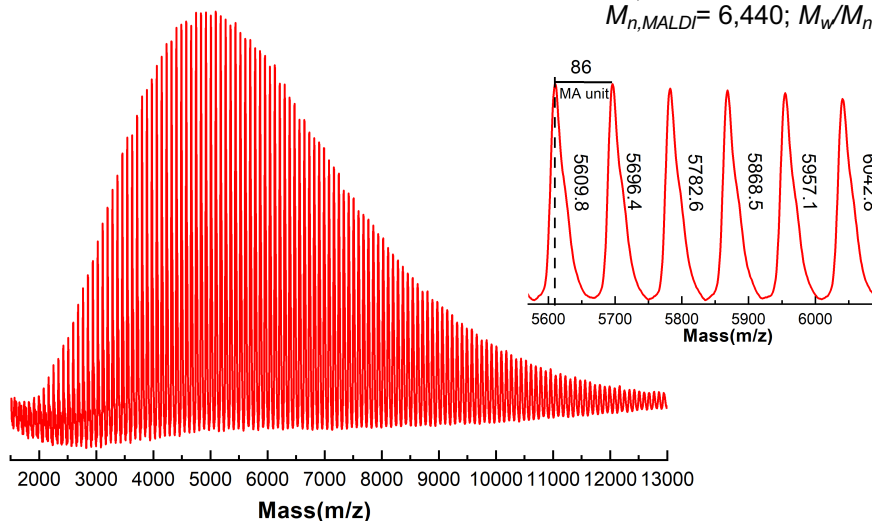

a) **PMA before thioetherification**

Conversion = 83%
M_{th}= 4,610
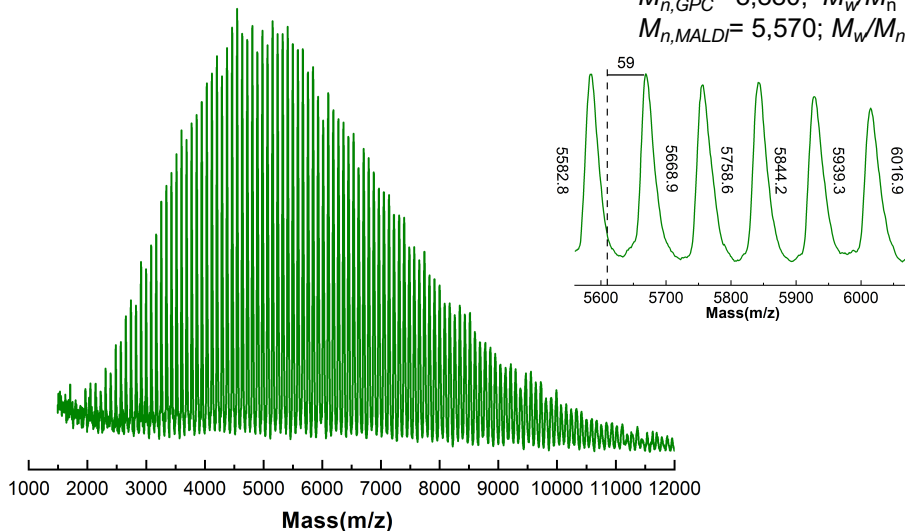$M_{n,GPC}$= 8,460; M_w/M_n= 1.34
$M_{n,MALDI}$= 6,440; M_w/M_n= 1.18

b) **PMA after thioetherification**

Conversion = 83%
M_{th}= 4,610
$M_{n,GPC}$= 8,880; M_w/M_n= 1.31
$M_{n,MALDI}$= 5,570; M_w/M_n= 1.19

Appendix 27. ^{1}H NMR spectra at 400 MHz of α,ω-di(bromo)PMA at: (a) 83% conversion (M_n = 8,460 and M_w/M_n = 1.34), ([MA]$_0$/[BPE]$_0$/[Me$_6$-TREN]$_0$ = 60/1/0.2); (b) 92% conversion (M_n = 6,420 and M_w/M_n = 1.27) ([MA]$_0$/[BPE]$_0$/[Me$_6$-TREN]$_0$/[TREN]$_0$ = 60/1/0.1/0.1); (c) 95% conversion (M_n = 7,690 and M_w/M_n =1.15) ([MA]$_0$/[BPE]$_0$/[TREN]$_0$ = 60/1/0.2); Polymerization conditions: MA = 2 mL, DMSO = 1.5 mL and non-activated 9 cm Cu(0) wire of 20 gauge. The signals at 7.26 ppm and 5.30 ppm are due to the partially non-deuterated residues of CDCl$_3$ and dichloromethane, respectively.

87
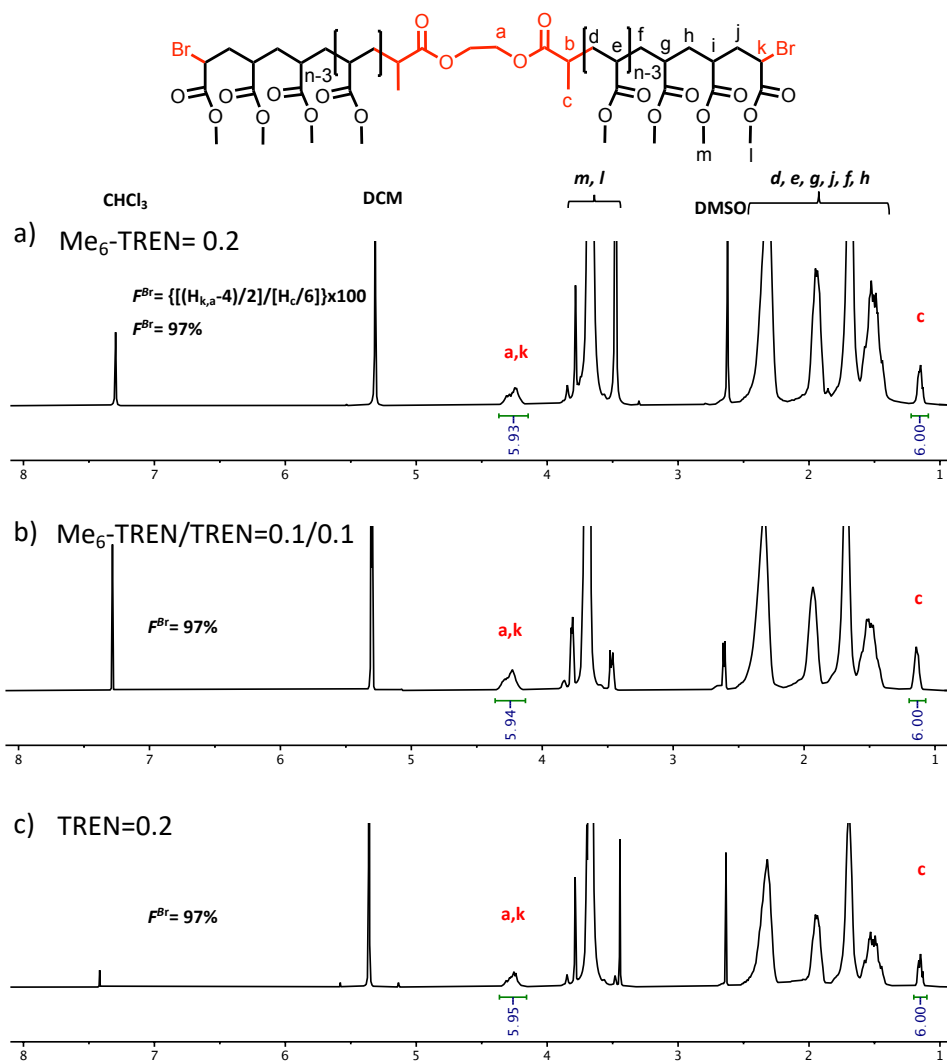
Appendix 28. ^{1}H NMR spectra at 400 MHz of α,ω-di(phenylthio)PMA at: (a) 83% conversion (M_n = 8,880 and M_w/M_n = 1.19), ([MA]$_0$/[BPE]$_0$/[Me$_6$-TREN]$_0$ = 60/1/0.2); (b) 90% conversion (M_n = 7,140 and M_w/M_n = 1.27), ([MA]$_0$/[BPE]$_0$/[Me$_6$-TREN]$_0$/[TREN]$_0$ = 60/1/0.1/0.1); (c) 96% conversion (M_n = 8,180 and M_w/M_n =1.13), ([MA]$_0$/[BPE]$_0$/[TREN]$_0$ = 60/1/0.2); Polymerization conditions: MA = 2 mL, DMSO = 1.5 mL and non-activated 9 cm Cu(0) wire of 20 gauge. The signals at 7.26 ppm and 5.30 ppm are due to the partially non-deuterated residues of CDCl$_3$ and dichloromethane, respectively.

$F^{SPh}= [(H_n/4)/(H_c/6)]\times100$

F^{SPh}= 98%

F^{SPh}= 96%

F^{SPh}= 98%

88
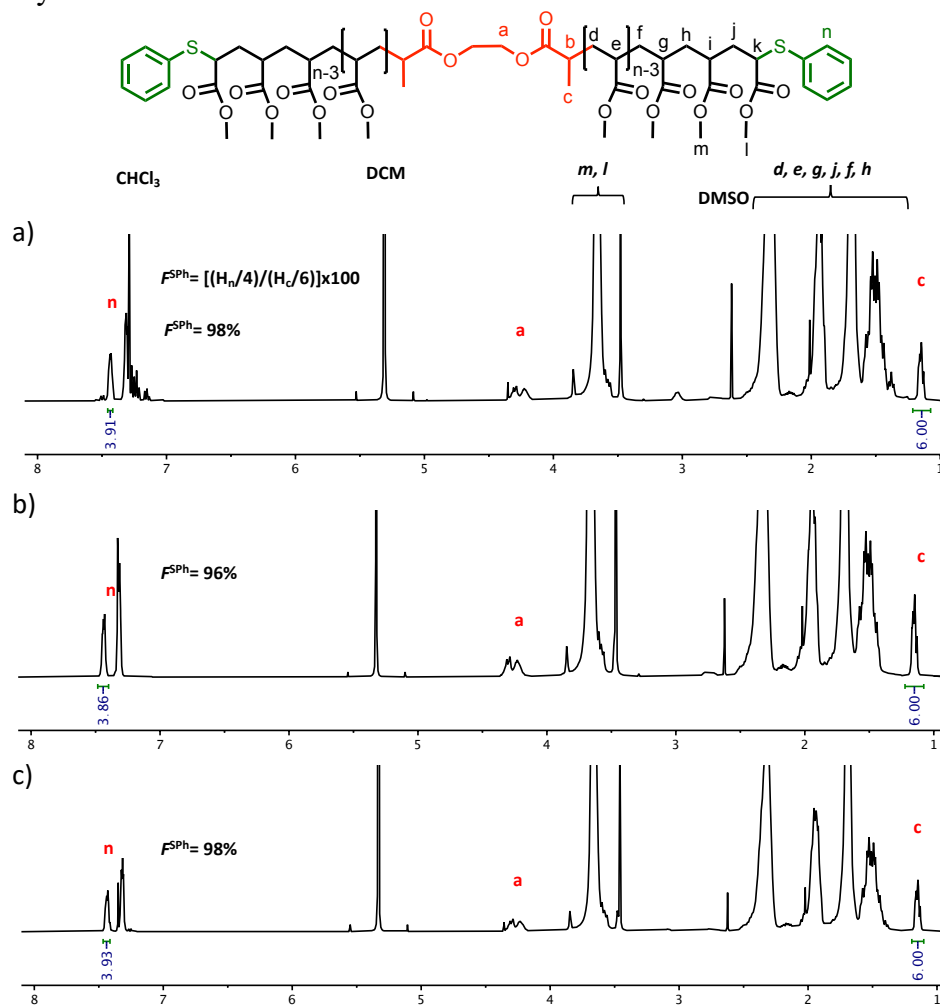
Appendix 29. MALDI-TOF of PMA-Br isolated at 92 % from SET-LRP of MA in DMSO solution initiated with BPE and catalyzed by non-activated Cu(0) wire at 25 °C; (a) before thio-bromo "click" reaction; (b) After thio-bromo "click" reaction. Reaction conditions: MA = 2 mL, DMSO = 1.50 mL, $[MA]_0/[BPE]_0/[Me_6-TREN]_0/[TREN]_0 = 60/1/0.1/0.1$, 9.0 cm of 20 gauge Cu(0) wire. The dotted line in expansion after thioeterification shows the original peak from before thioeterification, while 59 represents the increase in molar mass after thioeterification i.e., $2*[SC_6H_5 (109, 2)–Br (79, 9)] = 58.57$ for each chain end.
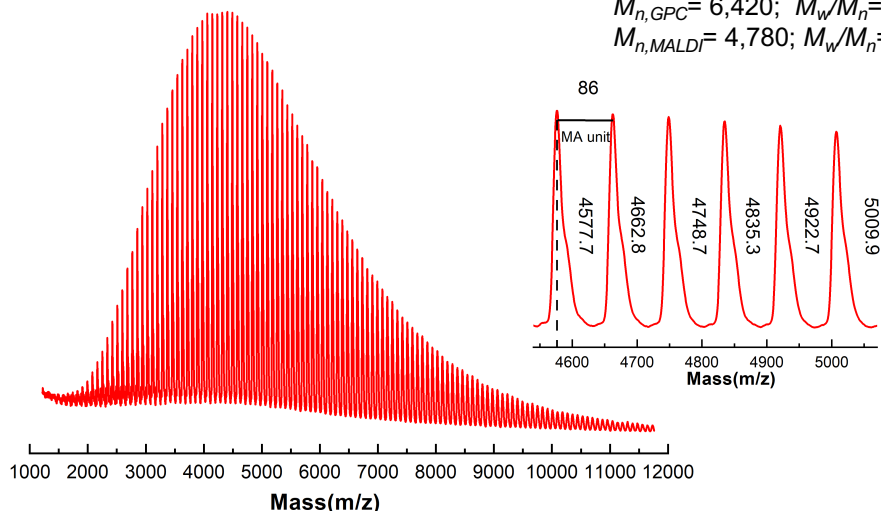
a) PMA before thioetherification

Conversion = 92%
M_{th}= 5,080
$M_{n,GPC}$= 6,420; M_w/M_n= 1.27
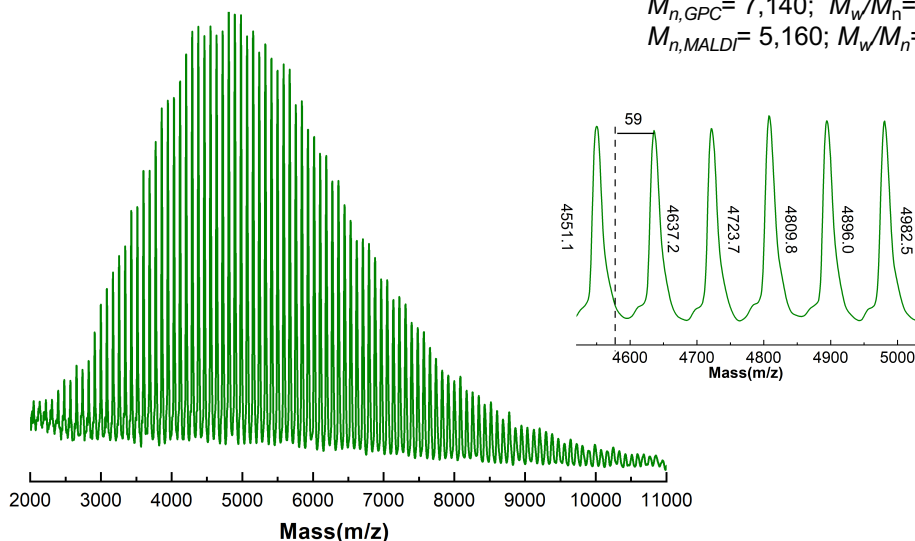$M_{n,MALDI}$= 4,780; M_w/M_n= 1.20

b) PMA after thioetherification

Conversion = 92%
M_{th}= 4,080
$M_{n,GPC}$= 7,140; M_w/M_n= 1.27
$M_{n,MALDI}$= 5,160; M_w/M_n= 1.15

Appendix 30. MALDI-TOF of PMA-Br isolated at 95 % from SET-LRP of MA in DMSO solution initiated with BPE and catalyzed by non-activated Cu(0) wire at 25 °C; (a) before thio-bromo "click" reaction; (b) after thio-bromo "click" reaction. Reaction conditions: MA = 2 mL, DMSO = 1.50 mL, $[MA]_0/[BPE]_0/[TREN]_0$ = 60/1/0.2, 9.0 cm of 20 gauge Cu(0) wire. The dotted line in expansion after thioeterification shows the original peak from before thioeterification, while 59 represents the increase in molar mass after thioeterification i.e., $2*[SC_6H_5 (109, 2)–Br (79, 9)]$ = 58.57 for each chain end.

a) **PMA before thioetherification**

Conversion = 95%
M_{th}= 5,230
$M_{n,GPC}$= 7,690; M_w/M_n= 1.14
$M_{n,MALDI}$= 5,620; M_w/M_n= 1.15
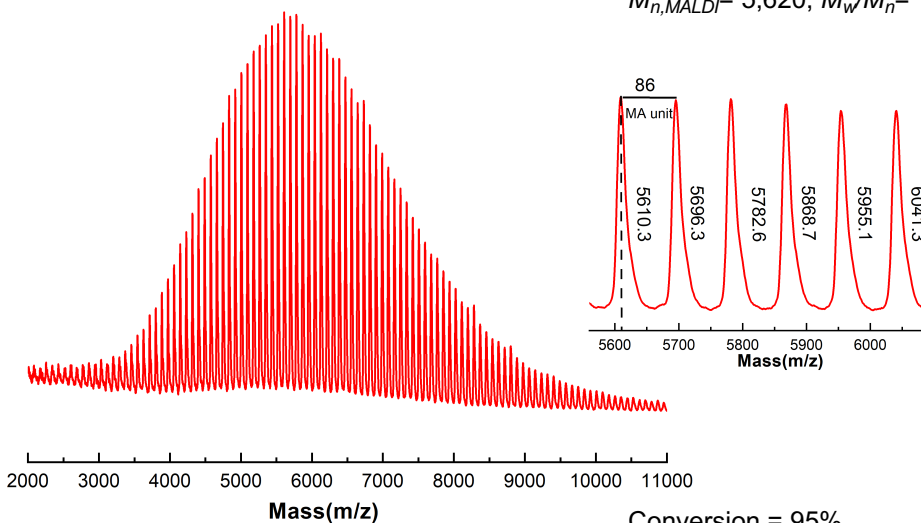
b) **PMA after thioetherification**

Conversion = 95%
M_{th}= 5,230
$M_{n,GPC}$= 8,180; M_w/M_n= 1.13
$M_{n,MALDI}$= 5,890; M_w/M_n= 1.20